NMDA RECEPTORS IN HIBERNATING ARCTIC GROUND SQUIRRELS

By

Huiwen Zhao

RECOMMENDED:

Advisory committee chair

Chair, Department of Chemistry and Biochemistry

APPROVED:

Dean, College of Natural Science and Mathematics

Dean of the Graduate School

October 11, 2005

Date

NMDA RECEPTORS IN HIBERNATING ARCTIC GROUND SQUIRRELS

A

THESIS

Presented to the Faculty

Of the University of Alaska Fairbanks

In Partial Fulfillment of the Requirements

For the Degree of

DOCTOR OF PHILOSOPHY

By

Huiwen Zhao, M.S.

Fairbanks, Alaska

December 2005

Abstract

Hibernation is a unique physiological state characterized by suppressed metabolism and body temperature that is interrupted by multiple, brief periods of arousal throughout the hibernation season. Blood flow fluctuates during hibernation and arousal in a reperfusion-like manner without causing neurological damage. Previous studies show that hippocampal slices from hibernating animals tolerate experimental oxygen nutrient deprivation and N-methyl-D-aspartate (NMDA) toxicity better than slices from euthermic animals. However, the cellular mechanisms underlying these examples of tolerance remain unclear.

Tolerance to NMDA toxicity suggests that modulation of NMDA receptors (NMDAR) contributes to intrinsic tissue tolerance in slices from hibernating Arctic ground squirrels (hAGS, *Spermophilus parryii*). NMDAR are one subtype of glutamate receptors. NMDAR play critical roles in excitatory synaptic transmission, synaptic plasticity, learning and memory, and excitotoxicity. NMDAR1 (NR1) is a fundamental subunit of NMDAR and required for receptor function.

The main focus of the current project was to test the hypothesis that NMDAR are down-regulated in hAGS compared with interbout euthermic AGS (ibeAGS) and to explore the potential mechanisms of this down-regulation. NMDAR function can be modulated by protein phosphorylation, subunit composition, and internalization. Hence, the aim of chapter 2 was to determine the distribution of NR1 in hAGS and ibeAGS using immunohistochemistry. The aim of chapter 3 was to examine NMDAR function in cultured hippocampal slices from hAGS, ibeAGS, and rats using calcium imaging, and to

investigate potential modulation of NMDAR such as phosphorylation and internalization for altered function using western blot analysis. Given that synaptic remodeling and functional changes after arousal from hibernation, and NMDAR play an important role in learning and memory, the aim of chapter 4 was to address the effects of hibernation on learning and memory in AGS using an active avoidance task.

Here, we report that NMDAR in hAGS are down-regulated via decreased phosphorylation of NR1. This down-regulation is not due to changes in NR1 distribution and internalization. In addition, the fraction of NR1 in the functional membrane pool in AGS is less than in rats. These findings provide evidence that modulation of NMDAR contributes to neuroprotection observed in hAGS.

TABLE OF CONTENTS

Page

Page

LIST OF FIGURES

LIST OF TABLES

LIST OF APPENDICES

ACKNOWLEDGEMENTS

The work for this thesis could not be finished without the support and encouragement of many people. It is a pleasure to have this opportunity to express my gratitude to all of them.

First of all, I would like to express my gratitude to my advisor, Dr. Kelly Drew, for giving me the opportunity to study at UAF and work in her lab. I am grateful for her many years of scientific instruction, her enthusiasm, knowledge, and integral view on research, all of which have made a deep impression on me. She could not realize how much I have learned from her: the art of doing research, the art of writing, and the art of thinking.... Moreover, her encouragement always pushes me forward and provides me with the confidence to face anything. I am very glad that I have come to know her in my life.

I would also like to thank my committee members: Drs. Lawrence Duffy, Abel Bult-Ito, and Lique Coolen. I am grateful for Dr. Duffy's financial support and scientific suggestions. Many thanks to Dr. Bult-Ito for his generosity in allowing me to use his lab facilities and for giving me great suggestions on both research and my career. Also, thanks to Dr. Coolen for her constructive suggestions in both immunohistochemistry and western blotting experiments. Thank you all for your valuable comments on my thesis and manuscripts.

I would like to acknowledge the Department of Chemistry and Biochemistry as well as the Biochemistry and Molecular Biology program for giving me the opportunity to study in their department and program. Special thanks to Dr. Thomas Clausen for his kind support for all my grant and scholarship applications and to Sheila Chapin for her kind assistance in everything.

This work has been supported and funded by the Alaskan Basic Neuroscience Program (NIH U54-NS 41069 funded by NINDS, NIMH, NCRR, and NCMHD) and Alaska EPSCoR (ESP-0092040 and EPS-0346770 fund by NSF). I thank them all for their confidence in me.

I would like to thank Dr. Sherri Christen for her selfless instruction in western blotting techniques, her valuable discussion, and her collaboration. I also thank Austin Ross for her help in tissue preparation and for her collaboration as a group, Maegan Weltzin for her wonderful collaboration in behavioral studies during the past few years, and many other past and present lab members in Dr. Drew's lab, all of whose names I can not list here. I hope they know how much I appreciate their help.

I also thank Dr. John Buchholz, Charles Hewitt (Loma Linda University, CA), Drs. Edward.Lachica (Bioptechs, PA), Osama Ogawa (CWRU, OH), and Carlos Arnaiz (Coulbourn Instruments, PA) for technical assistance in Ca^{2+} imaging, western blotting, and learning behavioral experiments. Without them, I could not have finished this work.

I feel a deep sense of gratitude to my parents who always support me through everything. I also thank my brother for the support he has offered in his own way.

Finally, I particularly thank my husband and our son for their love, understanding, and support at all times.

Chapter 1

General Introduction

1. 1 Overview of hibernation

1. 1. 1 Hibernation physiology

Hibernation is a survival strategy of hibernators when food is scarce and day length decreases during long, cold winters. Arctic ground squirrels (AGS, *Spermophilus parryii*) are the main focus of this project. AGS are mainly found in Alaska, the Yukon Territory, and northern British Columbia in Canada. In general, AGS begin hibernating in September and arouse in May. During hibernation, body temperature drops, respiration rate slows down, and animals are difficult to arouse. Hibernation is a unique physiological state characterized by periods of reduced metabolic activity and body temperature that is interrupted at regular intervals by brief periods of arousal where metabolism rapidly returns to euthermic (non-hibernating) levels. Hibernating animals experience multiple rounds of arousal followed by a return to hibernation throughout the hibernation season (Fig. 1. 1, Lust et al., 1989; Frerichs et al., 1994; Carey et al., 2003).

1. 1. 2 Hibernation is a natural model of neuroprotection

Hibernation, as a natural model of neuroprotection, is known both *in vivo* and *in vitro* (Drew et al., 2004, Frerichs et al., 1994, Zhou et al., 2001). Heart rate decreases upon entrance into hibernation, resulting in an 80-90% reduction in blood flow to the brain and other organs. During arousal from hibernation, lower oxygen delivery

accompanied with lower blood flow is replaced by rapid increases in blood flow (up to 300% of minimum hibernating level). Fluctuations in blood flow during the hibernation cycle are in a reperfusion-like manner without causing any neurological damage (Frerichs et al., 1994; Ma et al., 2005). Such dramatic fluctuation in cerebral blood flow causes swings in energy supply and would produce severe damage or death in humans. For instance, stroke, the third killer in America, is the consequence of an interruption of cerebral blood flow, which causes symptoms ranging from a passing weakness to profound paralysis, coma, and death (Heiss et al., 1992; Garcia, 1992).

An *in vitro* study demonstrates that hippocampal slices from hibernating 13-lined ground squirrels tolerate experimental ischemia better than slices from euthermic 13-lined ground squirrels (Frerichs et al., 1998). Recent work from Dr. Drew's lab shows that hippocampal slices from hibernating AGS tolerate oxygen nutrient deprivation and N-methyl-D-aspartate (NMDA), even at high concentrations, better than slices from interbout euthermic AGS (Ross et al., in press).

Furthermore, an *in vivo* study also provides evidence that hibernating AGS brain tolerates a penetrating brain injury caused by insertion of a microdialysis probe (Zhou et al., 2001). Tissue damage is attenuated in hibernating AGS compared to euthermic AGS 3 days after the implantation of microdialysis probes in the striatum of brain.

How do hibernating animals tolerate dramatic swings in blood flow and brain trauma? Study of hibernation physiology may address some medical problems and offer clues to how humans might be protected from stroke, traumatic brain injury and

neurodegenerative disease. The purpose of the current project (chapter 2 and chapter 3) is therefore, to investigate the potential neuroprotective mechanisms in hibernating AGS.

1. 1. 3 Hibernation is a natural model of adult synaptic plasticity

Hibernation is a natural model of adult mammalian synaptic plasticity, evidenced by pronounced synaptic remodeling observed in the hippocampus from ground squirrels during hibernation, 2 h and 24 h after arousal (Popov and Bocharova, 1992; Popov et al., 1992; Malínský and Polách, 1985; Weltzin et al., in press). For example, CA3 apical dendritic branching, spine densities, dendritic spine profile areas, and the number of postsynaptic densities per spine all decrease during torpor in ground squirrels (*Spermophilus undalatus*), an Arctic species closely related to AGS. Within hours after arousal from hibernation, hippocampal synaptic parameters increase beyond pre-hibernation levels and peak at about 2-3 h after arousal. By 24 h after arousal, dendritic re-growth has started to subside, but remains larger than during torpor (Popov and Bocharova, 1992; Popov et al., 1992).

The natural synaptic restructuring observed in adult ground squirrels may provide a unique opportunity to study the functional consequences of synaptic reorganization. For instance, Mihailovic et al. (1968) reported that arousal from hibernation enhanced learning in ground squirrels suggesting that synaptic remodeling during arousal may indeed have a functional correlation. McNamara and Riedesel (1973) and Millesi et al. (2001) have assessed how hibernation influences learning acquired prior to hibernation, but these studies have produced mixed effects of hibernation on learning. Therefore, the

purpose of the current project (chapter 4) is to examine how hibernation affects cognitive function in AGS.

1. 2 Overview of NMDA receptors

1. 2. 1 Classification of glutamate receptors

N-methyl-D-aspartate receptors (NMDAR) are one subtype of glutamate receptors. Glutamate receptors play an important role in neuronal development, synaptic plasticity, learning and memory and cell death (Collingridge and Singer, 1990; Monaghan et al., 1989). Glutamate receptors include ligand gated ion channels (ionotropic glutamate receptors) and G-protein coupled receptors (metabotropic glutamate receptors) (Table 1. 1). Metabotropic glutamate receptors regulate synaptic transmission and neuronal excitability through activation or inhibition of various G-protein coupled effectors. Their effects are relatively slower in onset and longer-lasting compared with the effects of ionotropic glutamate receptors. Ionotropic glutamate receptors allow ions such as sodium and calcium to pass through the channels. The ionotropic glutamate receptors are further subdivided into three groups, including alpha-amino-3-hydroxy-5-methyl-4-isoxazolepropionic acid receptors (AMPAR), NMDAR, and kainite receptors based on selective pharmacology (Monaghan et al., 1989).

1. 2. 2 Subunit composition of NMDAR

NMDAR were first identified due to the selective activation by NMDA. NMDAR are primarily composed of the NMDAR1 (NR1) subunit, NMDAR2A-D (NR2A-D)

subunits, and sometimes NMDAR3A-B (NR3A-B) subunits. In general, these subunits assemble as heterotetramers in the endoplasmic reticulum to form functional channels. After processing in the Golgi apparatus, mature NMDAR are targeted to synaptic and extrasynaptic sites (Scott et al., 2001; Monyer et al., 1992; McIlhinney et al., 1998; Ozawa et al., 1998). NMDAR share a common basic structure with other ligand-gated receptors. NR1 subunits are generated from one single gene that undergoes extensive splice variation in both N-terminals and C-terminals to form eight separate splice variants. NR2 subunits are generated from four different genes (NR2A-D). Functional NMDAR are formed by at least one NR1 subunit in various combinations with NR2A-D subunits. NR1 is required for functional NMDAR, while NR2 subunits play regulatory roles (Carroll and Zukin, 2002). The different combinations of NR1 and NR2 subunits may confer different physiological and pharmacological properties on the receptors (Monyer et al., 1994, Stephenson, 2001).

1. 2. 3 Pharmacological characteristics of NMDAR

NMDAR complexes possess multiple binding sites on both the NR1 subunit and NR2 subunit (Fig. 1. 2, Lynch and Guttermann, 2001). For instance, there is a glutamate binding site and a polyamine binding site in the NR2 subunit, a glycine binding site in the NR1 subunit, as well as other binding sites for Mg^{2+} and Zn^{2+} ions. Both NMDAR agonists such as glutamate and NMDAR competitive antagonists such as L-2-amino-5-phosphonovalerate (AP5) bind the receptor through the glutamate binding site. Spermine, spermidine, and phencyclidine bind the receptor through the polyamine binding site. All

compounds and ions that act at binding sites of NMDAR may modulate NMDAR activity.

1. 2. 4 Activation of NMDAR

At the resting membrane potential, NMDAR is inactivated due to voltage-dependent block of the channel pore by the Mg^{2+} ion. Although NMDAR have higher affinity for glutamate than AMPA and kinate receptors, NMDA receptors can only be activated after membrane depolarization induced by intense activation of AMPA and kainate receptors and subsequent removal of magnesium from the channel pore. Once they are activated, channel opening permits an influx of Na^{+} and Ca^{2+} ions, and an efflux of K^{+} ions. NMDAR have a high permeability to calcium ions and NMDAR mediated calcium influx is the major synaptically controlled mechanism of calcium influx (Dingledine et al., 1999). When energy is scarce, excessive discharge of glutamate will cause excessive levels of NMDA receptor activation and then trigger cell death (Szatkowski and Attwell, 1994). Although other non-NMDA glutamate receptors such as AMPAR also allow calcium ion influx, the calcium influx through AMPAR is relatively small and subunit dependent (Bennett et al., 1996). Therefore, NMDAR have attracted significant attention in the past two decades due to their high Ca^{2+}-permeablity and their key roles in synaptic plasticity and excitotoxicity (Ascher and Nowak, 1987; Choi, 1995).

1. 2. 5 NMDAR modulation

NMDAR contribute significantly to excitatory synaptic transmission throughout the mammalian central nervous system. NMDAR also play critical roles in synaptic plasticity, long-term potentiation (LTP), long-term depression (LTD), learning and memory, and excitotoxicity, which depend on the levels of receptor activation (Cummings et al., 1996; Zucker, 1999; Choi, 1995). The function of synaptic NMDA receptors needs to be tightly regulated in order to perform the appropriate function in neurons (Barria and Malinow, 2002). NMDAR function can be modulated by protein phosphorylation, ATP and Ca^{2+}-dependant depolymerization of actin, desensitization, cations, pH, and redox agents (Liu and Zhang, 2000). In addition, multiple proteins that associate with the intracellular domains of NMDAR subunits can modulate NMDAR function by effecting the insertion of NMDAR at synaptic sites (Scott et al., 2001).

Protein phosphorylation is a major mechanism in the regulation of NMDAR function (Liu and Zhang, 2000). NMDAR function is activated by phosphorylation and inactivated by dephosphorylation. Protein kinase C (PKC), cAMP-dependent protein kinases (PKA) and protein tyrosine kinases increase NMDAR channel activity, while protein tyrosine phosphatases and serine/threonine phosphatases decrease NMDAR channel activity. The NR1 subunit is phosphorylated by PKA on Serine 890 and 897, and by PKC on Serine 896.

1. 3 Hibernation and NMDAR

Heterothermic mammals such as ground squirrels tolerate ischemia better than homeothermic mammals such as rats both *in vivo* and *in vitro* (Drew et al., 2004; Frerichs et al., 1998). This tolerance is enhanced in the hibernating state compared with the non-hibernating state (euthermy). However, the cellular mechanisms underlying this tolerance remain unclear. Intracellular calcium is a ubiquitous second messenger integrating many cellular processes, including neuronal development, gene expression, synaptic plasticity, and neuronal death (Siesjo, 1990). Calcium overload through NMDAR is a major trigger of ischemia-induced neuronal death. Recent work showed that hippocampal slices from hibernating AGS tolerate oxygen nutrient deprivation and NMDA, even at high concentrations, better than slices from interbout euthermic AGS (Ross et al., in press). Tolerance to NMDA suggests that modulation of NMDAR contributes to intrinsic tissue tolerance in slices from hibernating AGS. Previous studies have also shown that modulation of NMDAR contributes to hypoxia and ischemia tolerance in developing brains of rats and piglets (Mishra et al., 2001, Fritz et al., 2002) and allows western painted turtles (*Chrysemys picta*) to tolerate long-term anoxia (Bickler et al., 1998).

1. 4 Scopes and aims of the current project

The main focus of the current project was to test the hypothesis that NMDAR are down-regulated in hibernating AGS compared with euthermic AGS. This decreased function could involve changes in NMDAR expression and distribution, internalization, and NMDAR modulation in hibernating AGS. NMDAR also play a role in learning and

memory. An additional focus of the current project was to examine the hypothesis that arousal from hibernation enhances the cognitive function in AGS. The aims were therefore:

1. To determine the distribution of the NR1 subunit of NMDAR in hibernating AGS and interbout euthermic AGS using immunohistochemistry.
2. To examine NMDAR function in cultured hippocampal slices from hibernating AGS, interbout euthermic AGS, and rats using calcium imaging.
3. To investigate NMDAR modulation and internalization as potential mechanisms for altered function using western blot analysis.
4. To address the effects of hibernation on learning and memory in AGS using an active avoidance task.

1. 5 References

Ascher P. and Nowak L. (1986) A patch-clamp study of excitatory amino acid activated channels. *Adv Exp Med Biol* 203, 507-511.

Barria A. and Malinow R. (2002) Subunit-specific NMDA receptor trafficking to synapses. *Neuron* 35, 345-353.

Bennett M. V., Pellegrini-Giampietro D. E., Gorter J. A., Aronica E., Connor J. A. and Zukin R. S. (1996) The GluR2 hypothesis: Ca(++)-permeable AMPA receptors in delayed neurodegeneration. *Cold Spring Harb Symp Quant Biol* 61, 373-384.

Bickler P. E. (1998) Reduction of NMDA receptor activity in cerebrocortex of turtles (Chrysemys picta) during 6 wk of anoxia. *Am J Physiol* 275, R86-91.

Carey H. V., Andrews M. T. and Martin S. L. (2003) Mammalian hibernation: cellular and molecular responses to depressed metabolism and low temperature. *Physiol Rev* 83, 1153-1181.

Carroll R. C. and Zukin R. S. (2002) NMDA-receptor trafficking and targeting: implications for synaptic transmission and plasticity. *Trends Neurosci* 25, 571-577.

Choi D. W. (1995) Calcium: still center-stage in hypoxic-ischemic neuronal death. *Trends Neurosci* 18, 58-60.

Collingridge G. L. and Singer W. (1990) Excitatory amino acid receptors and synaptic plasticity. *Trends Pharmacol Sci* 11, 290-296.

Cummings J. A., Mulkey R. M., Nicoll R. A. and Malenka R. C. (1996) Ca^{2+} signaling requirements for long-term depression in the hippocampus. *Neuron* 16, 825-833.

Dingledine R., Borges K., Bowie D. and Traynelis S. F. (1999) The glutamate receptor ion channels. *Pharmacol Rev* 51, 7-61.

Dave K. R., Prado R., Raval A. P., Drew K. L. and Perez-Pinzon M. A. (2005) The arctic ground squirrel brain resists cardiac arrest during euthermia. Submitted to *Stroke*

Drew K. L., Harris M. B., LaManna J. C., Smith M. A., Zhu X. W. and Ma Y. L. (2004) Hypoxia tolerance in mammalian heterotherms. *J Exp Biol* 207, 3155-3162.

Frerichs K. U. and Hallenbeck J. M. (1998) Hibernation in ground squirrels induces state and species-specific tolerance to hypoxia and aglycemia: an in vitro study in hippocampal slices. *J Cereb Blood Flow Metab* 18, 168-175.

Frerichs K. U., Kennedy C., Sokoloff L. and Hallenbeck J. M. (1994) Local cerebral blood flow during hibernation, a model of natural tolerance to "cerebral ischemia". *J Cereb Blood Flow Metab* 14, 193-205.

Fritz K. I., Zubrow A. B., Mishra O. P. and Delivoria-Papadopoulos M. (2002) NMDA receptor modification during graded hypoxia in the cerebral cortex of newborn piglets. *Biol Neonate* 82, 46-52.

Garcia J. H. (1992) The evolution of brain infarcts. A review. *J Neuropathol Exp Neurol* 51, 387-393.

Heiss W. D., Huber M., Fink G. R., Herholz K., Pietrzyk U., Wagner R. and Wienhard K. (1992) Progressive derangement of periinfarct viable tissue in ischemic stroke. *J Cereb Blood Flow Metab* 12, 193-203.

Lust W. D., Wheaton A. B., Feussner G. and Passonneau J. (1989) Metabolism in the hamster brain during hibernation and arousal. *Brain Res* 489, 12-20.

Lynch D. R. and Guttmann R. P. (2001) NMDA receptor pharmacology: perspectives from molecular biology. *Curr Drug Targets* 2, 215-231.

Ma Y. L., Zhu X., Rivera P. M., Toien O., Barnes B. M., Lamanna J. C., Smith M. A. and Drew K. L. (2005) Absence of Cellular Stress in Brain Following Hypoxia Induced by Arousal from Hibernation in Arctic Ground Squirrels. *Am J Physiol Regul Integr Comp Physiol.* Jun. 23.

Malinsky J. and Polach A. (1985) Changes of synaptic apparatus in the brain cortex of the hedgehog during hibernation (a quantitative Golgi and electron microscopic study). *Acta Univ Palacki Olomuc Fac Med* 108, 109-115.

McIlhinney R. A., Le Bourdelles B., Molnar E., Tricaud N., Streit P. and Whiting P. J. (1998) Assembly intracellular targeting and cell surface expression of the human N-methyl-D-aspartate receptor subunits NR1a and NR2A in transfected cells. *Neuropharmacology* 37, 1355-1367.

McNamara M. C. and Riedesel M. L. (1973) Memory and hibernation in Citellus lateralis. *Science* 179, 92-94.

Mihailovic L., Petrovic-Minic B., Protic S. and Divac I. (1968) Effects of hibernation on learning and retention. *Nature* 218, 191-192.

Millesi E., Prossinger H., Dittami J. P. and Fieder M. (2001) Hibernation effects on memory in European ground squirrels (Spermophilus citellus). *J Biol Rhythms* 16, 264-271.

Mishra O. P. and Delivoria-Papadopoulos M. (2001) Effect of graded hypoxia on high-affinity Ca^{2+}-ATPase activity in cortical neuronal nuclei of newborn piglets. *Neurochem Res* 26, 1335-1341.

Monaghan D. T., Bridges R. J. and Cotman C. W. (1989) The excitatory amino acid receptors: their classes, pharmacology, and distinct properties in the function of the central nervous system. *Annu Rev Pharmacol Toxicol* 29, 365-402.

Monyer H., Burnashev N., Laurie D. J., Sakmann B. and Seeburg P. H. (1994) Developmental and regional expression in the rat brain and functional properties of four NMDA receptors. *Neuron* 12, 529-540.

Ozawa S., Kamiya H. and Tsuzuki K. (1998) Glutamate receptors in the mammalian central nervous system. *Prog Neurobiol* 54, 581-618.

Popov V. I. and Bocharova L. S. (1992a) Hibernation-induced structural changes in synaptic contacts between mossy fibres and hippocampal pyramidal neurons. *Neuroscience* 48, 53-62.

Popov V. I., Bocharova L. S. and Bragin A. G. (1992b) Repeated changes of dendritic morphology in the hippocampus of ground squirrels in the course of hibernation. *Neuroscience* 48, 45-51.

Ross A. P., Christian S. L., Zhao H. W. and Drew K. L. (2005) Persistent tolerance to oxygen and nutrient deprivation and N-methyl-D-aspartate in cultured hippocampal slices from hibernating Arctic ground squirrel. *J Cereb Blood Flow Metab* in press.

Scott D. B., Blanpied T. A., Swanson G. T., Zhang C. and Ehlers M. D. (2001) An NMDA receptor ER retention signal regulated by phosphorylation and alternative splicing. *J Neurosci* 21, 3063-3072.

Siesjo B. K. (1990) Calcium in the brain under physiological and pathological conditions. *Eur Neurol* 30 Suppl 2, 3-9; discussion 39-41.

Stephenson F. A. (2001) Subunit characterization of NMDA receptors. *Curr Drug Targets* 2, 233-239.

Szatkowski M. and Attwell D. (1994) Triggering and execution of neuronal death in brain ischaemia: two phases of glutamate release by different mechanisms. *Trends Neurosci* 17, 359-365.

Weltzin M., Zhao H. W., Drew K. L., and Bucci D. J. (2005) Arousal from Hibernation Alters Contextual Learning and Memory. *Behav Brain Res*, in press

Zhou F., Zhu X., Castellani R. J., Stimmelmayr R., Perry G., Smith M. A. and Drew K. L. (2001) Hibernation, a model of neuroprotection. *Am J Pathol* 158, 2145-2151.

Zucker R. S. (1999) Calcium- and activity-dependent synaptic plasticity. *Curr Opin Neurobiol* 9, 305-313.

Table 1. 1 Classification of glutamate receptors

Glutamate receptors	Subtype	Subunits
Ionotropic receptors	NMDAR	NR1
		NR2A-D
		NR3
	AMPAR	GluR1-4
	Kianate	GluR5-7
		KA1, 2
Metabotropic receptors	Group I	mGlu1
		mGlu5
	Group II	mGlu2
		mGlu3
	Group III	mGlu4
		mGlu6
		mGlu7
		mGlu8

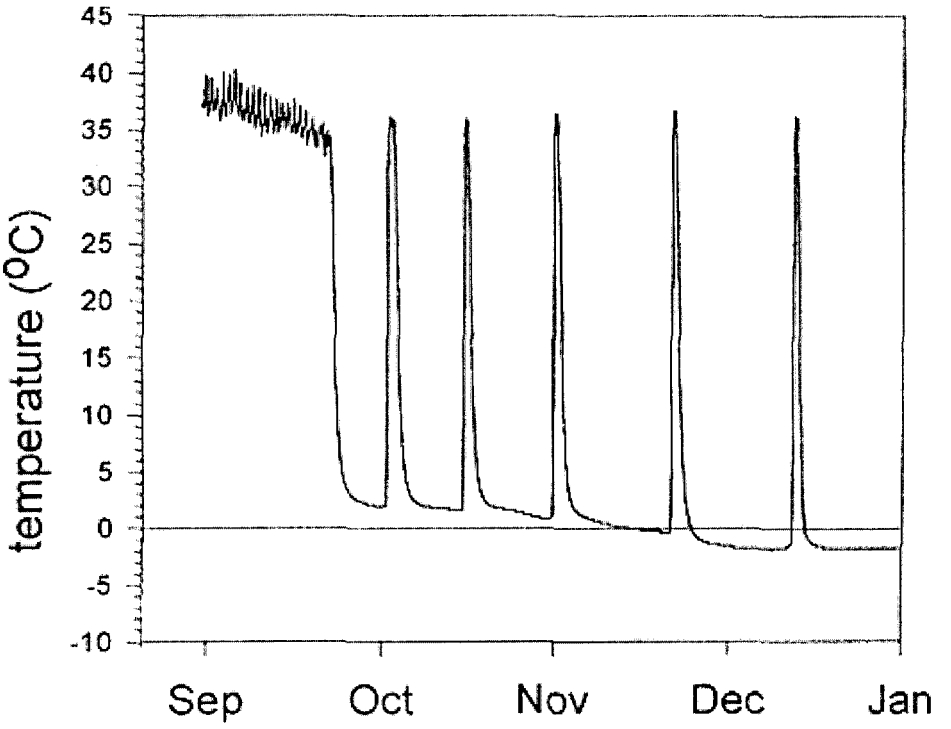

Fig. 1. 1. Body temperature changes in AGS over the course of the hibernation season. Data are shown for first half of the 7-mo-long hibernation season. Adapted from Boyer et al. (1998) with permission.

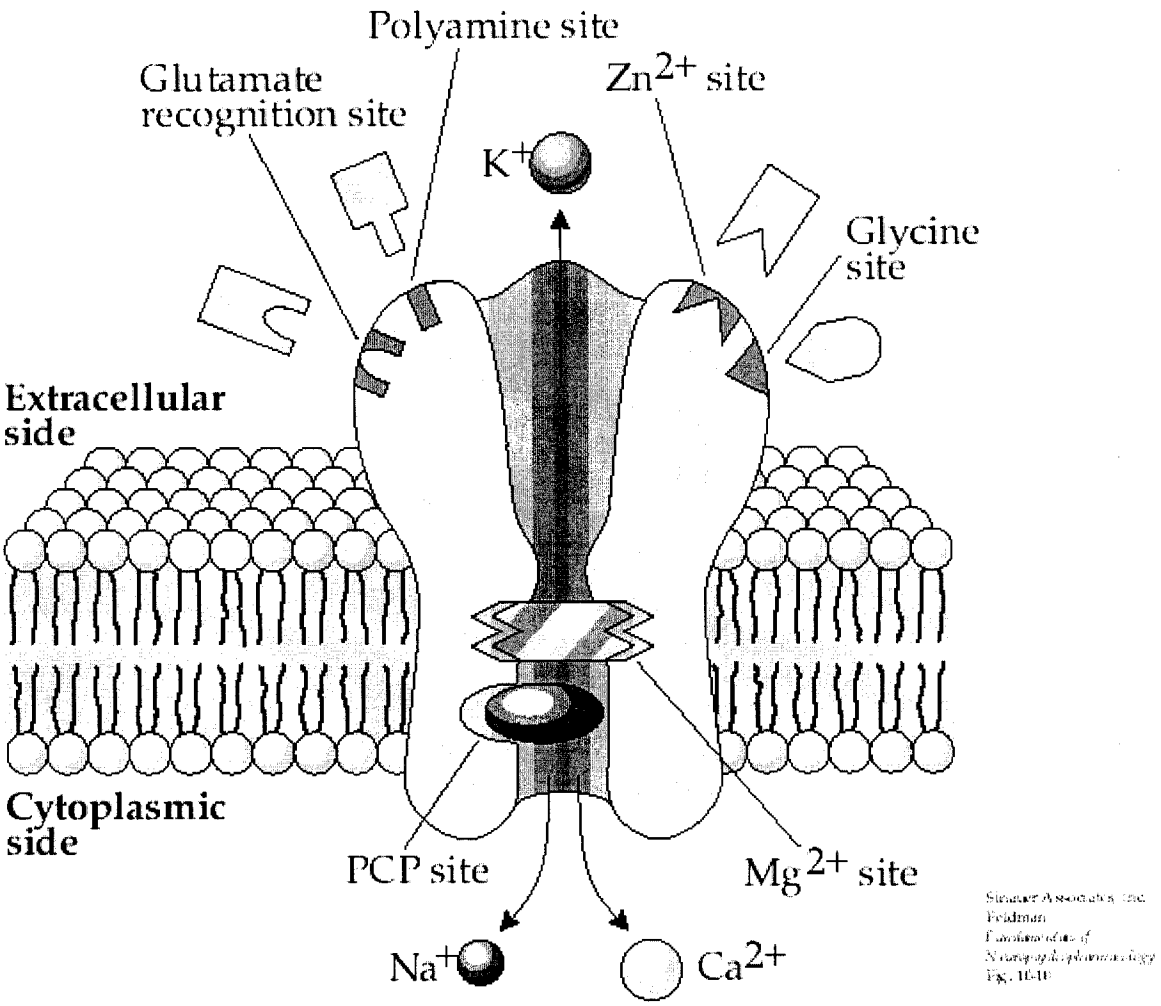

Fig. 1. 2. Schematic representation of the NMDAR complex. The NMDAR complex possesses a glutamate recognition site to which receptor agonists and competititve antagonists bind, as well as other binding sites for glycine, polyamines such as spermine, spermidine, phencyclidine (PCP) and the ions Mg^{2+} and Zn^{2+}. Channel opening permits an influx of Na^+ and Ca^{2+} ions, and an efflux of K^+ ions. From http://www.chemistry.emory.edu/justice/chem190j/EAAreceptors.htm

Chapter 2*

Distribution of NMDA Receptor Subunit NR1 in Arctic Ground Squirrel Central Nervous System

2. 1 Abstract

Hibernation is a natural model of neuroprotection and adult synaptic plasticity. NMDA receptors (NMDAR), which play key roles in synaptic plasticity and excitotoxicity, have not been characterized in hibernating animals. All NMDAR consist of at least one NMDAR1 (NR1) subunit, which is required for receptor function. Localization of NR1 reflects localization of the majority, if not all, NMDAR complexes. The purpose of this study, therefore, was to characterize the distribution of NR1 subunits in Arctic ground squirrels (AGS, *Spermophilus parryii*) central nervous system using immunohistochemistry. In addition, hippocampal neurons show morphological changes after arousal from hibernation. Hence, a subsequent aim was to assess one of these morphological changes, specifically cell somata size in NR1 stained sections in three hippocampal regions (CA1, CA3, and dentate gyrus). For the first time, we report the expression and distribution of NR1 in AGS, which was similar for hibernating AGS and euthermic AGS. Moreover, we show a significant decrease in size of hippocampal CA1 and dentate gyrus NR1-expressing neuronal somata during hibernation.

---

* This chapter was submitted to J Comp Neurol and authors are Zhao HW, Castillo MR, Christian SL, Bult-Ito A, and Drew KL.

2. 2 Introduction

Heterothermic mammals, i.e., mammals that hibernate, provide extreme examples of neuroprotection in both the hibernating and euthermic (non-hibernating) state (Frerichs and Hallenbeck, 1998; Zhou et al., 2001; Ma et al., 2005; Ross et al., in press; Dave et al., unpublished observation). These animals also show pronounced synaptic plasticity (Popov et al., 1992a; Popov and Bocharova, 1992b) and evidence of adult cognitive enhancement following arousal from hibernation (Mihailovic et al., 1968; Weltzin et al., in press). N-methyl-D-aspartate receptors (NMDAR) play essential roles in excitotoxicity, synaptic plasticity and learning and memory (Moriyoshi et al., 1991), yet no studies have begun to characterize NMDAR in heterothermic species.

NMDAR have three major subunits: NMDAR1 (NR1), NMDAR2A-D (NR2A-D), and NMDAR3 (NR3). Localization of NR1 reflects localization of the majority, if not all, NMDAR complexes (Forrest et al., 1994; Sakimura et al., 1995; Nakanishi, 1992). All functional NMDAR consist of at least one NR1 subunit in various combinations with two or more NR2A-D subunits, and sometimes include the NR3 subunit. NR1 is expressed throughout the brain and throughout all stages of development. The purpose of this study therefore was, to characterize the distribution of NR1 subunits in the central nervous system of Arctic ground squirrels (AGS, *Spermophilus parryii*) using a NR1 antibody that has been well characterized in rats and other species such as mouse, monkey, and human (Johnson et al., 1996; Bilak et al., 1995; Siegel et al., 1994; Huntley et al., 1994).

The hippocampus shows structural (Popov and Bocharova, 1992a; Popov et al., 1992b) and functional changes (Weltzin et al., in press) after arousal from hibernation. Popov et al. (1992b) report a decrease in volume of CA3 somata during hibernation in *Spermophilus undalatus*, an Arctic species closely related to AGS. In their study, the volume of neuronal cell bodies was measured in gallocyanin-stained paraffin sections. Gallocyanin is a nuclear stain, and, therefore, decreased volume could only be attributed to the nucleus and not to the entire cell body (Schulte et al., 1991). Other studies show changes in nuclear size, but not cell bodies in taste receptor cells during hibernation (Popov et al., 1999). The majority of NMDAR are expressed on the surface of neurons, especially in the synaptic plasma membrane (Monaghan and Cotman, 1985; Kharazia et al., 1996). Thus, we measured cell body size in NR1 stained sections in three hippocampal regions [CA1, CA3, and dentate gyrus (DG)]. Here, for the first time we report the distribution of NR1 in AGS using immunohistochemistry and show significant changes in the size of hippocampal CA1 and dentate gyrus neuronal somata during hibernation.

2. 3 Materials and methods

2. 3. 1 *Antibodies*

Mouse anti-NR1 monoclonal antibody (Cat# MAb363, Chemicon, Temecula, CA) was used for immunohistochemistry and subsequent semi-quantitative western blot analysis. This antibody recognizes a peptide (116 KD) corresponding to amino acids 660-811 of the NR1 subunit, which is located at the extracellular loop between the third and

fourth transmembrane regions. Mouse anti-β-actin monoclonal antibody (Cat# 5316, Sigma-Aldrich Corp. St. Louis, MO) was used as a loading control for western blotting. This antibody recognizes an epitope (42 kD) located on the C-terminal end of actin conserved in all actin isoforms.

2. 3. 2 *Animals*

The Institutional Animal Care and Use Committee of the University of Alaska Fairbanks approved all animal procedures. AGS were trapped on the northern slope of the Brooks Range, Alaska in July under permit from the Alaska Department of Fish and Game. AGS were screened for salmonella and quarantined for at least 14 days. All AGS were housed individually in cages at an ambient temperature (T_a) of approximately 18°C, fed approximately 40 g of Mazuri Rodent Chow per day, and kept on natural lighting for 64° latitude until they were moved to environmental chambers. In August, AGS were fed 10-15 sunflower seeds each day for two weeks before being moved to environmental chambers where they were housed at T_a of approximately 2°C, 4 hr: 20 hr light: dark, and fed rodent chow *ad libitum*.

Groups of AGS (hibernating AGS and euthermic AGS, n = 4 per group) were matched for age, sex, and body weight. At the time of tissue collection, hibernating AGS had experienced at least three bouts of torpor and were at least three days into their current bout. Respiratory rate was less than five breaths per minute, and wood shavings placed on an animal's back 24 hr previously remained undisturbed. Euthermic AGS had experienced at least two bouts of torpor. For the immunohistochemistry experiment,

euthermic AGS were naturally aroused in the cold chamber (T_a, 2°C). For the western blotting experiment, euthermic AGS were aroused by transferring to a warm room (T_a, 18°C) and tissue was collected approximately 24 hr later. Their respiration rate was more than 80 breaths per minute, body temperature was more than 35.5°C, and they quickly responded to touch.

2. 3. 3 *Immunohistochemistry*

Animals were anaesthetized with 5% halothane and maintained at 3% mixed with 100% oxygen, delivered at a flow rate of 1.5 L/min. Prior to perfusion, the descending aorta was clamped to achieve more efficient perfusion of the brain. AGS were perfused transcardially with saline for 5-10 min (600-800 ml) followed by 4% paraformaldehyde in 0.1 M phosphate buffer (pH 7.4) for 15-20 min (1000-2000 ml). Brains were quickly removed and post-fixed in 4% paraformaldehyde at 4°C overnight, and then cryoprotected in 30% sucrose until brains sank. Brains were rapidly frozen in isopentane at –30°C to –40°C, which was pre-cooled with dry ice or liquid N_2. Coronal sections were cut with a cryostat (Leica CM 1800) at 50 μm and stored in cyroprotectant (1% (w/v) polyvinylpyrrolidone, 30% sucrose, and 30% ethylene glycol in 0.1 M PBS) at –20°C until use.

All incubations were carried out with gentle agitation at room temperature unless otherwise stated. Sections were rinsed in PBS 6 times for 10 min each, and quenched with 0.5% H_2O_2 for 20 min. After rinsing for 30 min, sections were blocked with 5% normal goat serum in PBS for 2 hr and then were incubated overnight with anti-NR1

(1:1000). Sections were then washed in PBS 3 times for 10 min each and incubated with secondary antibody (biotinylated anti-mouse IgG, 1:200, Vector Laboratory, Burlingame, CA) for 30 min. The sections were washed with PBS and incubated in avidin-biotin-peroxidase (vectastain ABC kit, Vector Laboratory, Burlingame, CA) for 30 min, washed, and treated with 0.03% of 3′, 3-diaminobenzidine tetrahydrochloride (DAB, Sigma-Aldrich Corp.St. Louis, MO). After washing, the sections were mounted on slides and coversliped with Permount (Fisher, Pittsburgh, PA). PBS controls, in which either primary or secondary antibody was omitted and replaced by PBS, were run in every experiment under the same conditions. Images of immunostained brain slices were taken with a Zeiss Axioplan 2 imaging microscope (Zeiss, Germany). Subjective assessment of the level of staining was described using a relative scale from 0 to 4. The lowest level (0) indicates the level of staining seen in corresponding control sections and 4 indicates the level of densest staining.

The cell body area of pyramidal neurons in hippocampal CA1 and CA3 regions and granular cells in hippocampal dentate gyrus was compared in both hibernating AGS and euthermic AGS. For each region of interest, at least 30 or more neurons per animal within the dorsal hippocampus, corresponding to figures 32-34 of the rat Atlas (Paxinos and Watson, 1998), were measured by manually tracing around the perimeter of each cell body using Metamorph software 6.2 (Meridian Instrument Co., Kent, WA).

2. 3. 4 *Western blotting*

Because a difference in the total number of positive numbers or density of NR1-immunoreactivity could be influenced by cell size, we used western blotting to semi-quantitatively compare NR1 expression between hibernating and euthermic AGS. Animals (n = 4 per group) were anesthetized and brains were removed quickly after decapitation. Hippocampi were dissected, quickly frozen in liquid N_2, and stored at – 80°C.

Total protein lysate was prepared by homogenizing approximately 20-30 mg of hippocampal tissue in 200-300 µl (10 × volumes) of ice cold 1% NP-40 lysis buffer (50 mM Tris-HCl (pH 7.6), 0.02% sodium azide, 0.5% sodium deoxycholate, 0.1% SDS, 1% NP-40, 150 mM NaCl with protease/phosphatase inhibitors 1 mM phenylmethylsulfonyl fluoride, 1 mM sodium orthovanadate, 10 µg/ml leupeptin, 1 µg/ml aprotinin, and 1 µg/ml antipain) with a motor-driven polytron homogenizer for 30-40 seconds. Homogenates were left on ice for 40 min and then centrifuged at maximal speed for 10 minutes using a microcentrifuge. The supernatant was collected and termed total protein lysate.

Protein concentration was determined using the Bio-Rad protein assay kit (Bio-Rad, Hercules, CA). Twenty µg of protein was separated on 8% SDS-PAGE gels and then transferred to nitrocellulose membranes. After blocking with 5% milk in TBS (10 mM Tris-HCl (pH 7.5) and 150 mM NaCl) for 1 hr, the membranes were incubated with anti-NR1 (1:1000) in TBST (TBS, 0.1% Tween 20) with 1% bovine serum albumin overnight at 4°C with gentle agitation. The membranes were washed with TBST and

incubated with horseradish peroxidase-conjugated secondary antibody (anti-mouse IgG, 1:2000, Bio-Rad, Hercules, CA) for 1 hr. Immunoreactive bands were visualized using enhanced chemiluminescence (ECL, Perkin-Elmer, Boston, MA). Membranes were stripped by incubation with 10 mM Tris-HCl (pH 2), 150 mM NaCl for 30 min. Equal loading was then confirmed by reprobing with anti-actin (1:5000, Cat # 5316, Sigma-Aldrich Corp. St. Louis, MO) diluted in TBST with 1% bovine serum albumin. Scans of ECL exposures were analyzed using ImageQuant 5.2 software (Amersham Biosciences, Piscataway, NJ).

All data were analyzed using one-way ANOVA (Sigmastat Ver3.0, SYSSTAT Software Inc., Chicago, IL). Data were expressed as group means ± SEM. The criterion for statistical significance was $p<0.05$.

2. 4 Results

Controls: Specificity of anti-NR1 antibody (Fig. 2. 1a) and the secondary antibody in AGS brain slices was verified by replacing the primary antibody with PBS and by replacing the secondary antibody with PBS. Immunostaining was absent in these control sections.

Overall NR1 distribution: Immunoreactivity of anti-NR1 was widely distributed throughout the central nervous system in both euthermic AGS and hibernating AGS (see table 2. 1). No qualitative difference in NR1 distribution was noted between the two groups.

The densest staining with anti-NR1 antibody was found throughout the hippocampus. Staining was also dense in layers 2-3 and layer 5 of the cerebral cortex. Staining appeared to be moderate in the putamen and thalamus, and light to moderate in the hypothalamus. Immunostaining in other regions such as the olfactory bulb, cerebellum, and the brain stem was light, but some neurons and nuclei were moderately stained (Fig. 2. 1).

Immunostaining was described as neuronal staining and neuropilar staining. Neuronal staining indicates the staining of cell bodies without staining of the nucleus and major dendrites. Neuropilar staining includes the processes and unresolvable matrix between cells without tracing to specific cell bodies.

Olfactory bulb: Immunostaining of the main olfactory bulb (Fig. 2. 1b and Fig. 2. 2a) was very light in the glomerular layer (Gl) and internal plexiform layer (Ipl), and light in the external plexiform layer (EPI) and granular cell layer (Gro). Immunostaining of mitral cells (Mi) appeared to be denser than other areas. Some periglomerular cells (Pg) were stained very lightly in the edge between the glomerular layer and external plexiform layer of the olfactory bulb. Neuropilar staining of the olfactory bulb was light to moderate compared with other brain regions.

Cortex: Immunostaining of NR1 in the frontal association cortex (FrA), primary motor cortex (M1), and parietal association cortex (PtA) (Fig. 2. 2c, d, e) was surveyed. The overall laminar pattern of NR1 immunoreactivity was similar in most regions of the cerebral cortex. Immunostaining of NR1 was present in most layers. Neuropilar staining was light to moderate and homogeneous throughout the cortical layers. Neuronal staining

patterns in layers varied slightly with regions. Little or no staining was seen in the molecular layer (layer 1). The densest neuronal staining was found in the external granular layer (layer 2) and external pyramidal layer (layer 3). Since most immunostained small and middle sized pyramidal neurons in layer 2 and layer 3 were highly packed, the staining of layers 2-3 appeared to be noticeably denser than the other layers. In the frontal association cortex, neurons in layers 4-6 were stained lightly to moderately. The staining patterns of layers 4 to 6 in the primary motor cortex and parietal association cortex was similar. Neuronal staining in layer 4 was light. Large pyramidal neurons as well as their long vertically oriented dendrites in layer 5 were densely stained. Neuronal staining of the multiform layer (layer 6) was light to moderate.

Hippocampus: The NR1 antibody labeled almost all of the major fields of the hippocampus (Fig. 2. 1e, f and Fig. 2. 3a, b, c, d). Immunostaining of pyramidal neurons in CA1 and CA3 areas and granular neurons in dentate gryus was the densest. Staining of hilar polymorphic cells in the hilus of the dentate gyrus were moderate to dense. In the hippocapmus, neuronal staining was well defined on the plasma membrane. The dendrites of pyamidal neurons in CA1 and CA3 were clearly traced and intensely labeled. Neuropilar staining was light to moderate in dentate gyrus and CA1 including the stratum oriens (Or), stratum radiatum (Ra), stratum lacunosum-moleculare (LM), and stratum moleculare (Mo). Neuropilar staining was remarkably dense in the stratum lucidum of CA3 area in which apical dendrites of the CA3 pyramidal neurons are located.

Basal ganglia: The structure of the basal ganglia is slightly different in AGS compared with rats. In rats, the caudate nucleus and putamen are not separated by the

internal capsule. In contrast, the internal capsule clearly delineates the caudate nucleus and putamen in AGS. The overall neuropilar staining in the basal ganglia is light to moderate. Neuronal staining in putamen was moderate and slightly denser than in the caudate nucleus (Fig. 2. 1c and Fig. 2. 2b).

Thalamus and hypothalamus: Neuronal staining in the thalamus and hypothalamus varied with nuclei (Fig. 2. 1e). In the midline region of the thalamus (Fig. 2. 3 e, f), neuronal staining in the medial habenular nucleus (MHb) and posterior paraventricular nucleus of the thalamus (PVP) was moderate to dense. The central medial thalamic nucleus (CM) and reuniens thalamic nucleus (Re) were moderately stained and surrounded with light neuropilar staining. Both neuronal and neuropilar staining in the lateral habenular nucleus was light. Neuronal staining in the medial habenular nucleus (MHb) was moderate to dense. The ventral nuclear group (VP) and the posterior thalamus nuclear group (Po) were stained lightly to moderately. The most remarkable staining in the hypothalamus (Fig. 2. 1e and Fig. 2. 3g, h) was found in the arcuate nucleus (Arc) and median eminence (ME) where neuropilar staining was moderate to dense. Neuropilar staining in other areas of the hypothalamus was moderate but greater than in thalamus (Fig. 2. 1e). Light to moderate staining was found in the lateral hypothalamus (LH) and periventrical hypothalamic nucleus (Pe). At the base of the hypothalamus, the size of the optic tract (opt, Fig. 2. 1f) and optic chiasm (ox, Fig. 2. 3h) was considerably larger in AGS than in rats consistent with a well developed visual system in ground squirrels (Reme and Young, 1977).

Cerebellum: Overall, cerebellar cortex (Fig. 2. 4a) staining was light to moderate. Neuropilar staining in the molecular layer and granular layer was light. Some small stellate cells in the molecular layer were lightly stained, granular cells were uniformly stained and the cell membrane was not well defined. Purkinje cell dendritic branches were labeled lightly to moderately and could be traced in some cells. Staining of Purkinje cell bodies varied from light to moderate. Glial cells in white matter were lightly stained.

Brain stem and cervical spinal cord: Neuropilar staining in brain stem was light. Neuronal staining varied with nuclei. Large motor neurons in the hypoglossal nucleus (12) (Fig. 2. 4b, d) and neurons in the lateral vestibular nuclei (LVe, Fig. 2. 4c) were stained moderately. Light staining was found in the superior paraolivary nucleus (SPO), facial nucleus (7), lateral reticular nucleus (LRt), spinal trigeminal tract (sp5), and interpolar part of spinal 5 nucleus (Sp5I). In cervical spinal cord (Fig. 2. 4e), neuropilar staining was very light, and glia cells in the white matter (Fig. 2. 4f) were lightly stained. Staining of gray matter was relatively denser than that of white matter. Staining in laminae 1-3 and lamina 10 was light; staining in laminae 4-8 was very light to light. The staining of large motor neurons in lamina 9 was moderate (Fig. 2. 4g).

Smaller neurons in hibernating AGS: Distinct staining of the plasma membrane allowed for accurate tracing of cell bodies. The area of neurons in hippocampal sub-regions was measured and results are shown in table 2. 2. Neurons of CA1 and the dentate gyrus in hibernating AGS were 19% and 33% smaller than euthermic AGS,

respectively ($p<0.05$). The area of CA3 neurons was not different between these two groups.

NR1 expression in hippocampus: Expression of NR1 in the hippocampus evaluated semi-quantitatively using western blotting was similar between hibernating and euthermic AGS ($p>0.05$, Fig. 2. 5).

2. 5 Discussion

In the current study, we report that the cellular pattern of NR1 expression in AGS is widely distributed throughout the central nervous system. Hibernating AGS have similar NR1 expression patterns to euthermic AGS and the amount of NR1 protein in hippocampus does not differ between the two groups of animals. In contrast to NR1 expression, neuronal soma size decreases in CA1 and dentate gyrus during hibernation.

The overall staining pattern of NR1 in AGS was, for the most part, similar to that in rats and other species including mouse, monkey, human, rabbit, quail, platyfish, rehesus macaque, and turtle (Monaghan and Cotman, 1985; Paquet and Smith, 2000; Kuppenbender et al., 1999; Petralia et al., 1994a; Johnson et al., 1996; Petralia et al., 1994b; Chatha, 2000; Siegel et al., 1994; Siegel et al., 1995; Bilak et al., 1995; Watanabe et al., 1998; Huntley et al., 1994; Bonnot et al., 1996; Cornil et al., 2000; Flynn et al., 1997; Garyfallou et al., 1996; Keifer and Carr, 2000; Paquet et al., 1997). Description of NR1 expression and distribution as well as changes in neuronal size is a necessary first step toward investigating the role of NMDAR in neuroprotection and plasticity in AGS.

Most brain regions including the olfactory bulb, cerebral cortex, hippocampus, and the striatum showed immunostaining similar to NR1 distribution in rats (Monaghan and Cotman, 1985; Petralia et al., 1994b; Huntly et al., 1994; Bilak et al., 1995; Trombley and Westbrook, 1990). The densest staining was found in the hippocampus and cerebral cortex of AGS, consistent with RNA blot analysis, *in situ* hybridization, autoradiography, and immunohistochemistry in rats (Moriyoshi et al., 1991; Monahan and Cotman, 1985; Petralia et al., 1994b). Slight differences in the relative level of staining in some brain regions between AGS and rats were observed. For example, we found equally dense staining in CA1, CA3, dentate gyrus, and hilus regions in AGS hippocampus while, in rats, others have found denser staining in CA1 and CA3 (Petralia et al., 1994b) or in CA1, and the hilus region of the dentate gyrus (Johnson et al., 1996). These disparities may be due to strain or species differences or to a difference in antibodies used. Different antibodies produce different NR1 staining patterns (Johnson et al., 1996). In rats, Petralia et al. (1994b) found the densest staining in CA1 and CA3 and moderate staining in DG using an NR1 antibody raised in rabbit that recognizes a peptide corresponding to the C terminal residue 909-938. When Johnson and his colleagues used anti-rabbit NR1-C1 that recognizes polypeptide residue 864-900, another epitope on the C terminus of the NR1 subunit, they reported the densest labeling in CA1 and the hilus of the dentate gyrus. Therefore, differences in antibodies used might explain differences in expression patterns among these studies and our results.

In heterothermic animals, neurons in the hibernating state show many changes in structure (Jacobs, 1996; Reme and Young, 1977, Azzam et al., 2000) and these

structural changes may be related to energy conservation and or hypofunction. For instance, purkinje cell nucleoli of cerebellum are smaller in hibernating hedgehogs compared to euthermic hedgehogs (Giacometti et al., 1989). Cone cells in the retina of hibernating 13-lined ground squirrel undergo many changes including reduction in the diameters of the membranous discs as well as the size and number of mitochondria (Reme and Young, 1977). Future studies are warranted to address the mechanism and functional significance of decreased neuronal cell size in hibernating AGS.

Other cells outside of the central nervous system also show differences. Malatesta et al. (2002) found that the total cell and cytoplasm area of hepatocytes from hibernating dormice (*Muscardinus avellanarius*) was significantly reduced compared with those from euthermic dormice. High energy phosphates are maintained in hibernation, decreases in actin-ATP hydrolysis and turnover may contribute to energy conservation and changes in cell size (Lust et al., 1989; Storey, 1997). Malatesta et al. (2002) suggested that the change in cell structure was related to marked reduction in hepatocyte function found in the hibernating dormouse. Whether similar mechanisms are involved in neuronal cell size changes remains to be elucidated.

Our results show that the area of CA3 neuronal cell bodies in hibernating AGS is similar to that in euthermic AGS. This is in contrast to Popov's results (1992b). Popov et al. (1992b) using a nuclear stain reported that the soma volume of CA3 pyramidal neurons was smaller in hibernating ground squirrels than those in euthermic ground squirrels (*Spermophilus undalatus*). Because decreased volume reported by Popov et al (1992b) could only be attributed to the nucleus, discrepancies between these two studies

may result from differential modulation of the cytoskeleton that maintains the structure of the nucleus and the plasma membrane. Alternatively, the level of the hippocampus that was evaluated may have differed between the two studies and account for the discrepant results.

Interestingly, similar expression of NR1 in hibernating AGS and euthermic AGS hippocampus suggests that NR1 expression does not decrease with cell size. However, the tolerance of oxygen nutrient deprivation and NMDA observed in the hippocampal slices from hibernating animals suggests that the modulation of NMDAR is involved in the neuroprotection observed in hibernating animals (Frerichs and Hallenbeck, 1998; Ross et al., in press). Therefore, no difference in NR1 expression suggests that NMDAR function may be altered through other mechanisms in hibernating AGS, such as phosphorylation or internalization.

In summary, we report expression and distribution of NR1 in AGS brain that is independent of hibernating state and similar to other species. In addition, CA1 and dentate gyrus neuronal cell bodies are significantly smaller in hibernating AGS.

2. 6 Acknowledgements

This work was supported by Alaskan Basic Neuroscience Program (NIH U54-NS 41069 funded by NINDS, NIMH, NCRR, and NCMHD) and Alaska EPSCoR (ESP-0092040). Authors also thank Dr. Lique Coolen for critical review of the manuscript, and other helpful comments.

2. 7 Literature cited

Azzam N. A., Hallenbeck J. M. and Kachar B. (2000) Membrane changes during hibernation. *Nature* 407, 317-318.

Bilak S. R., Bilak M. M. and Morest D. K. (1995) NMDA receptor expression in the mouse cerebellar cortex. *Synapse* 20, 257-268.

Bonnot A., Corio M., Tramu G. and Viala D. (1996) Immunocytochemical distribution of ionotropic glutamate receptor subunits in the spinal cord of the rabbit. *J Chem Neuroanat* 11, 267-278.

Chatha B. T., Bernard V., Streit P. and Bolam J. P. (2000) Synaptic localization of ionotropic glutamate receptors in the rat substantia nigra. *Neuroscience* 101, 1037-1051.

Cornil C., Foidart A., Minet A. and Balthazart J. (2000) Immunocytochemical localization of ionotropic glutamate receptors subunits in the adult quail forebrain. *J Comp Neurol* 428, 577-608.

Dave K. R., Prado R., Raval A. P., Drew K. L. and Perez-Pinzon M. A. (2005) The arctic ground squirrel brain resists cardiac arrest during euthermia. Submitted to *Stroke*

Flynn K. M., Schreibman M. P. and Magliulo-Cepriano L. (1997) Developmental changes in NMDA receptor expression in the platyfish brain. *Brain Res* 771, 142-146.

Forrest D., Yuzaki M., Soares H. D., Ng L., Luk D. C., Sheng M., Stewart C. L., Morgan J. I., Connor J. A. and Curran T. (1994) Targeted disruption of NMDA receptor 1 gene abolishes NMDA response and results in neonatal death. *Neuron* 13, 325-338.

Frerichs K. U. and Hallenbeck J. M. (1998) Hibernation in ground squirrels induces state and species-specific tolerance to hypoxia and aglycemia: an *in vitro* study in hippocampal slices. *J Cereb Blood Flow Metab* 18, 168-175.

Garyfallou V. T., Kohama S. G. and Urbanski H. F. (1996) Distribution of NMDA and AMPA receptors in the cerebellar cortex of rhesus macaques. *Brain Res* 716, 22-28.

Giacometti S., Scherini E. and Bernocchi G. (1989) Seasonal changes in the nucleoli of Purkinje cells of the hedgehog cerebellum. *Brain Res* 488, 365-368.

Huntley G. W., Vickers J. C., Janssen W., Brose N., Heinemann S. F. and Morrison J. H. (1994) Distribution and synaptic localization of immunocytochemically identified NMDA receptor subunit proteins in sensory-motor and visual cortices of monkey and human. *J Neurosci* 14, 3603-3619.

Jacobs L. F. (1996) The economy of winter: phenotypic plasticity in behavior and brain structure. *Biol Bull* 191, 92-100.

Johnson R. R., Jiang X. and Burkhalter A. (1996) Regional and laminar differences in synaptic localization of NMDA receptor subunit NR1 splice variants in rat visual cortex and hippocampus. *J Comp Neurol* 368, 335-355.

Keifer J. and Carr M. T. (2000) Immunocytochemical localization of glutamate receptor subunits in the brain stem and cerebellum of the turtle Chrysemys picta. *J Comp Neurol* 427, 455-468.

Kharazia V. N., Phend K. D., Rustioni A. and Weinberg R. J. (1996) EM colocalization of AMPA and NMDA receptor subunits at synapses in rat cerebral cortex. *Neurosci Lett* 210, 37-40.

Kuppenbender K. D., Albers D. S., Iadarola M. J., Landwehrmeyer G. B. and Standaert D. G. (1999) Localization of alternatively spliced NMDAR1 glutamate receptor isoforms in rat striatal neurons. *J Comp Neurol* 415, 204-217.

Lust W. D., Wheaton A. B., Feussner G. and Passonneau J. (1989) Metabolism in the hamster brain during hibernation and arousal. *Brain Res* 489, 12-20.

Ma Y. L., Zhu X., Rivera P. M., Toien O., Barnes B. M., Lamanna J. C., Smith M. A. and Drew K. L. (2005) Absence of Cellular Stress in Brain Following Hypoxia Induced by Arousal from Hibernation in Arctic Ground Squirrels. *Am J Physiol Regul Integr Comp Physiol.*

Malatesta M., Zancanaro C., Baldelli B. and Gazzanelli G. (2002) Quantitative ultrastructural changes of hepatocyte constituents in euthermic, hibernating and arousing dormice (Muscardinus avellanarius). *Tissue Cell* 34, 397-405.

Mihailovic L., Petrovic-Minic B., Protic S. and Divac I. (1968) Effects of hibernation on learning and retention. *Nature* 218, 191-192.

Monaghan D. T. and Cotman C. W. (1985) Distribution of N-methyl-D-aspartate-sensitive L-[3H]glutamate-binding sites in rat brain. *J Neurosci* 5, 2909-2919.

Moriyoshi K., Masu M., Ishii T., Shigemoto R., Mizuno N. and Nakanishi S. (1991) Molecular cloning and characterization of the rat NMDA receptor. *Nature* 354, 31-37.

Nakanishi S. (1992) Molecular diversity of glutamate receptors and implications for brain function. *Science* 258, 597-603.

Paquet M., Tremblay M., Soghomonian J. J. and Smith Y. (1997) AMPA and NMDA glutamate receptor subunits in midbrain dopaminergic neurons in the squirrel monkey: an immunohistochemical and in situ hybridization study. *J Neurosci* 17, 1377-1396.

Paquet M. and Smith Y. (2000) Presynaptic NMDA receptor subunit immunoreactivity in GABAergic terminals in rat brain. *J Comp Neurol* 423, 330-347.

Paxinos G and Watson C. (1998) The rat brain in stereotaxic coordinates, 4th ed. San Diego: *Academics*

Petralia R. S., Wang Y. X. and Wenthold R. J. (1994a) The NMDA receptor subunits NR2A and NR2B show histological and ultrastructural localization patterns similar to those of NR1. *J Neurosci* 14, 6102-6120.

Petralia R. S., Yokotani N. and Wenthold R. J. (1994b) Light and electron microscope distribution of the NMDA receptor subunit NMDAR1 in the rat nervous system using a selective anti-peptide antibody. *J Neurosci* 14, 667-696.

Popov V. I. and Bocharova L. S. (1992a) Hibernation-induced structural changes in synaptic contacts between mossy fibres and hippocampal pyramidal neurons. *Neuroscience* 48, 53-62.

Popov V. I., Bocharova L. S. and Bragin A. G. (1992b) Repeated changes of dendritic morphology in the hippocampus of ground squirrels in the course of hibernation. *Neuroscience* 48, 45-51.

Popov V. I., Ignat'ev D. A. and Lindemann B. (1999) Ultrastructure of taste receptor cells in active and hibernating ground squirrels. *J Electron Microsc* (Tokyo) 48, 957-969.

Reme C. E. and Young R. W. (1977) The effects of hibernation on cone visual cells in the ground squirrel. *Invest Ophthalmol Vis Sci* 16, 815-840.

Ross A. P., Christian S. L., Zhao H. W. and Drew K. L. (2005) Persistent tolerance to oxygen and nutrient deprivation and N-methyl-D-aspartate in cultured hippocampal slices from hibernating Arctic ground squirrel. *J Cereb Blood Flow Metab* in press.

Sakimura K., Kutsuwada T., Ito I., Manabe T., Takayama C., Kushiya E., Yagi T., Aizawa S., Inoue Y., Sugiyama H. (1995) Reduced hippocampal LTP and spatial learning in mice lacking NMDA receptor epsilon 1 subunit. *Nature* 373, 151-155.

Schulte E. K., Lyon H. and Prento P. (1991) Gallocyanin chromalum as a nuclear stain in cytology. I. A cytophotometric comparison of the Husain-Watts Gallocyanin chromalum staining protocol with the Feulgen procedure. *Histochem J* 23, 241-245.

Siegel S. J., Brose N., Janssen W. G., Gasic G. P., Jahn R., Heinemann S. F. and Morrison J. H. (1994) Regional, cellular, and ultrastructural distribution of N-methyl-D-aspartate receptor subunit 1 in monkey hippocampus. *Proc Natl Acad Sci U S A* 91, 564-568.

Siegel S. J., Janssen W. G., Tullai J. W., Rogers S. W., Moran T., Heinemann S. F. and Morrison J. H. (1995) Distribution of the excitatory amino acid receptor subunits GluR2(4) in monkey hippocampus and colocalization with subunits GluR5-7 and NMDAR1. *J Neurosci* 15, 2707-2719.

Storey K. B. (1997) Metabolic regulation in mammalian hibernation: enzyme and protein adaptations. *Comp Biochem Physiol A Physiol* 118, 1115-1124.

Trombley P. Q. and Westbrook G. L. (1990) Excitatory synaptic transmission in cultures of rat olfactory bulb. *J Neurophysiol* 64, 598-606.

Watanabe M., Fukaya M., Sakimura K., Manabe T., Mishina M. and Inoue Y. (1998) Selective scarcity of NMDA receptor channel subunits in the stratum lucidum (mossy fibre-recipient layer) of the mouse hippocampal CA3 subfield. *Eur J Neurosci* 10, 478-487.

Weltzin M., Zhao H. W., Drew K. L., and Bucci D. J. (2005) Arousal from Hibernation Alters Contextual Learning and Memory. *Behav Brain Res*, in press

Zhou F., Zhu X., Castellani R. J., Stimmelmayr R., Perry G., Smith M. A. and Drew K. L. (2001) Hibernation, a model of neuroprotection. *Am J Pathol* 158, 2145-2151.

Table 2. 1 NR1 expression in AGS brain. *

Brain regions	Subjective assessment of level of staining
Olfactory region	
Anterior olfactory nucleus (AO)	2
Main olfactory bulb	
glomerular layer of olfactory bulb (GI)	1
periglomerular cell (Pg)	1
external plexiform layer olfactory bulb (EPI)	1.5
mitral cell layer of olfactory bulb (Mi)	2
internal plexiform layer olfactory bulb (Ipl)	1
granular cell layer of olfactory bulb (Gro)	1-1.5
Cortex	
Piriform cortex (pir)	3.5
Frontal association cortex (FrA) and Prelimbic cortex (PrL)	
Layer 1	0-0.5
Layer 2-3	2.5
Layer 4-6	2
Parietal association cortex (PtA) and Primary motor cortex (M1)	
Layer 1	0-0.5
Layer 2-3	3.5
Layer 4	2-2.5
Layer 5	3-3.5
Layer 6	2.5-3
Hippocampus	
CA1	
stratum oriens (Or)	1-1.5
Pyramidal layer (Py)	3.5-4
Stratum radiatum (Ra)	2.5
Stratum lacunosum-moleculare (LM)	1.5
CA3	
stratum oriens (Or)	1-1.5
Pyramidal layer (Py)	3-3.5
Stratum lucidum (Lu)	3
Dentate gyrus	
Molecular layer (Mo)	1.5
Granular layer (Gr)	3.5-4
Polymorph layer (hilus)	3-3.5
Amygdala	
Posterolateral cortical amygdale nucleus (PLCo)	2.5
Posteromeidal cortical amygdale nucleus (PMCo)	2.5
Dorsal endopiriform nucleus (Den)	1.5
Lateral amygdaloid nucleus (La)	2.5-3
Basolateral amygaloid nucleus (BL)	3

Table 2. 1 NR1 expression in AGS brain continued.

Septum	
Medial septal nucleus (MS)	2
Lateal septal nucleus, dorsal (LSD)	1
Lateal septal nucleus, intermediate (LSI)	1
Nucleus of horizontal limb diagonal band (HDB)	2
Nucleus of vertical limb diagonal band (VDB)	2
Basal ganglia	
Caudate nucleus	2-2.5
putamen	3
Nucleus accumbens core (Acbc)	2
Lateral global pallidum (LGP)	2
Ventral pallidum (VP)	2
Thalamus	
Lateral habenular nucleus (LHb)	2
Medial habenular nucleus (MHb)	3.5
Stria medullairs of thalamus (sm)	0-0.5
Paraventricular thalamic nucleus, posterior (PVP),	3-3.5
Intermediodorsal thalamic nucleus (IMD),	2.5-3
Centeral medial thalamic nucleus (CM),	3
Reuniens thalamic nucleus (Re)	3
Laterodorsal thalamic nucleus (LDV)	2.5-3
Ventral thalamic nuclear group (Vl, VM)	2.5-3
Ventral posterior thalamic neulear group (VPM, VPL)	2.5-3
Posterior thalamic nuclear group (Po)	2.5-3
Hypothalamus	
Lateral hypothalamic area (LH),	1.5
Magnocellular nucleus of lateral hypothamus	2.5
Dorsomedial nucleus, dorsal (DMD)	2
Perifornical nucleus (PeF)	2
Periventrical hypothalamic nucleus (Pe), neuropilar	1.5
Ventromed nucleus (VMH)	
Dorsomed part	2.5-3
Ventrolat part	2
Arcuate nucleus, medial part (ArcM)	3.5
Medial eminence (ME)	3.5
Suprachiasmatic nucleus (SCN)	1
Lateral preoptic area (LPO)	0.5-1
Supraopic nucleus (SO)	1
Midbrain	
Superficial gray layer of superior colliculus (SuG)	2
Optic nuclear layer of superior colliculus (OP)	1
Optic tract	0
Medial genic nucleus (MG)	1.5
Substantia nigra (SNR)	1.5
Commissural of superior colliculus (CSC)	0.5

Table 2. 1 NR1 expression in AGS brain continued.

Cerebral peduncle (CP)	0.5
Cerebellum	
Cerebellar cortex	
Molecular layer	2
Stellate cells	1.5
Granular layer	2
Purkinje cell body	2.5
Purkinje cell dendrities	2-2.5
Golgi cell	1.5-2
White matter	0-0.5
Glia	0.5
Brain stem	
Nucleus of the solitary trat, Parvicellular part (SolPC)	3-3.5
Nucleus of the solitary tract, medial part (SolM)	2
Subpostrema dorsal (SubPD)	3.5
Hypoglossal (12)	2.5-3
Lateral reticular nucleus (LRt)	2
Lateral recticular nucleus, parvicell (LRtPC)	1.5-2
Superior paraolivary nucleus (SPO)	1.5
Medial vestibular nuclei, magnocellular part (MVeMC)	2.5
Facial nucleus (7)	2
Inferior olive (IO)	2
Dorsal motor nucleus of vagus (10)	2
Spinal trigeminal tract (sp5)	0.5-1
Spinal 5 nucleus (Sp5C, Sp5O)	1-1.5
Cervical Spinal cord	
Lateral cervical nucleus (Latc)	1.5
Central cervical nucleus (CeCv)	2
Intermediomedial cell column (IMM)	1.5
Laminae I-III	2
Laminae IV-VIII	1.5
Motor neurons of laminae IX	2.5
Laminae X	1.5

* Note: Level of staining was described in the relative scale from 0 to 4, in which 0 indicates the level seen in corresponding control sections and 4 indicates the densest staining.

Table 2. 2 Comparison of neuronal soma area in AGS hippocampal subfields.

Subfields	Area of neurons (μm^2)	
	Hibernating AGS	Euthermic AGS
CA1	120 ± 6.7	167 ± 6.9 *
CA3	198.2 ± 8.8	204 ± 7.6
Dentate gyrus	49 ± 0.5	71 ± 2.4 *

* $p < 0.05$, n = 4 per group

Fig. 2. 1. Immunolabeling of NR1 in coronal sections of AGS brain from forebrain to cerebellum: a) Control section at the same level as the NR1 stained section show in of fig. 2. 1c. b -f) Olfactory bulb to cerebellum. opt, optic tract; ic, internal capsule; csc, commissural of the superior colliculus; SuG, superficial gray layer of the superior colliculus; Op, optic nerve layer of the superior colliculus; MG, medial geniculate nucleus; SNR, substantia nigra, reticular part; cp, cerebral peduncle, basal part. Scale bar in fig. 2. 1b, 100 μm, in others, 2.5 mm. Frames in fig. 2. 1e indicate the areas where neuronal soma size was measured.

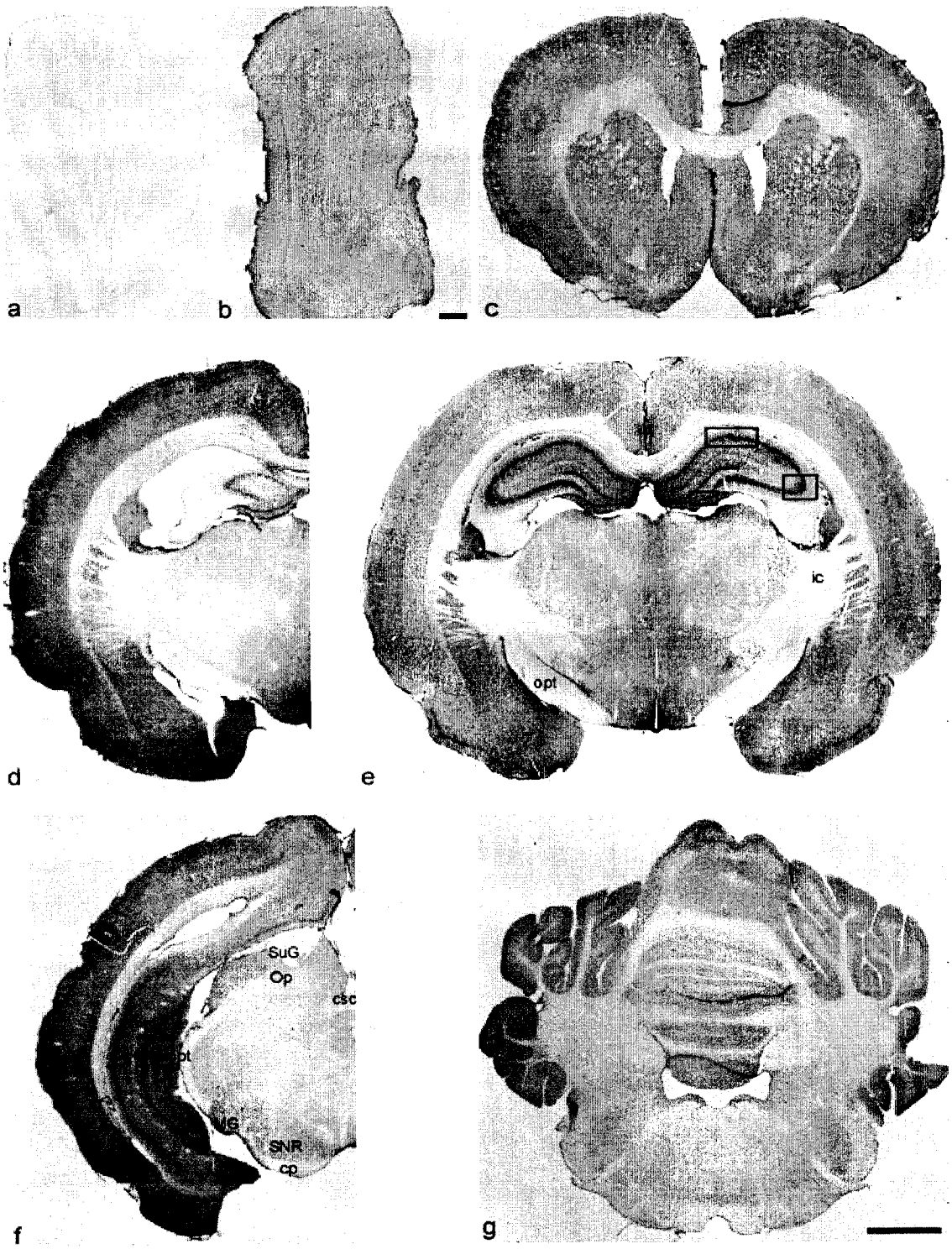

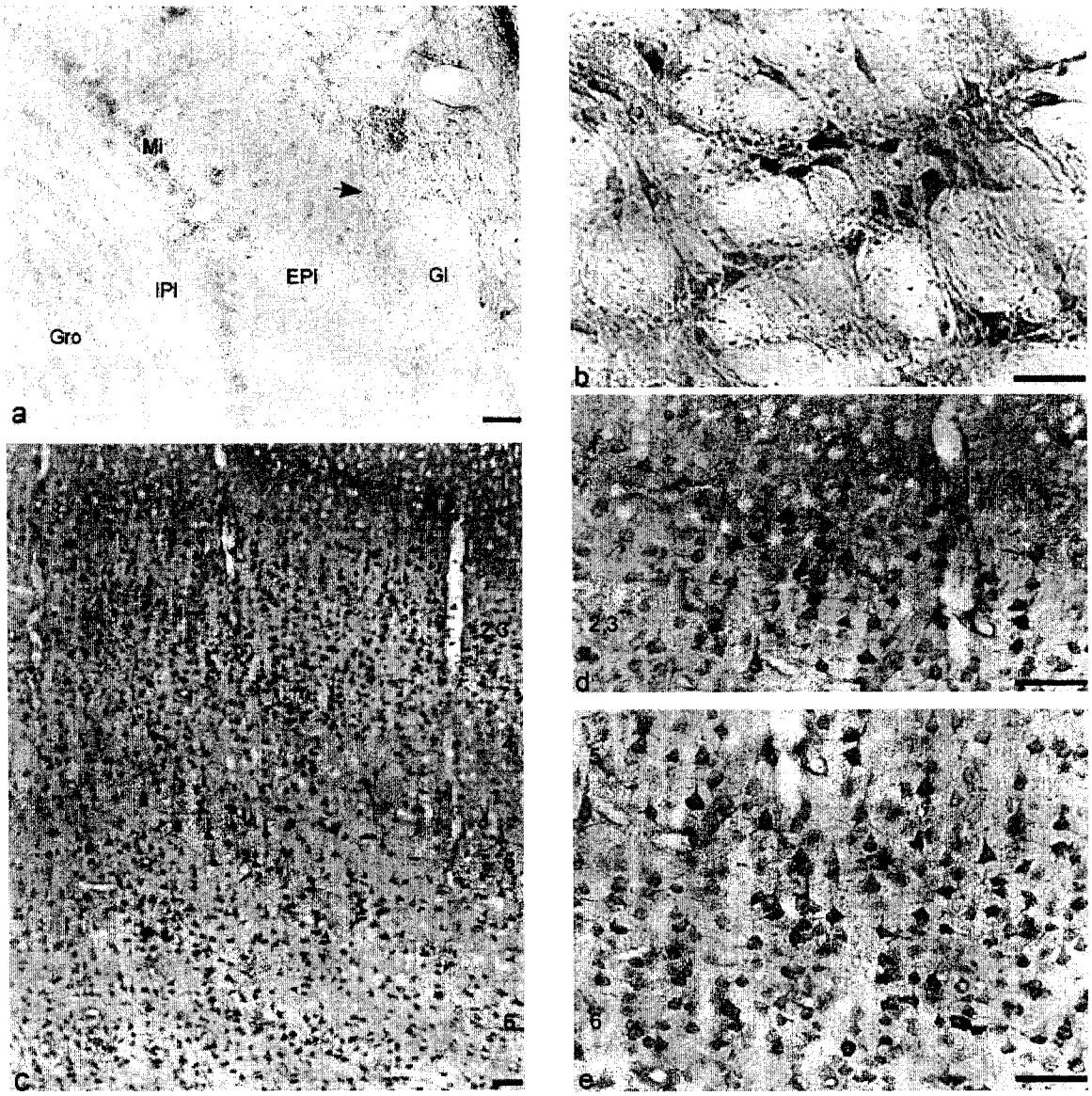

Fig. 2. 2. Olfactory bulb, putamen, and cerebral cortex: a) Main olfactory bulb, b) Putamen, c) Low power of cortex, d) Cortex layers 1-3, e) Cortex layers 5-6. GI, glomerular layer of olfactory bulb; EPI, external plexiform layer olfactory bulb; Mi, mitral cell layer of olfactory bulb; IPl, internal plexiform layer olfactory bulb; Gro, granular cell layer of olfactory bulb. Arrow indicates a periglomerular cell, Numbers in fig. 2. 2c, d, e indicate the layers of cortex. Scale bar, 50μm.

Fig. 2. 3. Hippocampus, thalamus, and hypothalamus: a) Low power of hippocampus, b) CA1, c) CA3, d) Dentate gyrus and hilus, e-f) Thalamus, g-h) Hypothalamus. Or, stratum oriens; Py, stratum pyramidale; Ra, stratum radiatum; LM, stratum lacunosum-moleculare; Mo, stratum moleculare; Gr, stratum granulare. Arrowheads indicate the stratum lucidum of CA3 region. Hi, hilus of dentate gyrus. MHb, medial habenular nucleus; sm, stria medullaris of the thalamus; PVP, paraventricular thalamus nucleus, posterior part; IMD, intermediodorsal thalamic area; CM, centeral medial thalamus nucleus; Re, reuniens thalamus nucleus; Pe, periventricular hypothalamus nucleus; ArcM, medial part of arcuate nucleus; ME, median eminence; LPO, lateral preoptic area; f, fornix; ox, optic chiasm. Arrowheads in fig. 2. 3a indicate the stratum lucidum of the CA3 region; Scale bar in fig. 2. 3a, 500 μm; and in fig. 2. 3b-h, 50 μm.

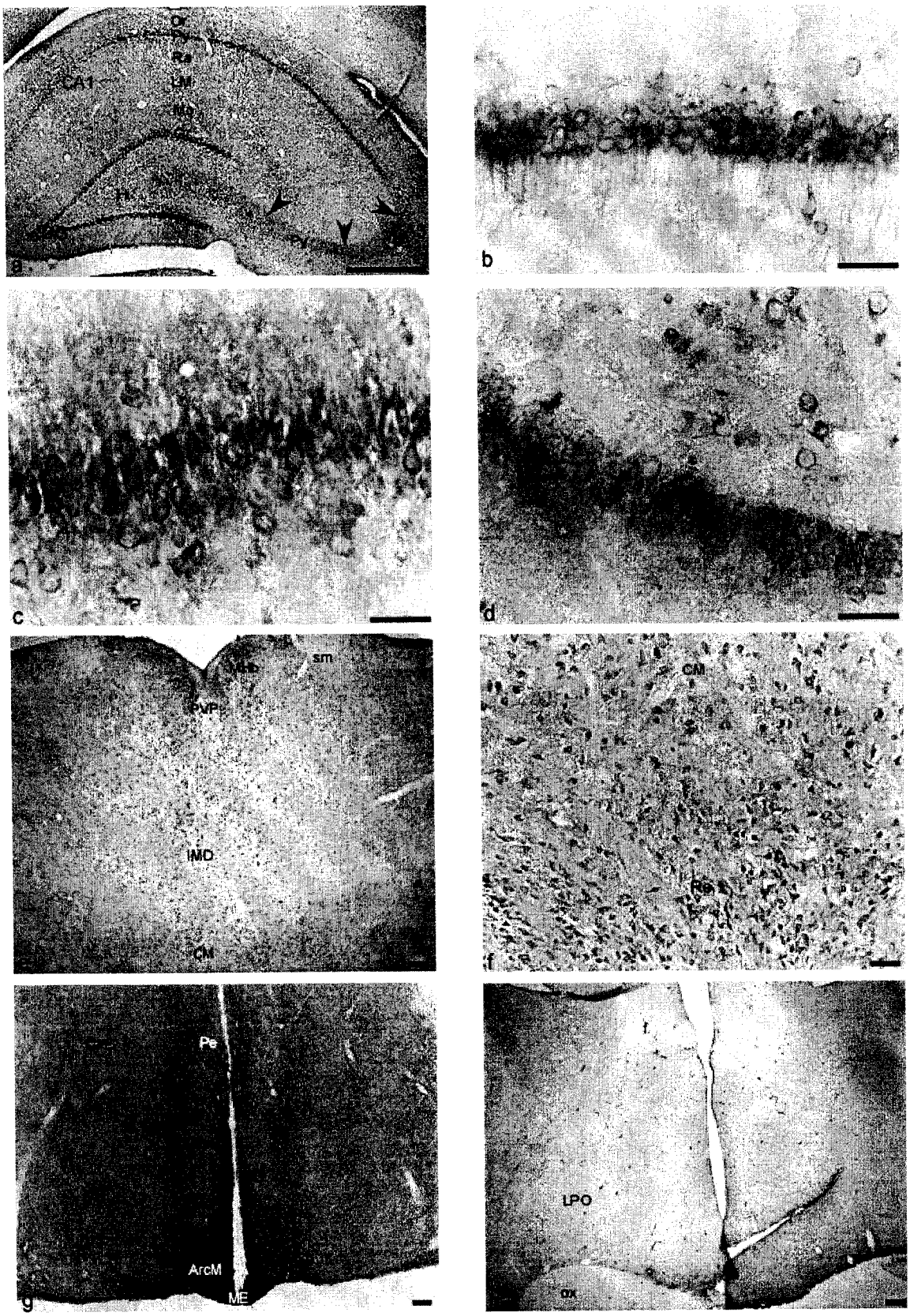

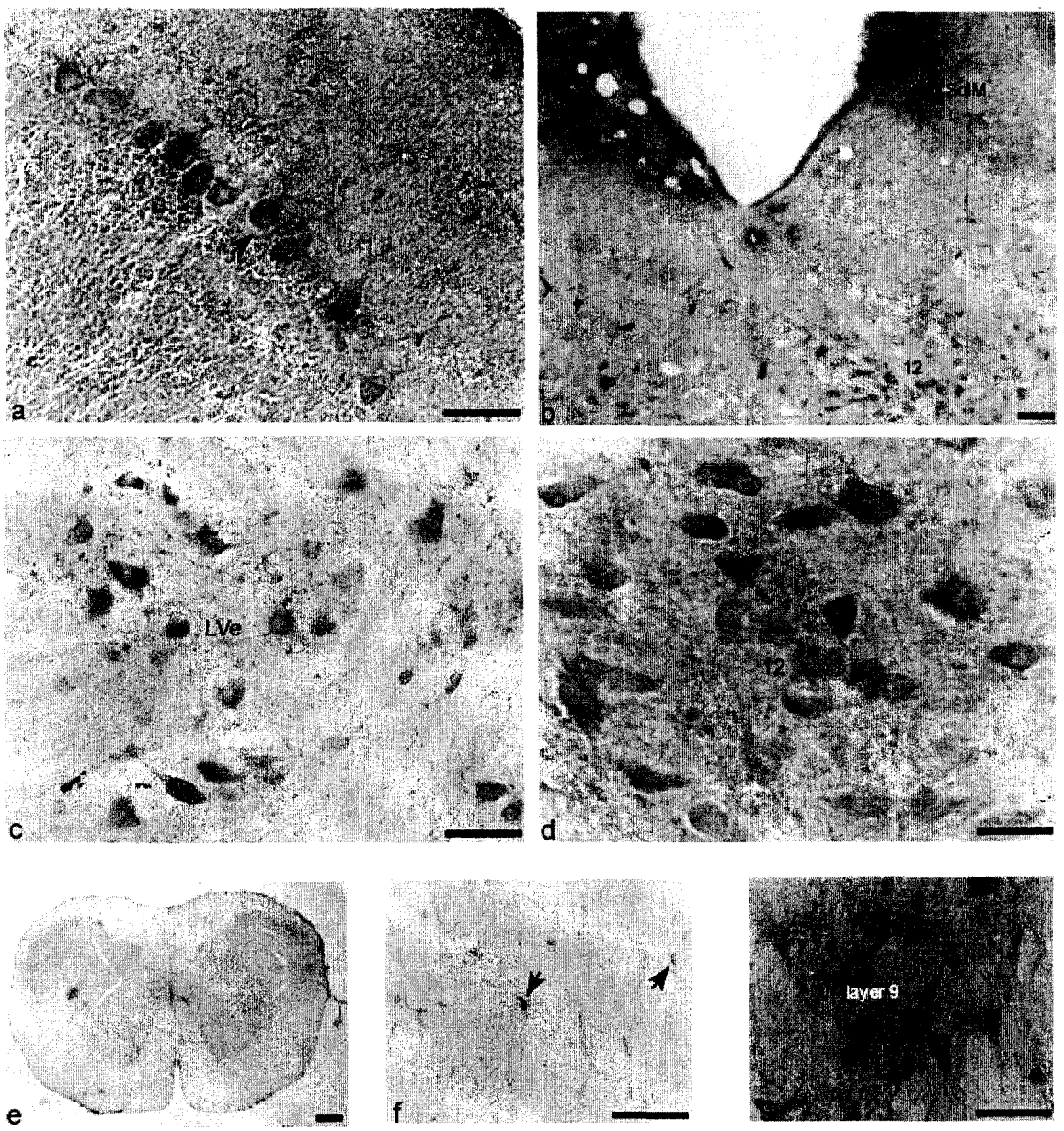

Fig. 2. 4. Cerebellum, brain stem, and cervical spinal cord. a) Cerebellar cortex, arrow indicates a Purkinje cell with two dendritic branches, b) brain stem, Nucleus of solitary tract, medial part. 12 indicates hypoglossal nucleus, also seen in d), c) Lateral vestibular nucleus, LVe, e) Spinal cord in lower power, f) glia cell in the white matter of spinal cord (C2); g) layer 9 of cervical spinal cord. Scale bar in e) is 200 μm, in others, 50 μm.

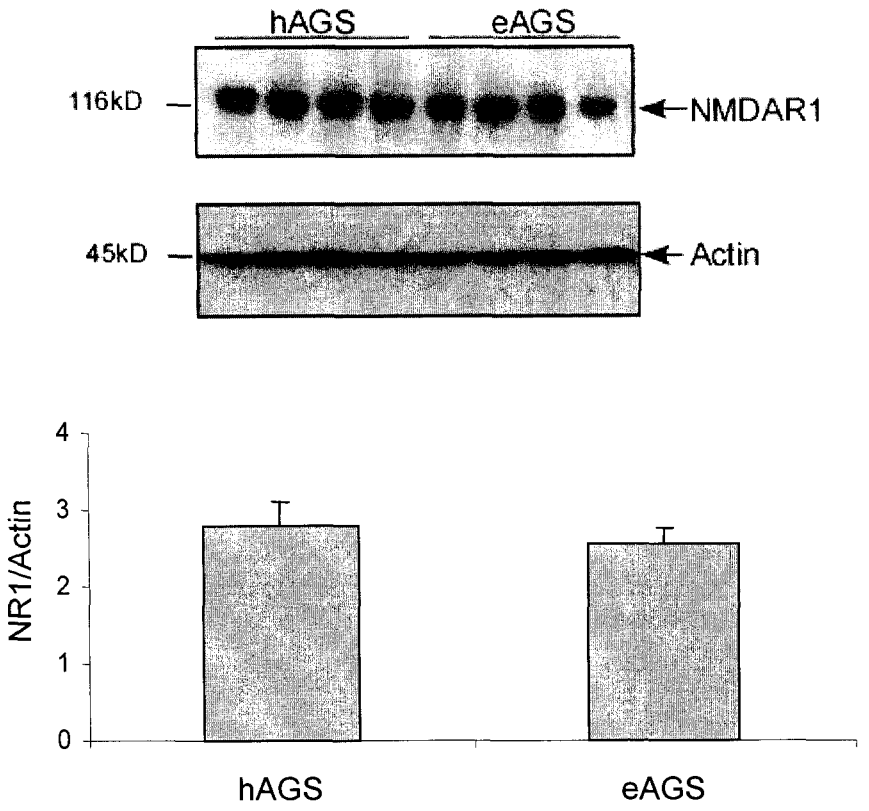

Fig. 2. 5. NR1 abundance comparison. NR1 abundance in total protein lysates prepared from hibernating AGS and euthermic AGS was similar ($p>0.05$). hAGS indicates hibernating AGS, eAGS indicates euthermic AGS.

Chapter 3*

Attenuation of NMDA receptor function in hibernating Arctic ground squirrels via decreased phosphorylation of NMDAR1

3. 1 Abstract

Heterothermic mammals such as ground squirrels tolerate ischemia better than homeothermic mammals such as rats both *in vivo* and *in vitro*, and this tolerance is enhanced in the hibernating state compared with the non-hibernating state (euthermy). However, the cellular mechanisms underlying this tolerance remain unclear. Calcium overload through NMDA receptors (NMDAR) is a major trigger of ischemia-induced neuronal death. The purpose of the current study was therefore to test the hypothesis that NMDAR are down-regulated in hibernating Arctic ground squirrels (hAGS, *Spermophilus parryii*) and to explore mechanisms of this down-regulation. To address this hypothesis, we used calcium imaging to examine NMDAR function in cultured hippocampal slices from hAGS, interbout euthermic AGS, and rats. Furthermore, we used western blot analysis to investigate NMDAR phosphorylation and internalization as potential mechanisms for altered function. We report that NMDAR function is suppressed in the hAGS due to decreased phosphorylation of NMDAR1 (NR1) subunit, a fundamental subunit required for functional NMDAR. Moreover, the fraction of NR1 in the functional membrane pool in AGS is less than in rats. Hence, modulation of NMDAR may contribute to the neuroprotection observed in hAGS.

---

* This chapter was submitted to *J Neurochemistry* and authors are Zhao HW, Ross AP, Christian SL, Buchholz JN, and Drew KL.

3. 2 Introduction

Stroke is a primary cause of disability in America, and studies in traditional laboratory animals such as rats have produced a poor yield of pharmacotherapies. Heterothermic mammals (e.g., ground squirrels) tolerate experimental hypoxia and ischemia significantly better than homeothermic mammals (e.g., rats) both *in vivo* and *in vitro* (Frerichs et al., 1998; Drew et al., 2004; Dave et al., unpublished observations). In addition, arousal from hibernation enhances learning in ground squirrels (Mihailovic et al., 1968; Weltzin et al, in press) suggesting that hibernation is a natural model of adult mammalian synaptic plasticity. However, the cellular mechanisms underlying these phenomena are largely unknown.

Intracellular calcium is a ubiquitous second messenger integrating many cellular processes, including neuronal development, gene expression, synaptic plasticity, and neuronal death (Siesjo, 1990). Intracellular calcium overload is essential for neuronal injury associated with ischemia and hypoxia (Budd, 1998). During ischemia and hypoxia, a decrease in ATP leads to loss of ion homeostasis, an increase in extracellular glutamate and activation of an excitotoxic cascade that leads to neuronal damage (Choi, 1995). Intracellular calcium overload originates from increased conductance of alpha-amino-3-hydroxy-5-methyl-4-isoxazolepropionic acid receptors (AMPAR), N-methyl-D-aspartate receptors (NMDAR), and voltage-gated calcium channels, as well as from release from intracellular stores (Tymianski et al., 1993). The NMDAR have attracted significant attention due to their high calcium permeablity and key roles in synaptic plasticity and excitotoxcity (Ascher and Nowak, 1987; Choi, 1995). Modulation of

NMDAR contributes to hypoxia and ischemia tolerance in developing brains of rats and piglets (Mishra et al., 2001, Fritz et al., 2002); and allows western painted turtles (*Chrysemys picta*) to tolerate long-term anoxia (Bickler et al., 1998).

We have recently found that hippocampal slices from hibernating Arctic ground squirrels (hAGS, *Spermophilus parryii*) tolerate oxygen nutrient deprivation and NMDA, even at high concentrations, better than slices from interbout euthermic AGS (ibeAGS) (Ross et al., in press). Tolerance to NMDA suggests that modulation of NMDAR contributes to intrinsic tissue tolerance in slices from hAGS. Functional NMDAR are heteromeric and formed by NMDAR1 (NR1) subunit in various combinations with NMDAR2A-D (NR2A-D) subunits (Carroll and Zukin, 2002). NR1 is required for functional NMDAR, while NR2 subunits play regulatory roles. Phosphorylation of NR1 and NR2 subunits enhances receptor function (Liu and Zhang, 2000). NMDAR function can also be modulated by internalization or altered insertion in the plasma membrane (Carroll and Zukin, 2002). The purpose of this study was, therefore, to test the hypothesis that NMDAR are down-regulated in hibernation and to explore mechanisms of this down-regulation. To test this hypothesis, we used calcium imaging to examine NMDAR function in cultured hippocampal slices from hAGS, ibeAGS, and rats. We also used western blot analysis to investigate NMDAR phosphorylation and internalization as potential mechanisms for altered function.

3. 3 Materials and methods

3. 3. 1 *Animals*: The Institutional Animal Care and Use Committee of the University of Alaska Fairbanks approved all animal procedures. AGS were trapped on the northern slope of the Brooks Range, Alaska, approximately 20 miles south of the Toolik Field Station of UAF (68°38' N, 149°38' W; elevation 809m) in July 2003 and 2004 under permit from Alaska Department of Fish and Game. Upon arrival at the university, AGS were quarantined for at least 14 days. All AGS were housed individually in cages at an ambient temperature (T_a) of approximately 18°C, fed approximately 40 g of Mazuri Rodent Chow per day, and kept on natural lighting for 64° latitude where the light:dark cycle changes from 20 hr: 4 hr to 16 hr: 8 hr. In early fall, AGS were fed 10-15 sunflower seeds each day for two weeks before being moved to environmental chambers to facilitate hibernation. After moving to the chamber, AGS were housed at a T_a of approximately 2°C and fed rodent chow *ad libitum*.

Groups of AGS (hAGS and ibeAGS) were matched for season, frequency and duration of torpor bouts, as well as age, sex, and body weight. Both hAGS and ibeAGS used in the current study had experienced at least three regular hibernation bouts lasting a minimum of four days each and three periods of interbout euthermy lasting approximately 24 hr each. hAGS were chosen if they were at least three days into their current torpor bout, their respiratory rate was less than five breaths per minute, and wood shavings placed on the animal's back 24 hr previously remained undisturbed. ibeAGS were chosen if their respiratory rate was more than 80 breaths per min, body temperature was greater than 35.5°C, and animals responded quickly to touch. All ibeAGS were

hibernating 12-16 hr prior to slice preparation and tissue collection, and had naturally aroused from hibernation in the past 12-16 hr.

Since the majority of AGS were female, female Wistar rats were used as positive controls. Rats were obtained from Simonsen Laboratories (Gilroy, CA), quarantined for at least 7 days, and kept at a T_a of approximately 21°C until euthanasia.

3. 3. 2 *Tissue preparation*: For calcium imaging studies, hippocampal slices were prepared from female hAGS, ibeAGS, and 28 to 34-day-old female Wistar rats. Prior to slice preparation, 12 mm diameter Millicell-CM inserts (Millipore, Bedford, MA, USA) were placed in a 24-well plate and equilibrated with 0.5 ml of Neurobasal™ Adult media supplemented with anti-oxidant free B-27 serum substitute (GIBCO, Grand Island, NY), 0.025 mM glutamate, 0.5 mM glutamine, and 1% streptomycin-penicillin (Sigma, USA) for 1 hr at 37°C. Animals were anaesthetized with 5% halothane and maintained at 3% mixed with 100% oxygen, delivered at a flow rate of 1.5 L/min. After decapitation, brains were rapidly removed into ice-cold Hibernate™ Adult medium (Brain Bits, Springfield, IL). Hippocampi were dissected, embedded in 3% agar, and cut at a thickness of 300 μm using a vibraslicer (World Precision Instruments, Inc., Sarasota, FL). One slice was placed on each insert, and slices were cultured at 37°C in a 5% CO_2 US Autoflow CO_2 Water-Jacketed humidified incubator (NuAire, Plymouth, MN).

3. 3. 3 *Ca^{2+} imaging*: After 24 hr in culture, slices were loaded by replacing Neurobasal with 0.5 ml perfusion buffer ((mM) NaCl 101, KCl 4.6, $CaCl_2$ 1.8, $MgCl_2$ 0.81, HEPES

10, and Dextrose 21) containing 10 μM fura-2 acetoxyl methyl (fura-2AM, Molecular Probes, Eugene, OR), 0.12% DMSO, 0.02% pluronic acid (Molecular Probes, Eugene, OR) and 0.5% BSA. Slices were loaded at 37°C for 1 hr in the dark. After loading, individual slices were transferred to a heated chamber mounted on the stage of a Zeiss Axiovert S-100 inverted microscope, in which the temperature of the chamber was maintained at 37°C by a Delta T4 Culture Dish Controller (Bioptechs, Butler, PA). Individual slices were perfused for another 30 min at 1.2 ml/min with a peristaltic pump before imaging to allow for esterase activity (Bioptach, Bulter, PA). The CA1 area of the hippocampal slices was excited alternately at wavelengths of 340 and 380 nm using a high-speed wavelength-switching device (Lambda 10-C, Shutter, Novato, CA). Fluorescence intensity at 510 nm was recorded through a 40×, 0.60 LD ACHROPLAN objective with a photometric KAF 1400-G2 low light level digital camera. Data were recorded using Metafluor imaging analysis software 6.1 (Meridian Instrument Co., Kent, WA).

Free intracellular calcium concentration ($[Ca^{2+}]_i$) was calculated using the following equation: $[Ca^{2+}]_i = K_d \times S_f \times (R-R_{min})/ (R_{max}-R)$. Calibration of K_d (259 nM) has been described in detail in Vanterpool et al. (2005). In brief, K_d was determined using a standard calibration buffer kit (Molecular Probes, Eugene, OR). R_{max} was measured by application of 10 μM ionomycin (Molecular Probes, Eugene, OR) in perfusion buffer, and R_{min} was measure by application of calcium free buffer (1.8 mM $CaCl_2$ in perfusion buffer was replaced with 10mM EGTA). S_f was defined as the ratio of fluorescence intensity at 380 nm in free calcium vs. saturated calcium. Ionomycin (10 μM) and

glutamate (1 mM) were dissolved in perfusion buffer and were pulse delivered to slices. To investigate contribution of NMDAR to glutamate-induced increase in $[Ca^{2+}]_i$, slices were perfused with D, L-2-amino-5-phosphonovalerate (AP5) in a final concentration of 200 μM (Sigma-Aldrich Corp. St. Louis, MO). AP5, dissolved in perfusate, was applied for 15 to 20 min prior to and during application of a second pulse of glutamate. In some experiments, a second pulse of glutamate was applied in the absence of AP5 to examine if the glutamate response was reproducible on the slices.

3. 3. 4 ***Tissue and protein lysate preparation*:** Brain tissues were prepared from female, 28 to 34-day-old rats, and hAGS and ibeAGS in both sexes. Animals were lightly anesthetized; brains were removed quickly after decapitation. Hippocampi were dissected, quick frozen in liquid N2, and stored at –80°C.

Total protein lysate preparation: Approximately 20-30 mg of hippocampal tissue was homogenized in 200-300 μl (10 × volumes) of ice cold 1% NP-40 lysis buffer (50 mM Tris-HCl (pH 7.6), 0.02% sodium azide, 0.5% sodium deoxycholate, 0.1% SDS, 1% NP-40, 150 mM NaCl) with protease/phosphatase inhibitors including 1 mM phenylmethylsulfonyl fluoride, 1 mM sodium orthovanadate, 10 μg/ml leupeptin, 1 μg/ml aprotinin, and 1 μg/ml antipain with a motor-driven polytron homogenizer for 30-40 seconds. Homogenate was left on ice for 40 min and then centrifuged at maximal speed for 10 min using a microcentrifuge. The supernatant was collected and termed total protein lysate.

Crude membrane/cytosolic preparation: Approximately 50-60 mg of hippocampal tissue was homogenized in 500-600 µl (10 × volume) of cold homogenization buffer (0.32 M sucrose, 10 mM HEPES (pH 7.4), 2 mM EDTA) with protease/phosphatase inhibitors including 0.1 mM phenylmethylsulfonyl fluoride, 1.5 µg/ml aprotinin, 10 µg/ml leupeptin, 1 mM sodium orthovanadate, and 10 µg/ml antipain using a glass-teflon homogenizer for 10-15 strokes. Homogenate was centrifuged at 1000 × g for 15 min to remove pelleted nuclear fraction (P1). Supernatant (S1) was then centrifuged at 200,000 × g for 15 min using the TLA100.2 rotor in a Beckman TL-100 ultracentrifuge (Beckman Coulter, Fullerton, CA) to yield a crude cytosolic fraction (S2) and a crude membrane pellet (P2). The crude membrane pellet (P2) was resuspended with homogenization buffer and centrifuged again at 200,000 × g for 15 min to yield the washed crude membrane pellet (P2′). The membrane fraction was prepared by resuspending P2′ in 200-250 µl (approximately 5 × volume) of HEPES-Lysis buffer (50 mM HEPES pH 7.4, 2 mM EDTA) and protease/phosphatase inhibitors.

3. 3. 5 ***Western blotting*****:** Protein concentration was determined using the Bio-Rad protein assay kit (Bio-Rad, Hercules, CA). Twenty µg of protein was separated on 8% SDS-PAGE gels and then transferred to nitrocellulose membranes. Rat brain microsomal preparation (Upstate, Lake Placid, NY) was used as a positive control in some experiments. After blocking with 5% milk in TBS (10 mM Tris-HCl (pH 7.5) and 150 mM NaCl) for 1 hr, the membranes were incubated with the primary antibody (anti-NR1, 1:1000, Cat # MAb 363, Chemicon, Temecula, CA; or anti-phospho NR1 (pNR1),

1:1000, Cat # 06-641, Upstate, Lake Placid, NY) in TBST (TBS and 0.1% Tween 20) with 1% bovine serum albumin overnight at 4°C with gentle agitation. The membranes were washed with TBST and incubated with horseradish peroxidase-conjugated secondary antibody (anti-mouse IgG, 1:2000, Bio-Rad, Hercules, CA) for 1 hr. Immunoreactive bands were visualized using enhanced chemiluminescence (ECL, Perkin-Elmer, Boston, MA). Membranes were stripped by incubation with 10 mM Tris-HCl (pH 2) and 150 mM NaCl for 30 min. Equal loading was then confirmed by reprobing with anti-tubulin β3 (1:1000 Cat # MAb1637, Chemicon, Temecula, CA); anti-Na^+, K^+ - ATP_{ase} β-1 (1:5000, Cat # 06-170,Upstate, Lake Placid, NY); or anti-actin (1:5000, Cat # 5316, Sigma-Aldrich Corp. St. Louis, MO) diluted in TBST with 1% bovine serum albumin respectively. Each membrane was reprobed a maximum of two times. Scans of ECL exposures were analyzed using ImageQuant 5.2 software (Amersham Biosciences, Piscataway, NJ).

3. 3. 6 *Statistics*

Data were expressed as group means ± SEM. Results were analyzed using one-way or two-way analysis of variance (ANOVA) and Student-Newman-Keuls method for post-hoc comparisons (Sigmastat Ver3.0, SYSSTAT Software Inc., Chicago, IL) or paired t-test where indicated. $p<0.05$ was considered significant.

3. 4 Results

3. 4. 1 Glutamate-induced $[Ca^{2+}]_i$ increase is similar in hAGS and ibeAGS

The resting $[Ca^{2+}]_i$ (nM) of hippocampal slices prepared from hAGS, ibeAGS, and rats was 95.2 ± 7.35, 89.7± 3.5, and 94.6± 6.3 respectively and there was no significant difference among groups. Glutamate induced a significant $[Ca^{2+}]_i$ increase in all groups compared with resting levels of Ca^{2+} ($p<0.001$, main effect of Treatment). Glutamate increased $[Ca^{2+}]_i$ to 391.2 ± 31.4 nM, 378.8 ± 37.2 nM, and 500.2 ± 39.0 nM in hAGS, ibeAGS and rats, respectively. No difference was found in glutamate-induced $[Ca^{2+}]_i$ increase between hAGS and ibeAGS, however, the glutamate-induced $[Ca^{2+}]_i$ in slices from rats was greater than in slices from hAGS or ibeAGS ($p<0.05$, Group x Treatment, Fig. 3. 1).

3. 4. 2 NMDAR function was suppressed in hAGS

To address the role of NMDAR in the glutamate-induced $[Ca^{2+}]_i$ increase, we treated slices with AP5, a competitive NMDAR antagonist. Glutamate-induced $[Ca^{2+}]_i$ increase was significantly attenuated in hippocampal slices prepared from rats and ibeAGS. In contrast, AP5 did not attenuate glutamate-induced rise in $[Ca^{2+}]_i$ in the hippocampal slices prepared from hAGS ($p<0.05$, Group x Treatment, Fig. 3. 2), suggesting that NMDAR did not contribute significantly to glutamate-induced increase in $[Ca^{2+}]_i$ in the hAGS.

In the absence of AP5, a second pulse of glutamate applied 5 to 10 min after the first pulse produced an increase in $[Ca^{2+}]_i$ that was 110% ± 11.5% of the first pulse ($n=5$, $p>0.05$, paired t-test).

3. 4. 3 Down-regulation of NMDAR function in hAGS via reduced phosphorylation of NR1

To begin to address the possible mechanisms of reduced NMDAR function in hAGS, we used western blots to examine phosphorylation of NR1 (pNR1), which enhances NMDAR activity. Since pNR1 was not detected in total protein lysate, we compared the ratio of pNR1 over NR1 in membrane fractions prepared from hAGS, ibeAGS, and rats. pNR1/NR1 was significantly lower in hAGS compared with ibeAGS and rats ($p<0.05$, effect of Group) (Fig. 3. 3), suggesting that decreased phosphorylation of NR1 contributes to down-regulation of NMDAR function in hAGS.

Purity of fractions was assessed using Na^+, K^+/ ATP_{ase} and tubulin as membrane and cytosolic markers respectively. We found that the membrane fraction is free of cytosolic components and that the cytosolic fraction contains low levels of membrane components (Fig. 3. 4). ibeAGS and hAGS did not differ in NR1 abundance in the membrane fraction. Interestingly, the ratio of NR1/Na^+, K^+-ATP_{ase} in the membrane fraction was significantly lower in AGS than in rats ($p<0.05$, effect of Group, Fig. 3. 5). However, the ratio of NR1/actin was significantly higher in AGS than in rats ($p< 0.05$, effect of Group, Fig. 3. 6). Moreover, NR1 abundance in the membrane fraction relative to total protein lysate was lower in AGS than in rats but was similar in hAGS and ibeAGS ($p<0.001$, effect of Group, Fig. 3. 7).

3. 5 Discussion

Here we report down-regulation of NMDAR function in hAGS and provide evidence that decreased phosphorylation of the NR1 subunit contributes to decreased function. Decreased NMDAR function likely contributes to pronounced protection from oxygen and nutrient deprivation and excitotoxicity in hippocampal slices from hAGS (Ross et al, in press).

Intracellular calcium is a crucial ion involved in neuronal development, gene expression, synaptic plasticity, and neuronal death (Choi, 1995). The resting level of $[Ca^{2+}]_i$ reported here for rats is 94.6 nM, which is similar to other studies (Michel et al., 2002; Raley-Susman et al., 2001; Colwell CS, 2001; Harris et al., 1998; Pottorf et al., 2000) and the resting level of $[Ca^{2+}]_i$ in AGS is similar to rats. Thus, a difference in resting $[Ca^{2+}]_i$ can not explain the previously observed tolerance of hAGS to experimental oxygen nutrient deprivation and NMDA (Ross et al, in press).

Effects of AP5 indicate that NMDAR do not contribute significantly to the glutamate-induced $[Ca^{2+}]_i$ increase in hAGS, suggesting that NMDAR function is down-regulated in hAGS. NMDAR function can be modulated by protein phosphorylation, ATP and Ca^{2+}-dependant depolymerization of actin, desensitization, cations, pH, and redox agents (Liu and Zhang, 2000). Our results showed that NR1 phosphorylation in hAGS was significantly decreased compared with ibeAGS and rats. Decreased phosphorylation is consistent with decreased NMDAR function. Decreased phosphorylation of NMDAR in turtle brain and newborn piglet brain is thought to contribute to anoxia and hypoxia/ischemia tolerance via maintenance of critical $[Ca^{2+}]_i$

(Bickler et al., 1998; Karen et al., 2002). Therefore, down-regulation of NMDAR via decreased phosphorylation could be a common mechanism adopted by hypoxia/ischemia-tolerant animals.

NMDAR function is activated by phosphorylation and inactivated by dephosphorylation. Protein kinase C, cAMP-dependent protein kinases (PKA) and protein tyrosine kinases increase NMDAR channel activity, while protein tyrosine phosphatases and serine/threonine phosphatases decrease NMDAR channel activity (Liu and Zhang, 2000). Our data show that phosphorylation of NR1 (Ser897) is decreased in hAGS compared with ibeAGS and rats. Ser897 is mainly phosphorylated by PKA, suggesting that activity of PKA may be lower or serine phosphatase activity may be higher in hAGS compared with ibeAGS and rat.

Although NMDAR are down-regulated in hAGS, glutamate induced a similar $[Ca^{2+}]_i$ increase in hAGS and ibeAGS. Igelmund et al. (1996) report that NMDA is less effective in inducing a change in extracellular calcium in hippocampal slices from hibernating golden hamster (*Mesocricetus auratus*) than in slices from warm-acclimated hamsters, consistent with the present findings. In contrast, AMPA is more effective in hibernating hamster slices than in warm-acclimated hamster slices at 37°C. Therefore, the similarity of glutamate-induced $[Ca^{2+}]_i$ increase between hAGS and ibeAGS may be due to the down-regulation of NMDAR and up-regulation of AMPAR. Alternatively, voltage gated calcium channels could be up-regulated in hibernation, although this is unlikely because of reported down-regulation of Q-type calcium channels in synaptosomes prepared from hibernating thirteen-lined ground squirrel (Gentile et al, 1996).

Although NMDAR are considered relatively stable compared with AMPAR, NMDAR can move in and out of the plasma membrane at a slow rate (Nong et al., 2004). Synaptic NMDAR function is regulated by NMDAR trafficking. NR1 abundance in both membrane fractions and total protein lysates is similar in hAGS and ibeAGS, suggesting that internalization of NR1 does not contribute to the down-regulation of NMDAR in hAGS. Although some membrane components are found in cytosolic fractions, NR1 is not detected in either hAGS or ibeAGS. These results further support that the internalization of NR1 does not play a role in the decreased NMDAR function in hAGS.

Interestingly, the proportion of NR1 expressed in the functional membrane pool in AGS is less than in rats. Combined with evidence for decreased glutamate-induced changes in $[Ca^{2+}]_i$ in AGS compared with rats, these data suggest that increased internalization or decreased insertion of NR1 may occur in AGS compared with rats.

In summary, we report that NMDAR are suppressed in the hAGS via reduced phosphorylation, and the fraction of NR1 in the functional membrane pool in AGS is smaller than in rats. The modulation of NMDAR may play an important role in the neuroprotection observed in hAGS (Zhou et al., 2001; Ross et al, in press).

3. 6 Acknowledgements

This work was supported by Alaskan Basic Neuroscience Program SNRP (NIH U54-NS 41069 funded by NINDS, NIMH, NCRR, and NCMHD) and Alaska EPSCoR (ESP-0092040 and EPS-0346770 funded by NSF). Authors also thank Charles Hewitt, Drs. Edward. Lachica and Osama Ogawa for technical instruction and Bodo Schulenburg for discussion and critical review of the manuscript.

3. 7 References

Ascher P. and Nowak L. (1986) A patch-clamp study of excitatory amino acid activated channels. *Adv Exp Med Biol* 203, 507-511.

Bickler P. E. (1998) Reduction of NMDA receptor activity in cerebrocortex of turtles (Chrysemys picta) during 6 wk of anoxia. *Am J Physiol* 275, R86-91.

Budd S. L. (1998) Mechanisms of neuronal damage in brain hypoxia/ischemia: focus on the role of mitochondrial calcium accumulation. *Pharmacol Ther* 80, 203-229.

Carroll R. C. and Zukin R. S. (2002) NMDA-receptor trafficking and targeting: implications for synaptic transmission and plasticity. *Trends Neurosci* 25, 571-577.

Choi D. W. (1995) Calcium: still center-stage in hypoxic-ischemic neuronal death. *Trends Neurosci* 18, 58-60.

Colwell C. S. (2001) NMDA-evoked calcium transients and currents in the suprachiasmatic nucleus: gating by the circadian system. *Eur J Neurosci* 13, 1420-1428.

Dave K. R., Prado R., Raval A. P., Drew K. L. and Perez-Pinzon M. A. (2005) The arctic ground squirrel brain resists cardiac arrest during euthermia. Submitted to *Stroke*

Drew K. L., Harris M. B., LaManna J. C., Smith M. A., Zhu X. W. and Ma Y. L. (2004) Hypoxia tolerance in mammalian heterotherms. *J Exp Biol* 207, 3155-3162.

Frerichs K. U. and Hallenbeck J. M. (1998) Hibernation in ground squirrels induces state and species-specific tolerance to hypoxia and aglycemia: an *in vitro* study in hippocampal slices. *J Cereb Blood Flow Metab* 18, 168-175.

Fritz K. I., Zubrow A. B., Mishra O. P. and Delivoria-Papadopoulos M. (2002) NMDA receptor modification during graded hypoxia in the cerebral cortex of newborn piglets. *Biol Neonate* 82, 46-52.

Gentile N. T., Spatz M., Brenner M., McCarron R. M. and Hallenbeck J. M. (1996) Decreased calcium accumulation in isolated nerve endings during hibernation in ground squirrels. *Neurochem Res* 21, 947-954.

Harris-White M. E., Zanotti S. A., Frautschy S. A. and Charles A. C. (1998) Spiral intercellular calcium waves in hippocampal slice cultures. *J Neurophysiol* 79, 1045-1052.

Igelmund P. (1996) Hibernation and hippocampal synaptic transmission. Adaptation to Cold: Tenth International Hibernation Symposium, (Spangenberger H., Nikmanesh F. Gh., Gabriel A., Lutke K., Zhao Y. Q., Bohm-Pinger M. M., Heinemann U., Hescheler J., and Klubmann F.W. eds), pp.159-166. University of New England Press, *Armidale*.

Liu Y., and Zhang J.T. (2000) Recent development in NMDA receptors. Chin Med J 113 (10):948-956 Michel S., Itri J. and Colwell C. S. (2002) Excitatory mechanisms in the suprachiasmatic nucleus: the role of AMPA/KA glutamate receptors. *J Neurophysiol* 88, 817-828.

Mihailovic L., Petrovic-Minic B., Protic S. and Divac I. (1968) Effects of hibernation on learning and retention. *Nature* 218, 191-192.

Mishra O. P., Fritz K. I. and Delivoria-Papadopoulos M. (2001) NMDA receptor and neonatal hypoxic brain injury. *Ment Retard Dev Disabil Res Rev* 7, 249-253.

Nong Y., Huang Y. Q. and Salter M. W. (2004) NMDA receptors are movin' in. Curr *Opin Neurobiol* 14, 353-361.

Pottorf W. J., Duckles S. P. and Buchholz J. N. (2000) Mechanisms of calcium buffering in adrenergic neurones and effects of ageing: testing the limits of homeostasis. *J Auton Pharmacol* 20, 63-75.

Raley-Susman K. M., Kass I. S., Cottrell J. E., Newman R. B., Chambers G. and Wang J. (2001) Sodium influx blockade and hypoxic damage to CA1 pyramidal neurons in rat hippocampal slices. *J Neurophysiol* 86, 2715-2726.

Ross A. P., Christian S. L., Zhao H. W. and Drew K. L. (2005) Persistent tolerance to oxygen and nutrient deprivation and N-methyl-D-aspartate in cultured hippocampal slices from hibernating Arctic ground squirrel. *J Cereb Blood Flow Metab* in press.

Siesjo B. K. (1990) Calcium in the brain under physiological and pathological conditions. *Eur Neurol* 30 Suppl 2, 3-9; discussion 39-41.

Tymianski M., Charlton M. P., Carlen P. L. and Tator C. H. (1993) Source specificity of early calcium neurotoxicity in cultured embryonic spinal neurons. *J Neurosci* 13, 2085-2104.

Vanterpool C. K., Pearce, W. J. and Buchholz, J. N. (2005) Advancing age alters rapid and spontaneous refilling of caffeine sensitive calcium stores in sympathetic superior cervical ganglion cells. *J Appl Physiology* 99, 963-971.

Weltzin M., Zhao H. W., Drew K. L., and Bucci D. J. (2005) Arousal from Hibernation Alters Contextual Learning and Memory. *Behav Brain Res*, in press

Zhou F., Zhu X., Castellani R. J., Stimmelmayr R., Perry G., Smith M. A. and Drew K. L. (2001) Hibernation, a model of neuroprotection. *Am J Pathol* 158, 2145-2151.

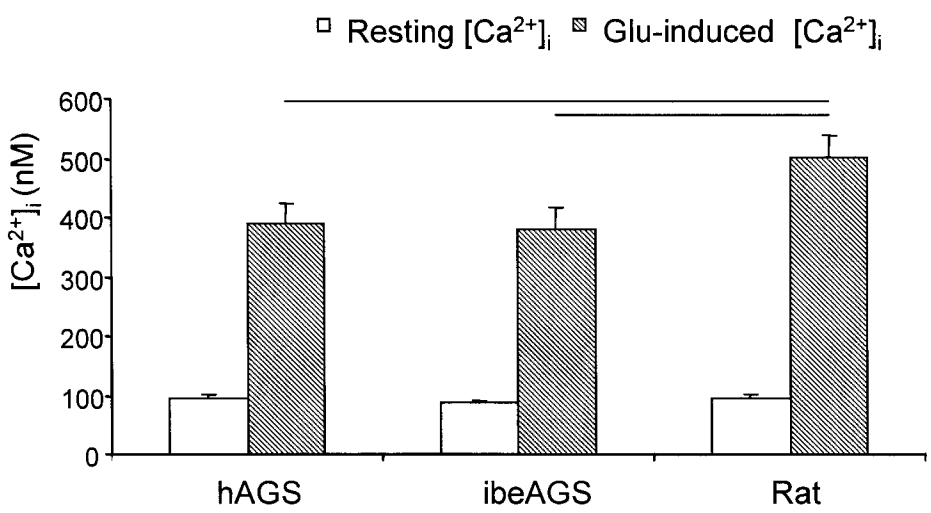

Fig. 3. 1. Glutamate effects on resting $[Ca^{2+}]_i$. hAGS, ibeAGS, and rat have similar resting $[Ca^{2+}]_i$ and glutamate induces a significant increase in $[Ca^{2+}]_i$ in all groups. Both ibeAGS and hAGS show less glutamate-induced $[Ca^{2+}]_i$ increase compared to rat. No difference is found between hAGS and ibeAGS, n=12-17 slices per group. Horizontal bars indicate significant difference between groups, $p<0.05$.

A.

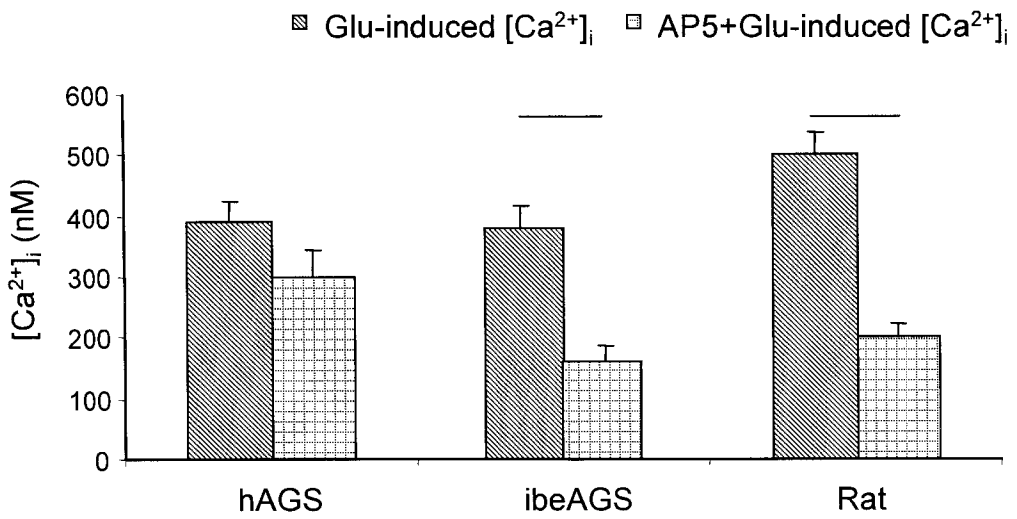

B.

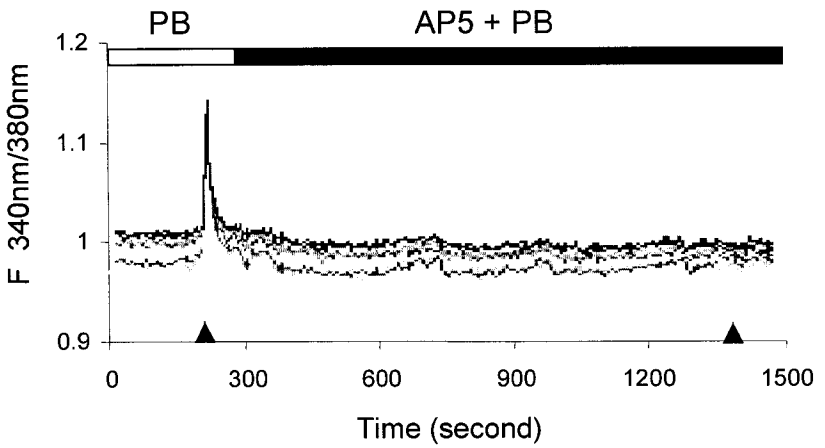

Fig. 3. 2. AP5 effects on glutamate-induced $[Ca^{2+}]_i$ increase. NMDAR function is suppressed in hAGS. A) AP5 blocks glutamate-induced $[Ca^{2+}]_i$ increase in slices from both rat and ibeAGS but not in hAGS, suggesting that NMDAR are suppressed in hibernation, n= 8-17 slices per group. Horizontal bars indicate significant difference between groups, $p<0.05$. B) A representative trace of a Ca^{2+} imaging experiment using fluorescence dye fura-2 in a hippocampal slice prepared from ibeAGS. White horizontal bar indicates perfusion with normal perfusion buffer (PB), black horizontal bar indicates perfusion with AP5 + PB. Arrowheads indicate the time point that a pulse of glutamate was given.

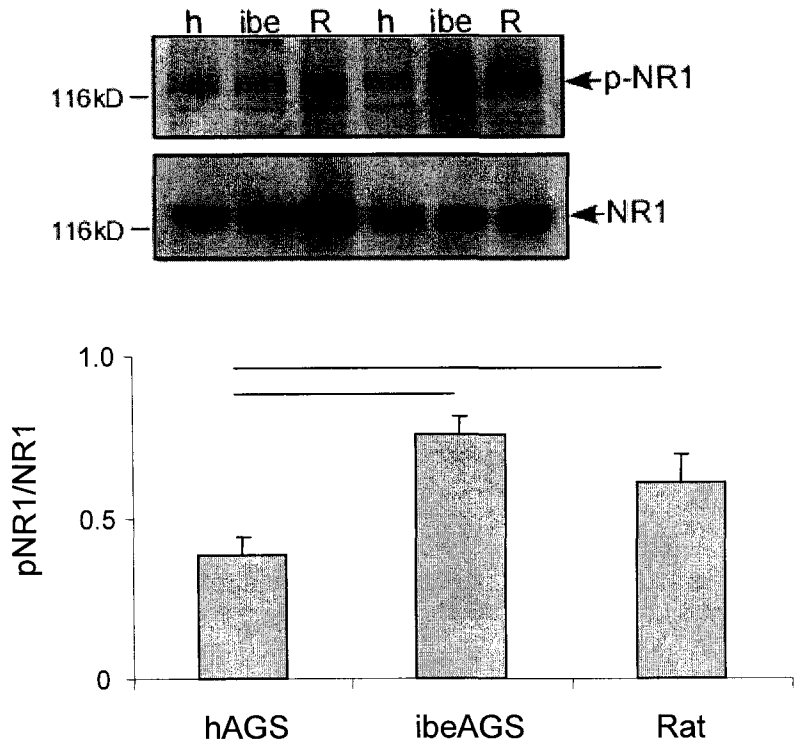

Fig. 3. 3. Decreased phosphorylation of NR1 in hAGS. pNR1/NR1 is decreased in hAGS compared with rat and ibeAGS, suggesting that suppressed NMDAR function is due to decreased phosphorylation of NR1 in hAGS. h indicates hAGS, ibe indicates ibeAGS, R indicates rat. Horizontal bars indicate significant difference between groups, $p<0.05$, n= 3-4 animals per group.

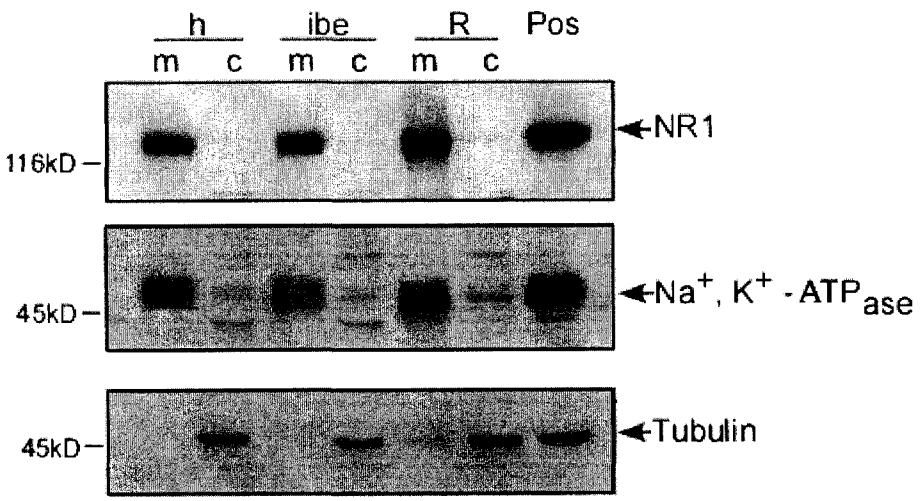

Fig. 3. 4. NR1 is most abundant in the membrane fraction. Purity of fractions was confirmed using Na^+, K^+- ATP_{ase} and tubulin as membrane and cytosolic markers. Membrane fraction is free of cytosolic components; cytosolic fraction contains low levels of membrane components. NR1 can not be detected in cytosolic fractions. h indicates hAGS, ibe indicates ibeAGS, R indicates rat, Pos indicates positive control.

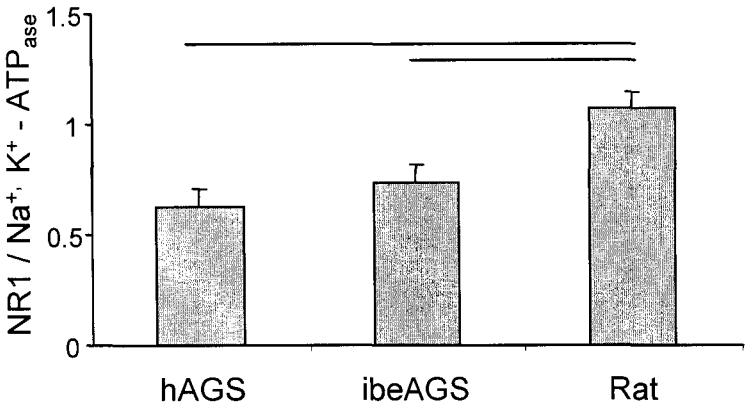

Fig. 3. 5. NR1 in the membrane fraction is similar in hAGS and ibeAGS.
Interestingly, NR1 abundance in the membrane fraction of both hAGS and ibeAGS is lower than in rats. Horizontal bars indicate significant difference between groups, $p<0.05$, n= 3 animals per group.

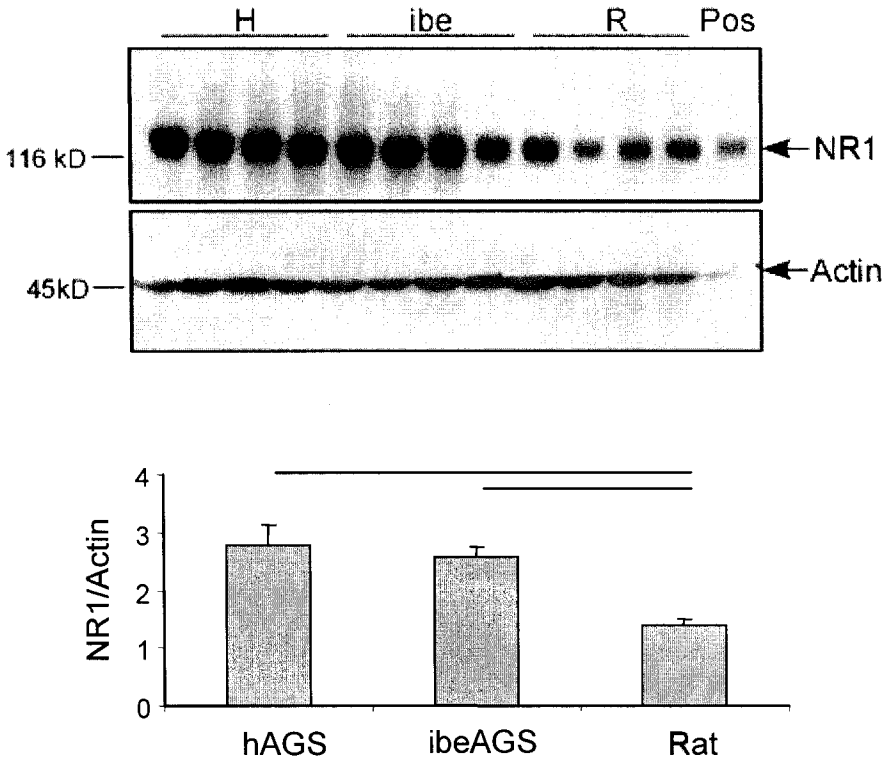

Fig. 3. 6. NR1 abundance in total protein lysate is higher in AGS than in rat. NR1 abundance in hAGS and ibeAGS are not different. h indicates hAGS, ibe indicates ibeAGS, R indicates rat, Pos indicates positive control. Horizontal bars indicate significant difference between groups, $p<0.05$, $n= 4$ animals per group.

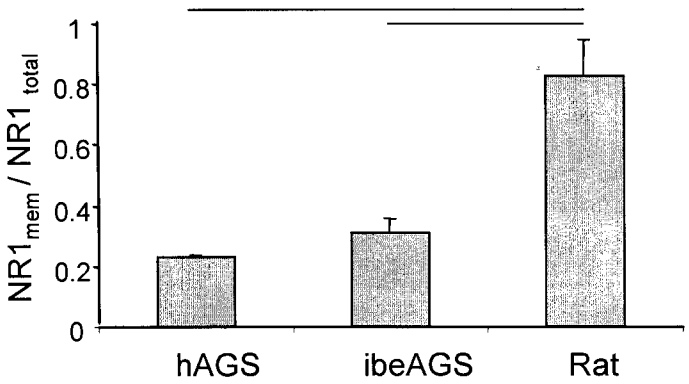

Fig. 3. 7. Fraction of NR1 in the functional membrane pool in AGS is smaller than in rats. Fraction of NR1 abundance in the membrane fraction ($NR1_{mem}$) relative to total protein lysate ($NR1_{total}$) is lower in AGS than in rats, but is similar in hAGS and ibeAGS. Horizontal bars indicate significant difference between groups, $p<0.001$, n= 3-4 animals per group.

Chapter 4*

Effects of Aversive Stimuli on Learning and Memory in Arctic Ground Squirrels

4. 1 Abstract

The present study was designed to assess effects of aversive stimuli on learning and memory in wild-caught Arctic ground squirrels (AGS, Spermophilus parryii) using an active avoidance learning paradigm. Results indicate that animals trained with low-value aversive stimuli (air puffs and lights) retained the task better than animals trained with high-value aversive stimuli (air puffs, lights and foot shock). Poor retention could not be explained by learning impairment, fear-induced freezing behavior or the effects of massed versus spaced training trials. Wild-caught AGS readily hibernate under laboratory conditions and provide a model of pronounced adult synaptic plasticity associated with emergence from hibernation. Characterization of learning and retention using active avoidance as well as other learning paradigms is a first step towards developing behavioral paradigms to assess cognitive function in this wild-trapped species. The present study shows that captive AGS are sensitive to aversive stimuli, argues for a direct effect on retention and suggests that high baseline levels of stress in a captive population may influence behavioral measures. The results further suggest that future studies of the effects of hibernation on learning and retention of active avoidance tasks employ low-level aversive stimuli.

---

* This chapter was published in *Behavioral Brain Research.* 2004; 151 (1-2): 219-224 and authors were Zhao HW, Bucci D, Weltzin M, and Drew KL.

4. 2 Introduction

Arctic ground squirrels (AGS, *Spermophilus parryii*) are indigenous to northern climates where the hibernation phenotype has evolved as an adaptation to extreme cold and food shortage during winter [2]. Hibernation is a unique condition characterized by metabolic suppression, decreased body temperature, and other physiological adaptations [7] that allow AGS to survive long arctic winters. Studying the effects of hibernation on learning and memory is of interest in light of evidence for pronounced synaptic remodeling of mossy fiber terminals in area CA3 of hippocampus during emergence from hibernation [18,19] as well as evidence that hibernation affects learning and memory. Previous reports about the effects of hibernation on learning and memory are inconsistent [15, 16, 17]; therefore, the topic remains worth studying.

In this experiment, an active two-way avoidance task was designed to assess AGS cognitive function. Active avoidance is a standard behavioral paradigm used to assess acquisition and retention of aversive events; a cognitive task of relevance to a prey species such as the AGS. Characterization of active avoidance in laboratory and domesticated species shows that optimal parameters vary widely between strains and species. In addition, aversive conditioning can result in a variety of responses (e.g., freezing versus running) that are dictated in part on the behavioral procedure as well as particular species being tested [4]. Given the number of novel and interesting questions related to learning, memory and synaptic plasticity that can be addressed in a hibernating species, the purpose of the present study was to characterize the effects of aversive

stimuli and hibernation on learning and retention of an active avoidance task in wild-caught, captive AGS.

4. 3 Materials and methods

4. 3. 1 Subjects

Arctic ground squirrels (AGS, *Spermophilus parryii)* were trapped on the northern slopes of the Brooks Range, Alaska, approximately 11 miles south of the Toolik Field Station of the University of Alaska Fairbanks (68°38' N, 149°38' W; elevation 809 m) in July 2001 under permit from Alaska Department of Fish and Game. Forty-eight male and female (37 juvenile and 11 adults) AGS, weighing 478 to 1130 g, were used in the experiment. Upon arrival, animals were screened for salmonella and quarantined for 14 days. All animals were housed individually in cages (21 cm high, X 46 cm wide, and X 31cm deep) and fed Mazuri Rodent Chow 40 g per day. Initially animals were housed at ambient temperature of 18-20 °C on an artificial 12:12 light: dark cycle. After training, two thirds of the animals were moved to an environmental chamber that mimicked their natural environment (2 °C and 4:20 light: dark). Of those animals housed in the cold chamber, some began to hibernate while others remained euthermic. Behavior of the animals in the cold chamber were checked and recorded daily for respiration rates and behavioral activity. Hibernation was indicated if respiratory rate was less than 6 per minute and wood shavings placed on animals back 24 hours previously remain undisturbed. All procedures were approved by the Institutional Animal Care and Use Committee of the University of Alaska Fairbanks.

4. 3. 2 Apparatus

The behavioral apparatus consisted of two behavioral chambers (Coulbourn Instruments, Allentown, PA) each measuring 35 cm high, X 53 cm wide, and X 26 cm deep, constructed of stainless steel and Plexiglass walls and sides. A stainless steel wall was placed between the chambers, with a 10 cm X 11 cm hole connecting the two sides. The grid floors consisted of metal bars, 0.5 cm in diameter, separated by 1.5 cm. The testing apparatus was enclosed in a sound-attenuated, ventilated box and connected to a computer. Graphic State Notation II (Data recording software, Coulbourn Instruments, Allentown, PA) was used to control the training procedure and monitor the escape response.

4. 3. 3 Behavioral Procedures

Animals were trained on an active two-way avoidance task using low or high aversive stimuli. At the beginning of each training session, an animal was placed in one side of the shuttle-box and given a 10-minute habituation period. A tone (4 kHz ~86 dB@10 cm, 30 sec duration) was used as the conditioned stimulus. Thirty seconds after presenting the tone, one of the two unconditioned stimuli was applied until the animal escaped to the adjacent compartment. The unconditioned stimulus was either a series of air puffs and light ("low aversive stimuli") or air puffs and light accompanied by a mild foot shock ("high aversive stimuli"). The air puffs (30 psi) were delivered via three outlets on the ends of the shuttle boxes in pulses of 0.3 sec on, 0.2 sec off; and light consisted of house and roof lights (313 Bayonet-type). The electric shock (0.2 mA) was delivered through the grid floor using a constant-current shock generator. An escape to

the opposite side of the chamber was defined as a learning trial. A two-minute resting interval occurred between trials. Trials were repeated for two hours/day. Training ended when animals reached a criterion of successful avoidance of the aversive stimuli on five consecutive trials. Animals that did not reach criterion within 20 days were eliminated from the experiment. Animals were retrained to criterion after a 44-day treatment period.

4. 3. 4 Behavioral Analyses

Behavioral indices of learning included a decrease in number of trials to reach criteria during training and retraining (retention), and a decrease in latency to escape. Latency was also assessed as a reflection of freezing, where larger latency to escape would be consistent with freezing behavior. Latency to escape was defined as the amount of time taken by each animal to cross into the safe side of the chamber after initiation of the tone. Retention was defined as the difference in number of trials to reach criterion between training and retraining. The number of trials to reach criterion and the latency to escape were analyzed using a three-way analysis of variance (ANOVA) with group (low or high aversive stimuli) and treatment (euthermic, hibernated or cold exposed euthermic) treated as between subjects variables and time (training and retraining) treated as a repeated measure (Glm procedure, SAS 1999-2001 by SAS Institute Inc., Cary, NC, USA). Individual graphs of latency to escape were displayed for each animal in parallel and inspected for trends. Results are reported as means ± SEM, and an alpha level of 0.05 was adopted for all statistical analyses.

4. 4 Results

Fifteen animals were eliminated from the study due to premature hibernation or failure to reach criterion after 20 days of training. Chi-square analysis shows that sex and age had no effect on failure to reach criteria ($p > 0.05$). Table 4. 1 shows group characteristics and the final number of animals in each group.

AGS trained with the high aversive stimuli performed differently than AGS trained with the low aversive stimuli. A repeated measure ANOVA revealed a significant interaction of group and time [$F(1,27)=5$, $p=0.03$], but no main effect of group or treatment, or a group X treatment X time interaction (p's>0.4). Post-hoc analyses revealed a trend towards fewer trials to reach criterion in the group receiving high aversive stimuli compared to the group that received low aversive stimuli ($p=0.06$), as shown in Figure 4. 1. Furthermore, animals in the low aversive stimuli group tended to require fewer trials to reach criterion upon retraining compared to the training phase ($p=0.07$).

Additional analyses of the performance of animals in the low versus high aversive stimuli groups included an assessment of the amount of time taken by each animal to cross into the safe side of the chamber (latency). Inspection of latency over trials revealed no time dependent effects. Indeed, no patterns were seen for latency to change in a consistent direction over time in any of the groups examined (data not shown). Latency did not differ between groups, as shown in Figure 4. 2. An ANOVA revealed no significant effect of group [$F(1,27)=0.09$, $p=0.77$] or time [$F(1,27)=0.09$, $p=0.76$], and no significant group time interaction [$F(1,27)=0.19$, $p=0.67$]. Lastly, the correlation

between the number of trials to reach criterion during training and retraining was assessed in the low and high aversive stimuli groups. As illustrated in Figure 4. 3, there was a significant correlation between number of trials to reach criterion during training and retraining in the low aversive stimuli group (r^2=0.59, p=0.0005), but not in the high aversive stimuli group (r^2=0.16, p=0.11).

4. 5 Discussion

The goal of the present study was to assess performance of wild-caught AGS in an active avoidance learning paradigm. Retention of the task was greater in the low-aversive stimuli group compared to the high-aversive stimuli group suggesting that low aversive stimuli are optimal for study of active avoidance in this species. Poor retention in the group of animals trained with higher aversive stimuli was somewhat unexpected since this group tended to perform better during the training phase.

This study is the first to show that attenuation of learning by aversive stimuli occurs at very low shock value in this population of wild caught animals, such that even minor amounts of shock (0.2mA) effects learning. Although it may be intuitively obvious that a wild-trapped species will be more sensitive to stress than a laboratory rat, this is the first systematic evaluation of effects of aversive stimuli on learning in these unique animals. Development of behavioral paradigms in hibernating species will provide tools to investigate relationships between learning and pronounced synaptic remodeling observed within hours following emergence from hibernation [18,19].

A variety of responses can be observed during aversive conditioning. The generation of a particular response depends on many factors, including the species being studied, the intensity of the aversive unconditioned stimulus, as well as various experimental contingencies [4]. For example, delivery of a foot shock in rats can result in running (e.g., avoidance behavior) or a freezing response (total motor immobility except for breathing) [3,8]. In addition, the frequency of conditioned response to a particular level of foot shock may vary in different species. For example, quite different levels of foot shock are used to generate similar levels of contextual freezing in mice versus rats [6,10]. Furthermore, it is has been demonstrated repeatedly that different levels of foot shock will alter the conditioned response. In laboratory rats, for example, increased intensity of foot shock beyond a certain level will generate a less conditioned response [4].

Potential explanations of results observed in AGS are considered in context of knowledge of active avoidance in other species. First, freezing behavior is often exhibited by animals in response to a fear-inducing stimulus such as foot shock [3]. Freezing is characterized by crouching behavior and the complete absence of movement, except for movement associated with respiration. In the present experiment, freezing would conflict with the behavior of interest, i.e. moving from the shock chamber to the safe chamber. Excessive freezing behavior might increase the number of trials needed to reach criterion because animals would tend to freeze and remain in the chamber in which shock was delivered. If this were the case, the time taken to move from the shock chamber to the no-shock chamber might be higher in the shock group. Assessment of latency to escape over

individual trials as well as over the entire training period, however, failed to show a difference between groups in the amount of time taken to move between the two chambers. Although freezing behavior cannot be ruled out unequivocally without visual observation, failure to detect a difference in latency to escape argues against a role for freezing behavior in the animals trained with high aversive stimuli.

Another possible explanation for the current findings involves group differences in the amount of trials received during training. Animals in the low aversive stimuli group tended to require more trials over a longer period of time to reach criterion during training compared to the high aversive stimuli group. Since training trials spaced out over a long time period typically result in improved learning and memory compared to trials massed together [12, 21], this might explain the difference in retention between the high aversive stimuli and low aversive stimuli groups. If so, a negative correlation between training and retraining performance might be expected, indicating that animals receiving more trials over a longer amount of time during training would require less trials to reach criterion during retraining. This, however, was not the case. In fact, animals trained with the low aversive stimuli demonstrated a significant positive correlation between training and retraining, supporting the conclusion that this group benefited from prior experience with the task compared to animals trained with high aversive stimuli. In contrast, performance during training was not a reliable predictor of retraining performance for animals in the high aversive stimuli group.

Prolonged exposure to stress (chronic stress) causes atrophy of apical dendrites in hippocampal neurons [13], possibly due to effects of corticosterone [22]. Chronic

unpredictable stress impairs long-term potentiation in rat hippocampal CA1 [1] and causes specific cognitive deficits in spatial learning and memory [13]. Extensive evidence shows that stress alters the neural morphology accompanied by deficits in learning and memory [11,14, 5]. Recently, Quervain et al. [20] have shown that the effect of stress on memory can be time dependent. For example, foot shock stress experienced 30 minutes, but not 2 minutes before a testing trial impaired retention of a spatial learning task. Thus, one interpretation of the present results is that although stress experienced immediately before a learning experience may confer an adaptive advantage by increasing the animal's attention to a potentially important stimulus, prolonged exposure to stress (chronic stress) possibly mediated by glucocortocoids in the hippocampus can adversely effect memory retrieval and retention.

Thus, in the present study, foot shock stress experienced during training might not be expected to impair learning. However, prolonged exposure to stress over several training days may have caused chronic stress and impaired memory consolidation and retrieval. Chronic stress during training may have negated any performance advantage conferred by previous training. Furthermore, the results of Quervain et al. support the notion that re-exposure to the training environment for 10 minutes prior to each retraining session may have resulted in increased glucocorticoid levels and impaired performance. Thus, while the primary purpose of the study was to assess a laboratory based learning paradigm in AGS, a novel, wild-caught, captive species, extrapolation of results to the wild suggests that a potential cost of prolonged exposure to a stressful stimulus may be poor long term retention of the event.

A related issue concerns the effects of cold stress associated with the pilot study of hibernation on retraining performance. More animals in the high aversive stimuli group did not hibernate, likely due to small sample size and variability typically observed in onset of hibernation after placement in the cold room. This group of animals was therefore exposed to the effects of cold stress during the intervening days between training and testing. Although this might have been expected to impair performance during retraining, results indicate that the behavior of animals in each of the three treatment conditions did not differ on any measure.

Characterization of learning and memory paradigms in AGS, a hibernating species, is a necessary step towards future studies of the effects of hibernation on learning and memory. Previous reports suggest that hibernation is a novel model of pronounced adult synaptic plasticity. Popov and colleagues [18,19] have shown that mossy fiber synapses in CA3 hippocampal neurons of ground squirrels (*Citellus undulates*) repeatedly undergo a striking structural transformation during hibernation. For example, dendritic spine profile area, the number of postsynaptic densities per spine and other parameters of synaptic density decrease during hibernation. Two hours after arousal from hibernation, these indices of synaptic density rebound and in some cases exceed levels in active (euthermic) animals [18,19]. Given the evidence for an association between synaptogenesis, learning and memory [9, 23], the synaptic changes occurring during hibernation and arousal from hibernation encourage future studies of the effects of hibernation on learning and memory. In addition to characterizing a behavioral paradigm for study of learning and memory in the AGS, a secondary goal of this study was to

perform a pilot study of the effects of hibernation on learning and memory. We report a large degree of variability in performance on the active avoidance task, which likely accounts for inability to detect an affect of hibernation given the small number of hibernating animals. Moreover, learning occurred over several days, so that immediate affects of hibernation, such as time dependent synaptogenesis, would be difficult to assess. Together, the present findings suggest that using low-aversive unconditioned stimuli, such as air puffs and light, in a paradigm that produces rapid learning may be more useful for examining the effects of hibernation on cognitive function.

4. 6 Acknowledgements

This work was supported by DARPA, Continuous Assisted Performance Program and by NS40169 funded in part by NINDS, NIMH, NCRR, NCMHD. Authors also thank Shufen Wu and Carlos Arnaiz for technical assistance and Alyssa R. Letourneau for discussion and critical review of the manuscript.

4. 7 References

1. Alfarez, D. Z., Joels, M., Krugers, H. J. Chronic unpredictable stress impairs long-term potention in rat hippocampal CA1 area and dentate gyrus in vitro. *Eur. J. Neurosce*, 2003;17(9): 1928-34.

2. Barnes, B. M. Freeze avoidance in a mammal: Temperatures below 0^{o}C in an arctic hibernator. *Science*, 1989; 244:1593-1594.

3. Blanchard, R. J. and Blanchard, D. C. Passive and active reactions to fear-eliciting stimuli. *Journal of Comparative Physiology and Psychology*, 1969; 68(1):129-135.

4. Bolles, R.C. Theory of Motivation (2^{nd} edition). Harper and Row, New York. 1975.

5. Bowman, R. E., Beck, K. D., Luine, V. N. Chronic stress effects on memory: sex differences in performance and monoaminergic activity. *Hom. Behav.*, 2003; 43(1): 48-59.

6. Bucci, D. J., Phillips, R. G., & Burwell, R. D. Contributions of postrhinal and perirhinal cortex to contextual information processing. *Behav Neurosci*, 2000; 114(5): 882-894.

7. Drew, K. L, Rice, M. E., Kuhn, T. B., Smith, M. A. Neuroprotective adaptations inhibernation: therapeutic implications for ischemia –reperfusion, traumatic brain injury and neurodegenerative diseases, *Free radical biology & Medicine*, 2001; 31(5): 563-573.

8. Fanselow, M.S. Conditional and unconditional components of postshock freezing. *Pavlovian Journal of Biological Sciences,* 1980; 15:177-182.

9. Geinisman, Y. Structural synaptic modifications associated with hippocampal LTP and behavioral learning. *Cerebral Cortex*, 2002; 10: 952-62.

10. Impey, S., Smith, D. M., Obrietan, K., Donahue, R., Wade, C., & Storm, D. R. Stimulation of cAMP response element(CRE)-mediated transcription during contextual learning. *Nature Neurosci*, 1998; 1(7): 595-601.

11. Kim, J. J. and Diamond, D. M. The stress hippocampus, synaptic plasticity and lost memories. *Nature reviews, Neuroscience*, 2002; 3: 453-462.

12. Lattal, K. M. Trial and intertrial durations in Pavlovian conditioning: issues of learning and performance. *Journal of Experimental Psychology: Animal Behavior Processes*, 1999; 25, 433- 450.

13. Magarinos, A. M., Verdugo, J. M. G., McEwen, B. Chronic stress alter synaptic terminal structure in hippocampus. *Proc. Natl. Acad. Sci.*, 1997; 94:14002-14008.

14. McEwen, B. S. and Sapolsky, R. M. Stress and cognitive function. *Current Opinions inNeurobiology*, 1995; 5: 205-216.

15. McNamara, M.C .and Riedesel, M.L. Memory and hibernation in Citellus literalis. *Science* 1973; 179: 92-94.

16. Mihailovic, L. J., Petrovc, B., Protic, S. and Divac, I. Effects of hibernation on learning and memory. *Nature*, 1968; 218:191-192.

17. Millesi, E., Prossinger, H., Dittami, J.P., and Fieder, M. Hibernation effects on memory in European ground squirrels (*Spermophilus citellus*). *Journal of Biological Rhythms*, 2001; 16: 264-271.

18. Popov, V. I. and Bocharova, L. S. Hibernation-induced structural changes in synaptic contacts between mossy fibres and hippocampal pyramidal neurons. *Neuroscience*, 1992; 48: 53-62.

19. Popov, V. I., Bocharova, L. S., and Bragin, A. G. Repeated changes of dendritic morphology in the hippocampus of ground squirrels in the course of hibernation. *Neuroscience*, 1992; 48; 45-51.

20. Quervain D. J. F., Roozendaal B., and McGaugh J. L. Stress and glucocorticoids impair retrieval of long-term spatial memory. *Nature*, 1998; 394: 787-790.

21. Rescorla, R. A. Behavioral studies of Pavlovian conditioning. *Annual Review of Neuroscience*, 1988; 11:329-352.

22. Wellman, C. L. Dendritic reorganization in pyramidal neurons in medial prefrontal cortex after chronic corticosterone administration. *J. Neurobiology*. 2001; 49(3): 245-53

23. Wright, J.W., Kramar, E.A., Meighan, S.E., and Harding, J.W. Extracellular matrix molecules, long-term potentiation, memory consolidation and the brain angiotensin system. *Peptides*. 2002; 1: 221-46.

Table 4. 1. Group characteristics

Number of AGS (n)		Low aversive stimuli (No shock)	High aversive stimuli (Shock, 0.2mA)
Total AGS before experiment		24	24
Sex	Female	13	13
	Male	11	11
Age	Adult	14	12
	Juvenile	10	12
Premature hibernation at 20 °C		1	2
Sex	Female	1	1
	Male	-	1
Age	Adult	1	-
	Juvenile	-	2
Failed to reach criteria after 20 day's training		7	5
Sex	Female	1	2
	Male	6	3
Age	Adult	4	3
	Juvenile	3	2
Remaining animals after experiment		16	17
Sex	Female	11	10
	Male	5	7
Age	Adult	3	3
	Juvenile	13	14
Treatment	Euthermic (T_a 20 °C)	5	6
	Euthermic (T_a 2 °C)	4	7
	Hibernation (T_a 2 °C)	7	4
Body Weight Range (g)		479-1042	500-1027

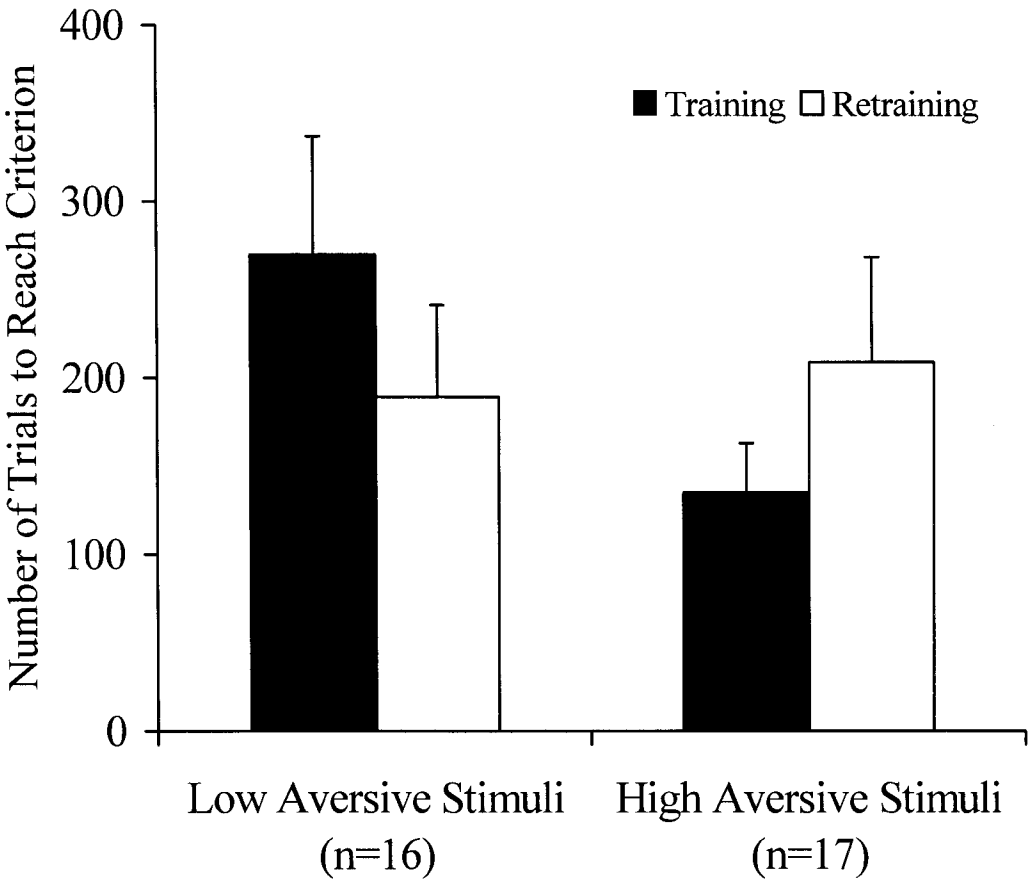

Figure 4. 1. AGS learned and remembered differently between two groups. AGS trained with the high aversive stimuli learned and remembered the task differently than AGS trained with the low aversive stimuli (p=0.03, Group X Time). Retention (the difference in number of trials to reach criterion between training and retraining) was enhanced in AGS trained using low aversive stimuli compared to those trained using the high aversive stimuli (p=0.03).

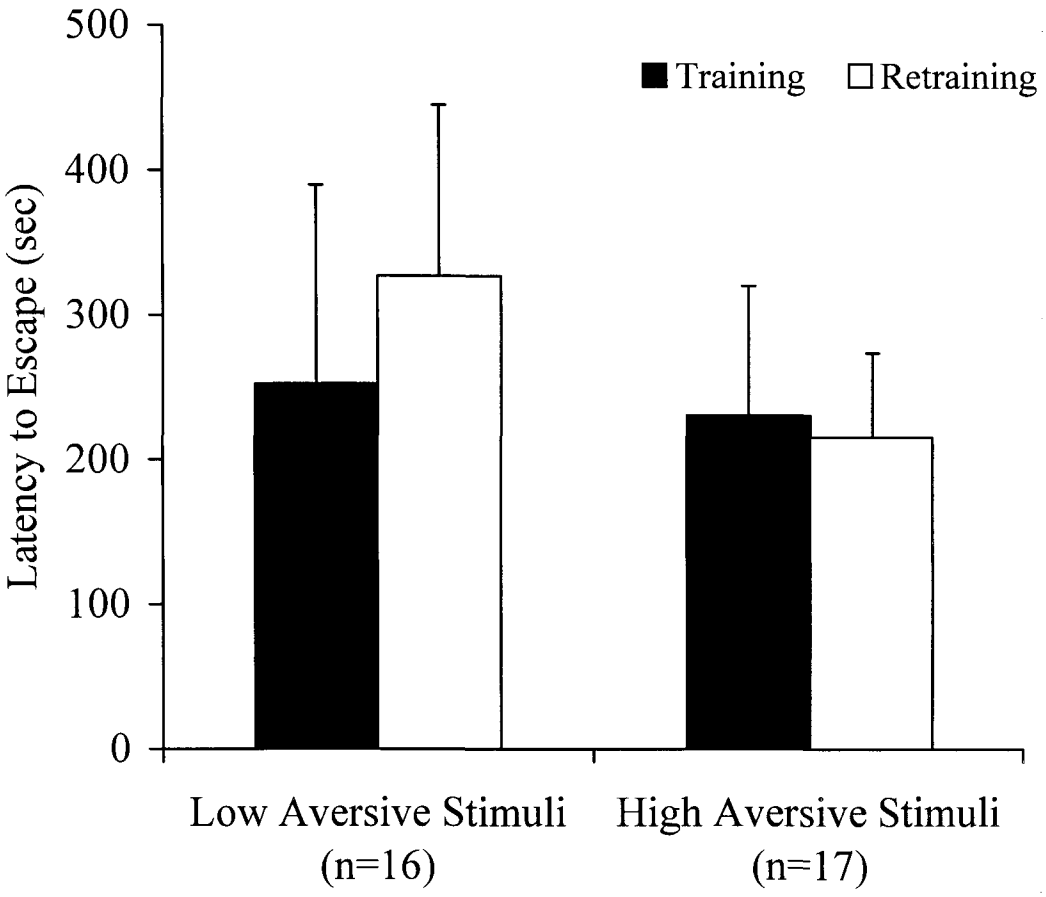

Figure 4. 2. Latency to escape is similar during training and retraining. There were no significant differences in the latency to escape during training and retraining.

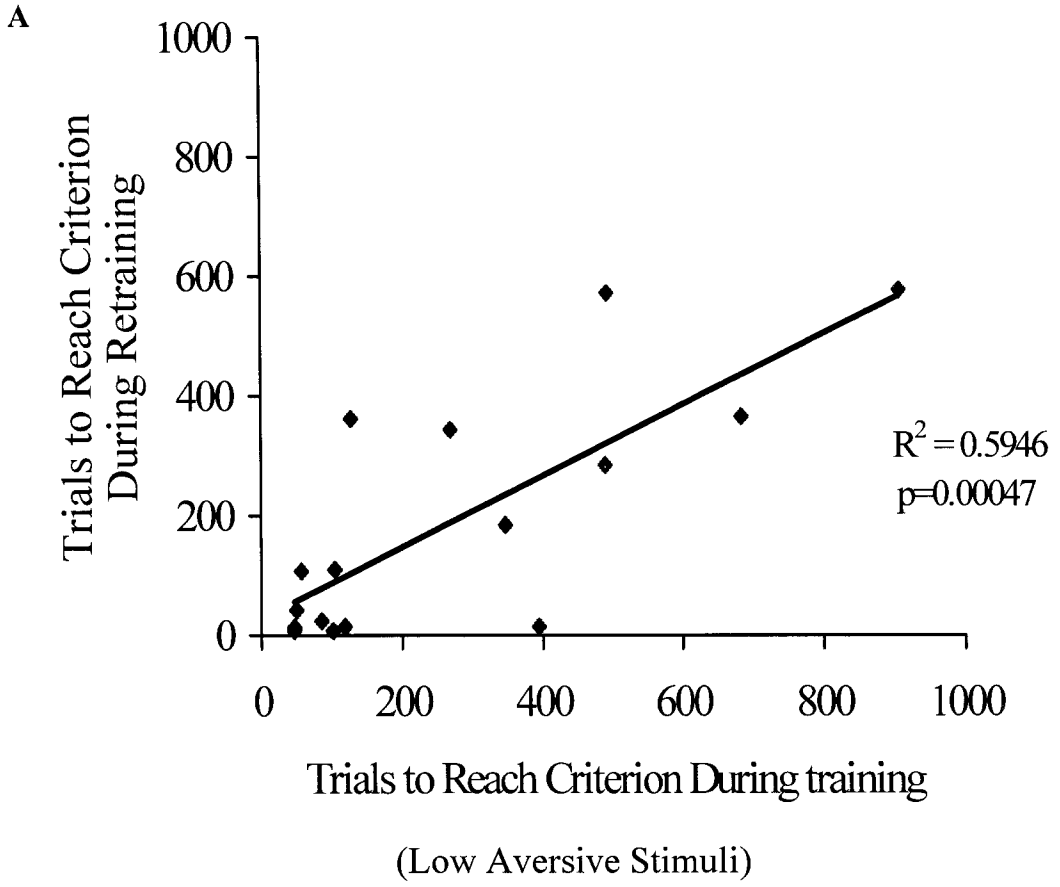

Figure 4. 3A. Trial numbers are correlated during training and retraining. The number of trials to reach criterion during training and retraining were significantly correlated in the low aversive stimuli group (p=0.0005; panel A).

B

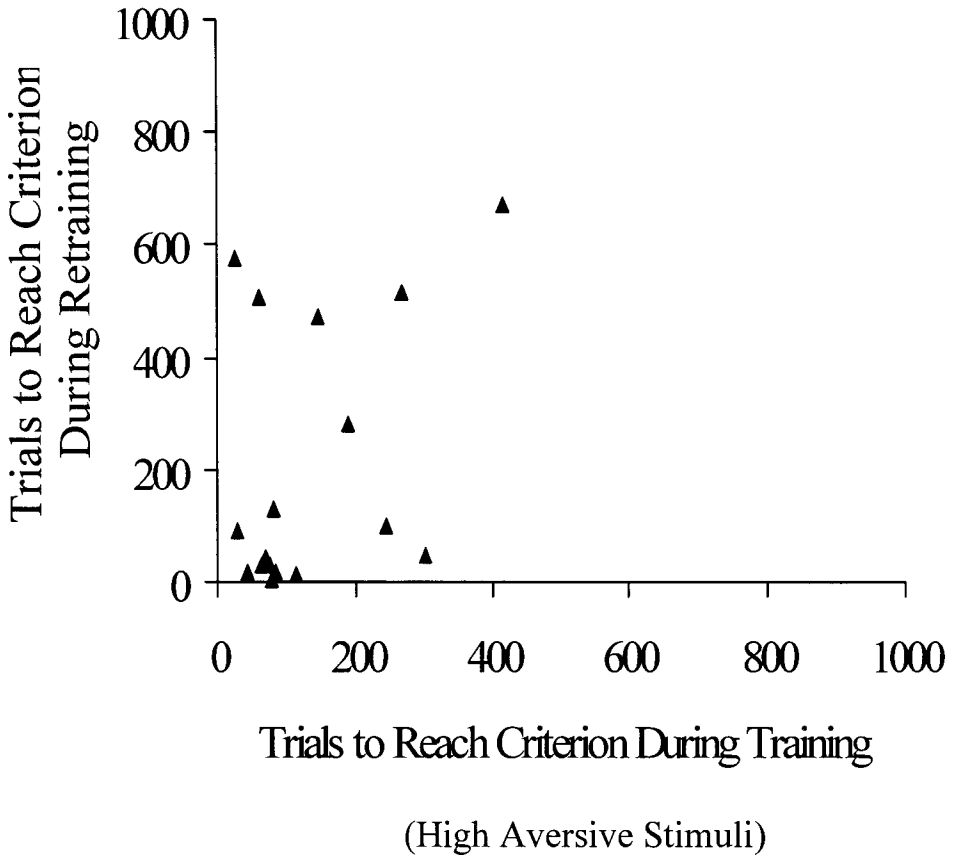

Figure 4. 3B. Trial numbers are correlated during training and retraining. The number of trials to reach criterion during training and retraining were significantly correlated in the low aversive stimuli group (p=0.0005; panel A), but not the high aversive stimuli group (panel B).

Chapter 5

General Discussion

5. 1 Findings of the current project

In the current project, we report that NMDAR in hAGS are down-regulated due to the decreased phosphorylation of the NR1 subunit. This down-regulation is not due to the changes in NR1 distribution and internalization in hAGS. In addition, the fraction of NR1 in the functional membrane pool in AGS is less than in rats. Altogether, these modulations of NMDAR may contribute to the neuroprotection previously observed in hAGS (Ross et al., in press).

5. 2 Glutamate excitotoxicity is Ca^{2+} source-dependent and amount-dependent

Calcium influx into cells has been termed the "final common pathway of cell death" (Schanne et al., 1979). Excessive Ca^{2+} accumulation has been implicated as a major trigger for neuronal injury. However, excitotoxic injury is Ca^{2+} source-dependent (Tymianski et al., 1993). Tymianski et al (1993) report that the neurotoxicity induced by glutamate far exceeded that induced by membrane depolarization with high K^+ although both stimuli induced the similar elevations in $[Ca^{2+}]_i$. More specifically, NMDAR are the major pathway of Ca^{2+} influx after glutamate stimulation (Choi, 1995; Tymianski et al., 1993). Previous studies show that NMDA-triggered cell death exceeded that triggered by non-NMDA receptors and other Ca^{2+} channels when $[Ca^{2+}]_i$ rise is similar, suggesting that the greater neurotoxicity of NMDAR as compared with other channels is not related

to the ability of NMDAR to trigger greater elevations in $[Ca^{2+}]_i$ (Tymianski et al., 1993). Nonetheless, brief exposure of NMDA can cause much more $^{45}Ca^{2+}$ influx than AMPA/kainate exposures. Therefore, excitotoxic injury is Ca^{2+} amount-dependant as well (Hartley et al., 1993; Eimerl and Schramm, 1994; Lu et al., 1996). Taken altogether, glutamate-induced excitotoxicity depends on the amount of $[Ca^{2+}]_i$ as well as the source of the increase in $[Ca^{2+}]_i$. Glutamate-induced $[Ca^{2+}]_i$ increase is significantly smaller in AGS compared with rats, and this may explain why both ibeGAS and hAGS tolerate ischemia and oxygen nutrient deprivation better than rats (Dave et al. unpublished observations, Ross et al., in press).

NMDAR are highly Ca^{2+}-permeable (MacDermott, 1986) and are capable of triggering widespread neurodegeneration, which is most closely linked to injury-initiating machinery (Tymianski et al., 1993; Rajdev and Reynolds, 1994). AMPA/kainate receptors are poorly permeable to Ca^{2+}, and more prolonged periods of activation of AMPA/kainate receptors are required for neurotoxicity (Koh et al., 1990; Choi, 1992). AMPA/kainite-induced neurotoxicity is thought to result from secondary Ca^{2+} influx via depolarization and subsequent activation of voltage-gated Ca^{2+} channels (Murphy and Miller, 1989; Weiss et al., 1990a) and release from intracellular stores. Although decreased NMDAR function results in a lower Ca^{2+} influx through NMDAR in hAGS, glutamate-induced $[Ca^{2+}]_i$ increase is similar in hAGS and ibeAGS, suggesting that the raise of $[Ca^{2+}]_i$ in hAGS may come from other sources. For instance, decreased NMDAR function in hAGS cause a decreased primary Ca^{2+} influx, in contrast, up-regulated other receptors such as AMPAR/kainite receptors may cause a increased secondary Ca^{2+} influx,

which has less toxic effects. In total, hAGS has a similar glutamate-induced $[Ca^{2+}]_i$ increase as ibeAGS. In the meantime, similar rise in $[Ca^{2+}]_i$ between hAGS and ibeAGS suggests that secondary sources of Ca^{2+} influx or release may be down-regulated in ibeAGS compared with hAGS, consistent with previous studies (Igelmund, et al., 1996). As discussed in chapter 3, Igelmund et al. (1996) found that NMDA was less effective in inducing a change in extracellular calcium in hippocampal slices from hibernating golden hamster (*Mesocricetus auratus*) than in slices from warm-acclimated hamsters, and AMPA is more effective in hibernating hamster slices than in warm-acclimated hamster slices at 37°C. Therefore, the similarity of glutamate-induced $[Ca^{2+}]_i$ increase between hAGS and ibeAGS may be due to the down-regulation of NMDAR and up-regulation of AMPAR in hAGS, or down-regulation of AMPAR in ibeAGS. Thus, a difference in the source of increased $[Ca^{2+}]_i$ appears to play a greater role in excitotoxicty than the overall magnitude of $[Ca^{2+}]_i$.

Although NMDAR are considered relatively stable compared with AMPAR, NMDAR can move in and out of the plasma membrane at a slow rate (Nong et al., 2004). Synaptic NMDAR function is regulated by NMDAR trafficking. NMDARs are found throughout the central nervous system and tend to be localized in dendritic spines as well as the soma (Craig et al., 1994; Dodt et al., 1998); however, they are also located at extrasynaptic sites (Sattler et al., 2000), which is involved in excitotoxicity (Cull-Candy et al., 2001). Differentially located NMDAR activation can initiate opposite effects on neuronal survival (Chazot, 2000, 2004). Activation of extrasynaptic NMDARs induces a loss of mitochondrial membrane potential, which is associated with glutamate-induced

toxicity. Synaptic NMDAR activation appears to have an antiapoptotic activity. We reported that both hAGS and ibeAGS tolerate ischemia and oxygen nutrient deprivation (Dave et al. unpublished observations, Ross et al., in press), suggesting that localization of NMDAR may also contribute to difference in tolerance between the species.

5. 3 Potential explanations of decreased NMDAR function in hAGS

NMDAR function can be modulated by subunit composition (Cull-Candy et al., 2003), protein phosphorylation, ATP and Ca^{2+}-dependant depolymerization of actin, desensitization, cations, pH, and redox agents (Liu and Zhang, 2000), as well as localization of receptors (Li et al., 2002).

In chapter 2, we report that hAGS have a similar NR1 distribution with euthermic AGS. Moreover, NR1 abundance in total protein lysate is similar in the two groups, suggesting that NR1 changes in distribution do not contribute to the down-regulation of NMDAR function in hAGS. As reviewed in chapter I, functional NMDAR are formed by NR1 subunits in various combinations with NR2A-D subunits. NR1 is required for functional NMDAR, while NR2 subunits play regulatory roles (Carroll and Zukin, 2002). The different combination of NR1 and NR2 subunits may confer different physiological and pharmacological properties on the receptors (Stephenson, 2001). For instance, radioligand studies on rat subunit recombinant NMDAR expressed in HEK 293 cells show a rank order of affinity for [^{3}H] glutamate as NR1/NR2B > NR1/NR2A ≈ NR1/NR2D > NR1/NR2C > NR1 (Laurie et al., 1994). Furthermore, oxygen sensitivity of NMDAR is affected by the difference in the subunit composition (Bickler et al., 2003).

Therefore, although NR1 distribution is similar, differences in NR2 subunit expression may contribute to decreased NMDAR function in hAGS, and warrant further investigation.

As discussed in chapter 3, protein phosphorylation is the major mechanism of NMDAR regulation. NMDAR function is activated by phosphorylation and inactivated by dephosphorylation. Protein kinase C (PKC), cAMP-dependent protein kinase (PKA), and protein tyrosine kinases increase NMDAR channel activity, while protein tyrosine phosphatases and serine/threonine phosphatase decrease NMDAR channel activity (Liu and Zhang, 2000). Data in chapter III show that phosphorylation of NR1 (Ser897) is decreased in hAGS compared with ibeAGS and rats. Ser897 residue in the NR1 subunit is mainly phosphorylated by PKA, suggesting that activity of PKA may be lower in hAGS and the activity of serine phosphatase may be higher in hAGS compared with ibeAGS and rat. Previous studies show that both temperature and hypoxia affect PKA function. PKA activity rapidly increases after exposure to short-term freezing in wood frog (*Rana sylvatica*) livers or short-term anoxic submergence in turtle (*Trachemys scripta elegans*) livers. However, after prolonged exposure to freezing and anoxia, PKA activity is suppressed (Holden and Storey, 1996; Mehrani and Storey, 1995). Therefore, suppressed PKA function may play a role in the down-regulation of NMDAR in hAGS. Both PKC and PKA can directly phosphorylate NR1, NR2A, and NR2B (Leonard et al., 1997). Therefore, in addition to the modulation by PKA, PKC may also be involved in the regulation of NMDAR function. PKC is known to phophorylate the Serine 896 residue in the NR1 subunit (Tingley et al., 1993). Mehrani et al. (1997) reported that

activity of PKC in hibernating bat brains decreased to 63% of the euthermic value; another study shows that PKC in bat brains was activated 5-fold during arousal from hibernation (Lee et al., 2002). These data support the involvement of phosphorylation in the modulation of NMDAR function in hAGS.

Normal brain function depends on the electrochemical gradient of key ions such as Na^+, K^+, and Ca^{2+} across the neuronal plasma membrane. Ion gradient maintenance requires constant energy input. Normally 50-60% of ATP is utilized to support those ion movements (Erecinska and Silver, 1994). The other 50% of ATP is used for ATP-dependent actin polymerization and depolymerization (Bernstein and Bamburg, 2003). During hibernation, metabolism decreases by 90% of non-hibernating level. Both actin-ATP hydrolysis and Na^+, K^+ - ATP_{ase} activity, as major energy consumers, may decrease in order to maintain the balance of ATP production and depletion (Lust et al., 1989; Storey, 1997). Suppression of ATP-dependent maintenance of the cytoskeleton is also evident from synaptic remodeling observed during hibernation cycle (Popov et al., 1992; Popov and Bocharova., 1992). Previous studies show that actin filament (F-actin) depolymerization leads to the use-dependent rundown of NMDAR activity; the rundown of NMDAR function is attenuated in the presence of intracellular ATP or is enhanced in the absence of ATP (Rosenmund and Westbrook, 1993; Norenberg et al., 1999). Hence, NMDAR function may be down-regulated in hAGS by suppressed metabolism and ATP-dependent maintenance of the actin cytoskeleton, which may act as a safety mechanism to prevent excessive influx of Ca^{2+} through NMDAR in torpid AGS.

Magnesium is an important cation, which can modulate NMDAR function by blocking the channel pore (liu and Zhang, 2000). NMDAR is strictly controlled by magnesium ions at physiological concentrations. During entrance into hibernation, elevation of blood plasma concentrations of potassium, calcium, and magnesium was found in golden hamsters (Ieglmund, et al., 1995). Hence, elevation of magnesium ions may inhibit NMDAR response.

Although the overall distribution of NR1 in hAGS and euthermic AGS is similar, a difference in the size of pyramidal neurons and granular cells in hippocampal CA1 is found. As discussed in chapter 2, brains from hibernating state showed many changes in structure compared with those from the euthermic state (Jacobs, 1996; Reme and Young, 1977, Azzam et al., 2000). For instance, smaller purkinje cell nucleoli of cerebellum (Giacometti et al., 1989) and reduced diameter of cone cells in the retina (Reme and Young, 1977) are found in hibernating animals. Moreover, reduced total cell and cytoplasm area of hepatocytes are found in the peripheral tissue of hibernating dormice compared with those from euthermic dormice (Malatesta et al., 2002). Interestingly, Malatesta et al. (2002) suggest that the change in cell structure is related to marked reduction in hepatocyte function found in the hibernating dormouse. Hence, decreased NMDAR function may be associated with the reduction in neuronal size in hAGS, which needs further investigation.

5. 4 Methodological considerations

The goal of chapter 4 was to assess cognitive function of wild-caught AGS using an active avoidance-learning paradigm. Active avoidance is a standard behavioral paradigm used to assess acquisition and retention of aversive events, a cognitive task of relevance to a prey species such as the wild-caught AGS. In this experiment, animals were trained on an active two-way avoidance task using low or high aversive stimuli. Based on the evidence of pronounced synaptic remodeling at 2 h and 24 h after arousal from hibernation (Popov and Bocharova, 1992; Popov et al., 1992; Malínský and Polách, 1985; Weltzin et al., in press), we expected that hibernation, as a natural model of pronounced adult synaptic plasticity, would enhance the cognitive function in AGS. However, due to a large degree of variability in performance on the active avoidance task and to the small number of hibernating animals studied, no effect of hibernation was observed. In addition, training and retraining occurred over several days, so the immediate effects of hibernation, such as time dependent synaptogenesis, were not detected in this study.

To further address the effect of hibernation on the cognitive function, which may be associated with synaptic restructuring in hippocampus, a learning paradigm involving a contextual fear conditioning task, known to rely on the hippocampus, was used to assess cognitive function at different time points, 3 h or 24 h after arousal from hibernation (Weltzin et al., in press). Unlike previous studies, this study specifically addressed hippocampal-related function and assessed learning at time points known to be associated with differences in dendritic morphology. The contextual learning and

memory were enhanced at 24h after arousal, but not 3h after arousal, suggesting that the burst in synaptic growth that peaks within 2-3 hours after arousal may not result in functional synapses until there is subsequent pruning and differentiation. Consistent with our findings, Matsuzaki et al. (2004) reported that smaller spines were preferred sites for LTP induction, suggesting that small spines play a leading role in initial learning, and larger spines appear to be resistant to LTP and possibly represent physical traces of long-term memory. Thus, it is important to select an appropriate task to study the behavioral performance in these wild-caught AGS.

5. 5 Conclusions of the studies in hibernation and NMDAR

Hibernation is a unique and highly regulated physiological state. As a natural model of neuroprotection and adult synaptic plasticity, studies of hibernation are encouraging and have potential to solve some medical problems in humans. The roles of NMDAR in synaptic plasticity and excitotoxicity have inspired a wide range of research into receptor potentiators to treat cognitive dysfunction and driven the search for antagonists as neuroprotective agents. The goal of the current project was to explore the potential association between NMDAR and hibernation. We report that NMDAR in hAGS are down-regulated due to the decreased phosphorylation of the NR1 subunit. This down-regulation is not due to the changes in NR1 distribution and internalization in hAGS. In addition, the fraction of NR1 in the membrane functional pool in AGS is less than in rats. These findings provide evidence for neuroprotection observed in hAGS. However, other mechanisms must be involved, which together with these findings act in

concert to contribute to neuroprotection. Further studies to explore other mechanisms are necessary to uncover the mechanisms underling hibernation and may direct us to alternative solutions to medical problems in humans.

5. 6 References

Azzam N. A., Hallenbeck J. M. and Kachar B. (2000) Membrane changes during hibernation. *Nature* 407, 317-318.

Bernstein B. W. and Bamburg J. R. (2003) Actin-ATP hydrolysis is a major energy drain for neurons. *J Neurosci* 23, 1-6.

Bickler P. E., Fahlman C. S. and Taylor D. M. (2003) Oxygen sensitivity of NMDA receptors: relationship to NR2 subunit composition and hypoxia tolerance of neonatal neurons. *Neuroscience* 118, 25-35.

Carroll R. C. and Zukin R. S. (2002) NMDA-receptor trafficking and targeting: implications for synaptic transmission and plasticity. *Trends Neurosci* 25, 571-577.

Chazot P. L. (2000) CP-101606 Pfizer Inc. *Curr Opin Investig Drugs* 1, 370-374.

Chazot P. L. (2004) The NMDA receptor NR2B subunit: a valid therapeutic target for multiple CNS pathologies. *Curr Med Chem* 11, 389-396.

Choi D. W. (1992) Excitotoxic cell death. *J Neurobiol* 23, 1261-1276.

Craig A. M., Blackstone C. D., Huganir R. L. and Banker G. (1994) Selective clustering of glutamate and gamma-aminobutyric acid receptors opposite terminals releasing the corresponding neurotransmitters. *Proc Natl Acad Sci U S A* 91, 12373-12377.

Cull-Candy S., Brickley S. and Farrant M. (2001) NMDA receptor subunits: diversity, development and disease. *Curr Opin Neurobiol* 11, 327-335.

Dave K. R., Prado R., Raval A. P., Drew K. L. and Perez-Pinzon M. A. (2005) The arctic ground squirrel brain resists cardiac arrest during euthermia. Submitted to *Stroke*.

Dodt H. U., Frick A., Kampe K. and Zieglgansberger W. (1998) NMDA and AMPA receptors on neocortical neurons are differentially distributed. *Eur J Neurosci* 10, 3351-3357.

Eimerl S. and Schramm M. (1994) The quantity of calcium that appears to induce neuronal death. *J Neurochem* 62, 1223-1226.

Erecinska M. and Silver I. A. (1994) Ions and energy in mammalian brain. *Prog Neurobiol* 43, 37-71.

Hartley D. M., Kurth M. C., Bjerkness L., Weiss J. H. and Choi D. W. (1993) Glutamate receptor-induced 45Ca2+ accumulation in cortical cell culture correlates with subsequent neuronal degeneration. *J Neurosci* 13, 1993-2000.

Holden C. P. and Storey K. B. (1996) Signal transduction, second messenger, and protein kinase responses during freezing exposures in wood frogs. *Am J Physiol* 271, R1205-1211.

Igelmund P. (1995) Modulation of synaptic transmission at low temperatures by hibernation-related changes in ionic microenvironment in hippocampal slices of golden hamsters. *Cryobiology* 32, 334-343.

Jacobs L. F. (1996) The economy of winter: phenotypic plasticity in behavior and brain structure. *Biol Bull* 191, 92-100.

Koh J. Y., Goldberg M. P., Hartley D. M. and Choi D. W. (1990) Non-NMDA receptor-mediated neurotoxicity in cortical culture. *J Neurosci* 10, 693-705.

Laurie D. J. and Seeburg P. H. (1994) Ligand affinities at recombinant N-methyl-D-aspartate receptors depend on subunit composition. *Eur J Pharmacol* 268, 335-345.

Lee M., Choi I. and Park K. (2002) Activation of stress signaling molecules in bat brain during arousal from hibernation. *J Neurochem* 82, 867-873.

Leonard A. S. and Hell J. W. (1997) Cyclic AMP-dependent protein kinase and protein kinase C phosphorylate N-methyl-D-aspartate receptors at different sites. *J Biol Chem* 272, 12107-12115.

Li B., Chen N., Luo T., Otsu Y., Murphy T. H. and Raymond L. A. (2002) Differential regulation of synaptic and extra-synaptic NMDA receptors. *Nat Neurosci* 5, 833-834.

Liu Y. and Zhang J. (2000) Recent development in NMDA receptors. *Chin Med J (Engl)* 113, 948-956.

Lu Y. M., Yin H. Z., Chiang J. and Weiss J. H. (1996) Ca(2+)-permeable AMPA/kainate and NMDA channels: high rate of Ca2+ influx underlies potent induction of injury. *J Neurosci* 16, 5457-5465.

Lust W. D., Wheaton A. B., Feussner G. and Passonneau J. (1989) Metabolism in the hamster brain during hibernation and arousal. *Brain Res* 489, 12-20.

MacDermott A. B., Mayer M. L., Westbrook G. L., Smith S. J. and Barker J. L. (1986) NMDA-receptor activation increases cytoplasmic calcium concentration in cultured spinal cord neurones. *Nature* 321, 519-522.

Malatesta M., Zancanaro C., Baldelli B. and Gazzanelli G. (2002) Quantitative ultrastructural changes of hepatocyte constituents in euthermic, hibernating and arousing dormice (Muscardinus avellanarius). *Tissue Cell* 34, 397-405.

Malinsky J. and Polach A. (1985) Changes of synaptic apparatus in the brain cortex of the hedgehog during hibernation (a quantitative Golgi and electron microscopic study). *Acta Univ Palacki Olomuc Fac Med* 108, 109-115.

Matsuzaki M., Honkura N., Ellis-Davies G. C. and Kasai H. (2004) Structural basis of long-term potentiation in single dendritic spines. *Nature* 429, 761-766.

Mehrani H. and Storey K. B. (1995) cAMP-dependent protein kinase and anoxia survival in turtles: purification and properties of liver PKA. *Mol Cell Biochem* 145, 81-88.

Mehrani H. and Storey K. B. (1997) Protein kinase C from bat brain: the enzyme from a hibernating mammal. *Neurochem Int* 31, 139-150.

Monyer H., Burnashev N., Laurie D. J., Sakmann B. and Seeburg P. H. (1994) Developmental and regional expression in the rat brain and functional properties of four NMDA receptors. *Neuron* 12, 529-540.

Murphy S. N. and Miller R. J. (1989) Regulation of Ca++ influx into striatal neurons by kainic acid. *J Pharmacol Exp Ther* 249, 184-193.

Norenberg W., Hofmann F., Illes P., Aktories K. and Meyer D. K. (1999) Rundown of somatodendritic N-methyl-D-aspartate (NMDA) receptor channels in rat hippocampal neurones: evidence for a role of the small GTPase RhoA. *Br J Pharmacol* 127, 1060-1063.

Popov V. I. and Bocharova L. S. (1992) Hibernation-induced structural changes in synaptic contacts between mossy fibres and hippocampal pyramidal neurons. *Neuroscience* 48, 53-62.

Popov V. I., Bocharova L. S. and Bragin A. G. (1992) Repeated changes of dendritic morphology in the hippocampus of ground squirrels in the course of hibernation. *Neuroscience* 48, 45-51.

Rajdev S. and Reynolds I. J. (1994) Glutamate-induced intracellular calcium changes and neurotoxicity in cortical neurons in vitro: effect of chemical ischemia. *Neuroscience* 62, 667-679.

Reme C. E. and Young R. W. (1977) The effects of hibernation on cone visual cells in the ground squirrel. *Invest Ophthalmol Vis Sci* 16, 815-840.

Rosenmund C. and Westbrook G. L. (1993) Calcium-induced actin depolymerization reduces NMDA channel activity. *Neuron* 10, 805-814.

Ross A. P., Christian S. L., Zhao H. W. and Drew K. L. (2005) Persistent tolerance to oxygen and nutrient deprivation and N-methyl-D-aspartate in cultured hippocampal slices from hibernating Arctic ground squirrel. *J Cereb Blood Flow Metab* in press.

Sattler R., Xiong Z., Lu W. Y., MacDonald J. F. and Tymianski M. (2000) Distinct roles of synaptic and extrasynaptic NMDA receptors in excitotoxicity. *J Neurosci* 20, 22-33.

Schanne F. A., Kane A. B., Young E. E. and Farber J. L. (1979) Calcium dependence of toxic cell death: a final common pathway. *Science* 206, 700-702.

Stephenson F. A. (2001) Subunit characterization of NMDA receptors. *Curr Drug Targets* 2, 233-239.

Storey K. B. (1997) Metabolic regulation in mammalian hibernation: enzyme and protein adaptations. *Comp Biochem Physiol A Physiol* 118, 1115-1124.

Tingley W. G., Roche K. W., Thompson A. K. and Huganir R. L. (1993) Regulation of NMDA receptor phosphorylation by alternative splicing of the C-terminal domain. *Nature* 364, 70-73.

Tymianski M., Charlton M. P., Carlen P. L. and Tator C. H. (1993) Source specificity of early calcium neurotoxicity in cultured embryonic spinal neurons. *J Neurosci* 13, 2085-2104.

Weltzin M., Zhao H. W., Drew K. L., and Bucci D. J. (2005) Arousal from Hibernation Alters Contextual Learning and Memory. *Behav Brain Res*, in press

Weiss J. H., Hartley D. M., Koh J. and Choi D. W. (1990) The calcium channel blocker nifedipine attenuates slow excitatory amino acid neurotoxicity. *Science* 247, 1474-1477.

Fig. 5. 1. Summary of findings. A). NR1 expression and NR1 abundance is similar in hAGS and ibeAGS, however, NR1 phosphorylation in hAGS is less than in ibeAGS. Interestingly, similar glutamate-induced $[Ca^{2+}]_i$ increase is similar between hAGS and ibeAGS, suggesting that other sources of Ca^{2+} influx or release in hAGS contributes to this glutamate-induced $[Ca^{2+}]_i$ increase. NR1 abundance is greater in rat than in AGS. NR1 phosphorylation in rats is similar as ibeAGS, but is significantly higher than in hAGS. Glutamate induces a greater $[Ca^{2+}]_i$ increase in rat compared with AGS. NMDAR, NMDA receptor; VGCC, voltage gated calcium channel; AMPAR, AMPA receptors; ER, endoplasmic reticulum. B) Possible mechanisms of decreased NMDAR function in hibernation. In addition, decreased pH, PKC activity, and increased Mg^{2+} that were described in other hibernating species, may also contribute to decreased NMDAR function in hAGS.

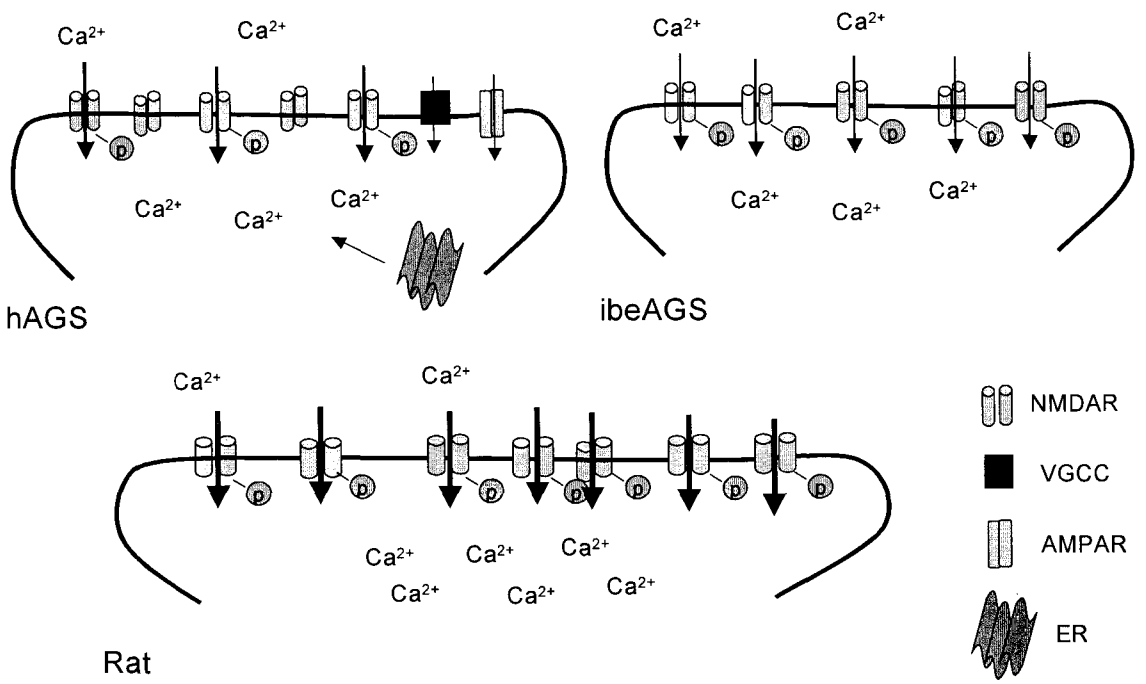

A.

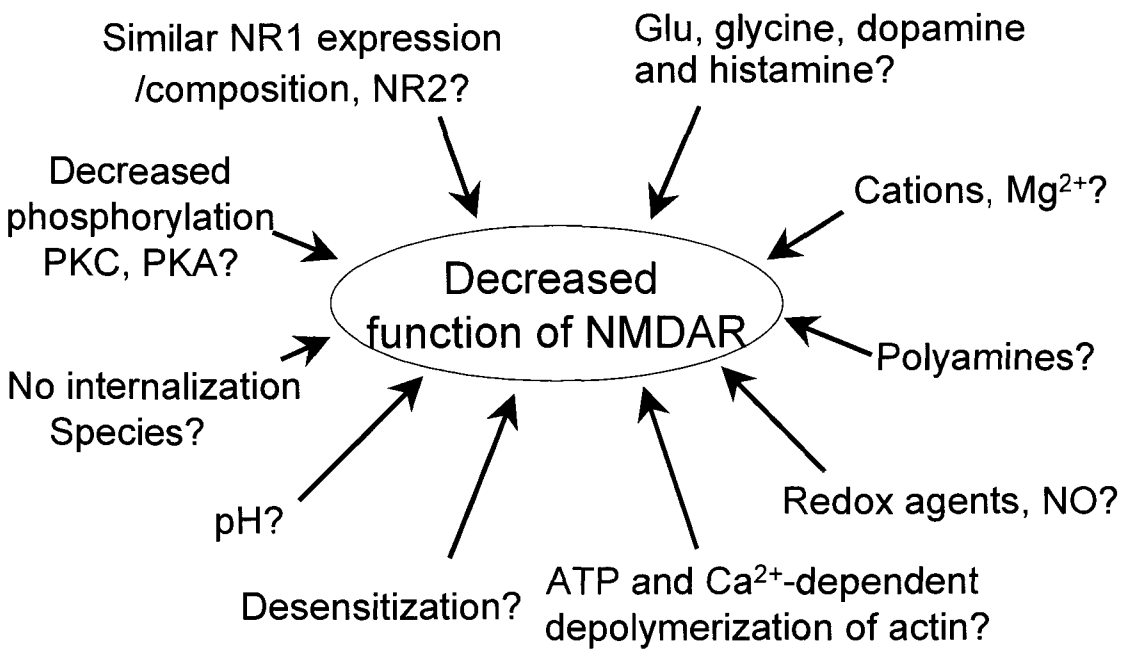

B

Appendix A: Immunohistochemistry protocol

1. All incubations were carried out with gentle agitation at room temperature unless otherwise stated
2. Pick the sections, put them in 4-compartment dishes, and rinse 6 × 10 min in PBS
3. Quench for 20min with solution prepared by adding 525 μl 30% H_2O_2 into 30ml PBS
4. Rinse 6 × 5 min in PBS
5. Block with 5 % normal goat serum (depending on the secondary antibody, for example, if the secondary antibody is anti-mouse IgG made in goat, blocking solution should be mixed with goat serum) in PBS for 2 hours
6. Incubate with the primary antibody (Mouse anti-NMDAR1 monoclonal antibody, 1:1000, Cat #: MAB 363, from Chemicon) in PBS with 3 % serum overnight at 4°C with gentle agitation.
7. Rinse 6 × 5 min in PBS
8. Incubate with secondary antibody (Biotinylated anti-mouse IgG (H+L) made in goat, 1:200 Cat #: BA-9200, Vector) with 5% goat serum in PBS
9. Prepare avidin-biotin-peroxidase solution (ABC, Vectastain ABC kit, Cat #: PK-6100) as follows: 9.86ml PBS +70μl A + 70μl B at least 30 min before using it
10. Rinse 6 × 5 min in PBS
11. Transfer to ABC solution for 30min
12. Rinse 6 × 5min in PBS

13. Prepare 3′, 3-diaminobenzidine tetrahydrochloride (DAB, Cat # 5905, Sigma) as followings: 9 mg DAB tablet in 30 ml PBS
14. Transfer to DAB solution for 5min, and then add 3 μl H_2O_2
15. Quick rinse for 3 times and regular rinse 6 × 5 min in PBS
16. Dry and dehydrated as below: 1 min 100% H2O→ 1 min 50% ETOH→ 1 min 70% ETOH→ 1 min 90% ETOH→ 2 min 100% ETOH→ 2 min 50%ETOH / 50% histoclear→ 2 min 70% ETOH / 30% histoclear→ 2 min 90% ETOH / 10% histoclear→ 2 min 100% histoclear→ 2+ min 100% histoclear
17. Mount sections on the slides and cover slip with permount

Appendix B: Membrane and cytosolic fractions preparation protocol

1. Be sure that all procedures are done with precooled reagents at 4°C.
2. Dissect out brain regions of interest (at least 40mg) into ice-cold into 10 volumes of ice-cold homogenization buffer (0.32 M sucrose, 10 mM HEPES pH 7.4, 2 mM EDTA, protease inhibitors, phosphatase inhibitors as below).

   To prepare 1ml homogenization buffer including the followings:

   - 0.8M Stock sucrose (54.76g in 200ml H_2O)→ take 400ul stock
   - 1M Stock HEPE (11.915g in 50ml H_2O) → take 10ul
   - 200mM EDTA (3,724g in 50ml H_2O) → take 10ul
   - Then add water 556.5ul
   - Inhibitor PMSF 100mM → take 1µl (final 0.1 mM)
   - Inhibitor Apr 1mg/ml → take 1.5µl (1.5µg/ml)
   - Inhibitor Leu 1mg/ml → take 10µl (10µg/ml)
   - Inhibitor Sodium Orthovandatre 100mM → take 10µl (1mM)
   - Inhibitor Antipan 10mg/ml→ take 1µl (10µg/ml)

3. Homogenize using 10-15 strokes of a glass-teflon homogenizer (original protocol use motor-driven glass-teflon himogenizer, but our hand-driven is fine). Never use polytron.
4. Spin at 1000 x g (3500 rpm) for 15 min using microcentrifuge at 4°C to remove pelleted nuclear fraction (P1).

5. Take supernatant (S1) and spin at ~200,000 x g (50,000 rpm for 30 min in 70.1 Ti rotor; or 62,000 rpm for 15 min in TLA100.3 rotor; or 67,000 rpm for 10-15 min in TLA 100.2 rotor) using ultracentrifuge and ultracentrifuge tubes to yield crude cytosol (S2) and crude membrane pellet (P2).
6. Resuspend pellet in homogenization buffer using pipette.
7. Spin again at ~200,000 x g to yield washed crude membrane pellet (P2').
8. Resuspend pellet in HEPES-Lysis buffer (50 mM HEPES pH 7.4, 2 mM EDTA, protease/phosphatase inhibitors).

   To prepare 1 ml HEPES-Lysis buffer:

   - 1M Stock HEPE (11.915g in 50ml H2O) → take 50ul
   - 200mM EDTA (3,724g in 50ml H2O) → take 10ul
   - Then add water 916.5ul
   - Inhibitor PMSF 100mM → take 1ul (final 0.1 mM)
   - Inhibitor Apr 1mg/ml → take 1.5ul (1.5ug/ml)
   - Inhibitor Leu 1mg/ml → take 10ul (10ug/ml)
   - Inhibitor Sodium Orthovandatre 100mM → take 10ul (1mM)
   - Inhibitor Antipan 10mg/ml → take 1ul (10ug/ml)

9. Measure protein concentration by Bio-Rad protein assay kit.
10. Aliquot and store at –80°C.

Appendix C: K_d calculation for fura-2

1. Calibration of Ca^{2+} Imager
   - Dissolve Fura-2 pentapotassium salt (F1200, Molecular Probes) in 1.2mL of Buffer A (Calicium calibration buffer Kit #2, C-3008) and store @ 4°C (stable for 90 days, **DO NOT FREEZE**) ---- This will give you 1 mM Stock fura-2 pentapotassium salt.
   - Turn Ca^{2+} imaging components ON in this order:
   - Xenon Lamp Power source
   - Turn on the LAMBDA10-C (shutter Instrument Filter Wheel controller) and ProScan (stage controller) (Right Switch on Back of Black Tower)
   - PC Monitor and PC
   - Open Metafluor, click New and 340/380, ratio, and control panel windows will pop out.
2. Buffer Dilutions @ 4μM Fura-2
   - Aliquot 500 μL of each buffer from A to K
   - Add 2.0 μL of 1mM Fura-2 pentapotassium salt to each aliquoted buffer.
   - Vortex well
   - Make a second Buffer E aliquot w/ no Fura-2 added.
   - Set microscope to Photo/Bi (Right one in and left one out)
   - Mount slide onto scope

- Add 50 μL of Buffer E to slide (100nM calcium with fura). Focus microscope until a sharp cone of light develops.
- Click *Focus* on the *control panel*, Set *Binning* to 8, *Exposure Time* to 2 sec (approximately setting, change them if you can't get good separation for 340/380), Gain to 3(4X), 1 MHz. Also click *Auto Scale box*, Use full chip for calibration, Change *Histogram* to *Linescan*. Close *Focus* window. Go to *Configure acquisition,* input the exposure time and binning.

3. Background: (Do not subtract back ground)
   - Replace slide w/ Buffer E (no Fura-2) and *Acquire One* image
   - *Configure: Image Display Controls*
   - Set *Low Threshold* for 340/380 for minimum black level (i.e. no gray, 340 & 380 as well, no need for ratio).
   - Acquire *Wavelength 1* Image for 340:
   - Acquire *Wavelength 2* Image for 380: Close
   - *References: Acquire background reference: View: Hide: Close*
4. Select region for calibration:
   - *Regions: Acquire Images:* set region for 340. *OK*
   - Mark area for calibration in 340, *Done*
   - Repeat on both 380 and 340/380 Ratio, *Done*. Then come back to 380 without acquiring image this time, just *Ok*, *Done*

5. Determine Sf:
    - On Control Panel choose *Log Data: OK: Application Microsoft Excel XP: OK*
    - Name the Excel data sheet and hit return.
    - Go back to MetaFluor.
    - In *control panel*, *Zero Clock*: to resume Acquisition. *Acquire* Data. Record for 1 min (Background Fluorescence)
    - *Pause Acquisition*, replace w/ Buffer A (zero Ca^{2+}), and record for 1 min.
    - *Pause Acquisition*, replace w/ Buffer K (sat. Ca^{2+}), and record for 1 min.
    - Save Excel File and close Excel program.
    - Image Display: View Calibration Images
6. Acquire Titration Standards:
    - *Calibration: Acquire Calibration Standards: Set Calibration Mode to Titration.*
    - Place slide onto objective, starting w/ Buffer A.
    - Enter [Ca^{2+}] in the *Value* box and *Acquire*.
    - Repeat for each buffer.
    - Correct all: Check *Subtract Background* only in here:
    - Save Calibration standard: OK
7. Calculate Calcium Titration Values:
    - *Calibration: Titration Calibration in Vitro*
    - Click number by each cell, Write down Ratio & Cal Value
    - Choose *Curve Fit* to view graph, close
    - Control: Close: File: Exit: No: Yes

APPROXIMATE SETTINGS FOR BACKGROUND SET-UP

380	**340**	**340/380**
D = Monochrome	Monochrome	Monochrome
BR = 61	48	51
C = 74	60	69
LT = 17	12	D min 1.0
HT = 3665	3665	D max 1.5

Focus: Toggle Shutter to change Wave Length to desired setting.

CORRECTED CALIBRATION VALUES			
No	RATIO	CAL VALUE	Ratio
1	0.411845	0.000 μm	
2	0.495221	0.017 μm	
3	0.608276	0.038 μm	
4	0.741000	0.065 μm	
5	0.90722	0.100 μm	
6	1.10582	0.150 μm	
7	1.46514	0.225 μm	
8	1.94154	0.351 μm	
9	2.07096	0.602 μm	
10	4.19266	1.350 μm	
11	5.67007	39.000 μm	

Appendix D: Ca^{2+} imaging protocol

1. Preparation:
   - Prepare HEPE-Neurobasal buffer containing (mM) NaCl 101, KCl 4.6, $CaCl_2$ 1.8, $MgCl_2$ 0.81, HEPES 10, and Dextrose 21)
   - Prepare Ca^{2+} free HEPE-Neurobasa buffer containing (NaCl 101, KCl 4.6, 10mM EGTA, $MgCl_2$ 0.81, HEPES 10, and Dextrose 21)
   - Prepare 10μM fura-2 solution 500 μl (for 24 well plate) with 0.5% BSA, 0.02% pluronic acid, and HEPE-Neurobasal buffer
   - Prepare Ionomycin (10 μM), Glu (1mM) and AP5 (200 μM) in HEPE-Neurobasal buffer
   - Load slices (on Millicell-CM insert) with fura2 in dark (covered with foil) at 37°C
   - Clean the dish and the rubber stopper with 70% alcohol
   - Rinse and fill the system with HEPE-Neurobasal buffer
2. Turn on Imaging Components:
   - Turn on Xenon Lamp Power
   - Turn on the LAMBDA10-C (shutter Instrument Filter Wheel controller) and ProScan (stage controller)
   - Turn on PC Monitor and PC:
3. Check Following:
   - Microscope set to Bi (i.e. right lever pushed in and left lever out)

- Use 10x objective, toggle the shutter 380 and locate CA1 area in the hippocampal slice
- Then focus using 40 x LD ACHROPLAN
- Close 380 shutter.

4. Initialize Software for New Experiment:
   - Open MetaFluro program:
   - Open New Experiment:New: (new exp. Screen appears)
5. Check Calibration Settings:
   - Calibration : Equation Calibration in vitro...(Kd)

     Kd = 259 ; Fmin = 72.3 ; Fmax = 10.7 ; Rmin = 0.25 ; Rmax = 2 .
   - Set microscope to Photo/Bi (i.e. microscope lever on left is pulled out & on the right is in)
6. Start focus:
   - Start Focus on the control pannel: Unclick Auto scale, toggle Shutter: Switch between 340 & 380
   - Determine the exposure time and binning state to capture a good image using the 380 nm exciter filter. (Want maximum intensity range between 340/380 w/out saturation)
   - Close Focus dialog box
   - Go to Configure Acquisition, fill the exposure time and binning in the 380nm. Close

- Go to Configure Experiment, click 340, 380nm: acquire, avg, show, update; click ratio: ratio (W1/W2) show, update; click Calcium: calibrated ratio 1 (not necessary). Ok

7. Edit Regions:
   - Regions : Select image for defining regions
   - Select ratio, Acquire Images, click OK
   - Set area around slice for graphing
   - Click Done Editing Regions
   - Repeat for 340 and 380, above steps
8. Set Display:
   - Set Display: Image Display Controls: Choose 380: Display=Monochrome
   - Adjust Brightness, Contrast, Low Threshold, High Threshold (use approximately settings on calibration), Repeat above 2 steps for 340
   - For Ratio 1: Choose Psuedocolor, this step only affect your view, but not results
   - Log measures to Dynamic Link to Excel 2000 (save in same folder as experiment), Back to MetaFluro, zero clock.
   - Open Events: add the event you want to do today, Run Experiment: Events
   - Run Experiment or Control: acquire
9. After experiment, flush the tubing and dish with 30-50 ml 10% bleach → 30-50ml 70% alcohol → 30-50ml milli-Q water→ run five more minute to empty perfusion system.
10. Precautions and possible trouble shooting:

- If you spill the solution on the objective, stop recording and wrap with Q-tips with 100% alcohol.
- After experiment, be sure to check stage and objective and always keep them clean and dry
- If you heard weird sound, it may come from filter wheel (it may tilt due to weight…), camera shutter (shutter is not fully closed…)
- If you need some accessories, go to www.bioptechs.com.